GEORGIA INSTITUTE OF TECHNOLOGY
OFFICE OF RESEARCH ADMINISTRATION

Date: 7 November 1969

RESEARCH PROJECT INITIATION

Project Title: Thermally Induced Flow Oscillations in Two Phase Flow Systems in Thermal Equilibrium

Project No.: ~~B-1113~~ E-25-608

Project Director: Dr. Novak Zuber

Sponsor: National Science Foundation

Agreement Period: From 15 October 1969 until 14 October 1971

Type Agreement: Grant No. GK-16023

Amount: $72,000 NSF Funds (B-1113)
21,573 GIT Contribution (E-1105)
$93,573 Total Budget

Grant Administrator

Dr. Royal E. Rostenbach
Acting Director
Engineering Energetics Program
Engineering Division
National Science Foundation
Washington, D. C. 20550

Reports Required

Annual - 14 October 1970

Final - Upon completion of project

Assigned to: School of Mechanical Engineering

COPIES TO:

- [x] Project Director
- [x] School Director
- [x] Dean of the College
- [x] Administrator of Research
- [x] Associate Controller (2)
- [x] Security-Reports-Property Office
- [x] Patent Coordinator
- [x] Library
- [x] Rich Electronic Computer Center
- [x] Photographic Laboratory
- [ ] EES Machine Shop
- [ ] EES Accounting Office

Other File B-1113

300. B-1113 (Sch)

RA-3 (4/65)

GEORGIA INSTITUTE OF TECHNOLOGY
OFFICE OF CONTRACT ADMINISTRATION

SPONSORED PROJECT TERMINATION

Date: September 15, 1976

Project Title: Thermally Induced Flow Oscillations in Two Phase Flow Systems in Thermal Equilibrium

Project No: E-25-608 (B-1113)

Project Director: Dr. Novak Zuber

Sponsor: National Science Foundation

Effective Termination Date: 3/31/73

Clearance of Accounting Charges: 3/31/73

Grant/Contract Closeout Actions Remaining:

- _ Final Invoice and Closing Documents
- X Final Fiscal Report
- _ Final Report of Inventions
- _ Govt. Property Inventory & Related Certificate
- _ Classified Material Certificate
- _ Other ______________________

Assigned to: Mechanical Engineering (School/Laboratory)

COPIES TO:

Project Director
Division Chief (EES)
School/Laboratory Director
Dean/Director—EES
Accounting Office
Procurement Office
Security Coordinator (OCA)
Reports Coordinator (OCA)

Library, Technical Reports Section
Office of Computing Services
Director, Physical Plant
EES Information Office
Project File (OCA)
Project Code (GTRI)
Other ______________________

CA–4 (3/76)

E-25-608

TWO-PHASE FRICTIONAL PRESSURE DROP IN LAMINAR, STRATIFIED FLOWS

A THESIS

Presented to

The Faculty of the Graduate Division

by

Larry Eugene Bowen

In Partial Fulfillment

of the Requirements for the Degree

Master of Science

in Mechanical Engineering

Georgia Institute of Technology

August, 1973

TWO-PHASE FRICTIONAL PRESSURE DROP IN LAMINAR, STRATIFIED FLOWS

A THESIS

Presented to

The Faculty of the Graduate Division

by

Larry Eugene Bowen

In Partial Fulfillment

of the Requirements for the Degree

Master of Science

in Mechanical Engineering

Georgia Institute of Technology

August, 1973

TWO-PHASE FRICTIONAL PRESSURE DROP

IN LAMINAR, STRATIFIED FLOWS

Approved:

____
Dr. Novak Zuber, Chairman

____
Dr. Ward O. Winer

____
Dr. Charles S. Martin

Date Approved by Chairman: Aug 13, 1973

ACKNOWLEDGMENTS

The author would like to express his gratitude and appreciation to Professor Novak Zuber for his timely assistance and invaluable advice during the author's thesis work. A special thanks is expressed to Dr. Zuber for obtaining several Russian works and aiding in their translation which were so necessary to the author's research. In addition, the author is indebted to Dr. Zuber for his efforts as chairman of the reading committee and for his review of the manuscript.

Acknowledgments are also presented to the two other members of the reading committee, Professor W. O. Winer, from the School of Mechanical Engineering, and Professor C. S. Martin, from the School of Civil Engineering, for their helpful suggestions.

The work presented in this thesis was carried out under the sponsorship of the Mechanics Division of the AFOSR Grant No. 70-1853 at the Georgia Institute of Technology. The author thanks the above organization for the financial provision for this research.

TABLE OF CONTENTS

LIST OF ILLUSTRATIONS

NOMENCLATURE

A_1	area occupied by phase 1
A_2	area occupied by phase 2
A_c	cross-sectional area
$\overline{\alpha}$	area-averaged void fraction, $\overline{\alpha} \equiv \frac{A_2}{A_c}$
b	length of the parallel plates
β	"flowing" volumetric concentration, $\beta \equiv \frac{Q_2}{Q_1+Q_2}$
C_1	constant defined by equation (15), Chapter I
C_2	constant defined by equation (16), Chapter I
D	diameter of circular pipe
D_H	hydraulic diameter, $D_H \equiv \frac{4A_c}{P_\omega}$
f_M	two-phase Moody friction factor
G	total mass flux, $G = \rho_1 j_1 + \rho_2 j_2$
h	distance between parallel plates
j	velocity for center of volume, $j = j_1 + j_2$
j_1	superficial velocity for phase 1, $j_1 = \frac{Q_1}{A_c}$
j_2	superficial velocity for phase 2, $j_2 = \frac{Q_2}{A_c}$
k	parameter defined by equation (16), Chapter III
ℓ	characteristic length
$(\frac{\Delta p}{L})$	pressure drop per unit length
ρ_1	density for phase 1
ρ_2	density for phase 2
ρ_m	mixture density

Q_1 volumetric flow rate for phase 1

Q_2 volumetric flow rate for phase 2

Φ_L square root of the two-phase frictional pressure drop to the frictional pressure drop that would result if the liquid phase occupied the entire pipe alone

Φ_G square root of the two-phase frictional pressure drop to the frictional pressure drop that would result if the gas phase occupied the entire pipe alone

Re_H Reynolds number based on hydraulic diameter

S "slip" ratio, $S \equiv \dfrac{\bar{v}_2}{\bar{v}_1}$

v_{fg} difference in specific volumes of saturated liquid and vapor

v_f specific volume of liquid

$\bar{v}_1$ average axial velocity for phase 1

$\bar{v}_2$ average axial velocity for phase 2

v_r relative velocity, $v_r \equiv \bar{v}_2 - \bar{v}_1$

v_m velocity for the center of mass

ν_m mixture kinematic viscosity

μ_1 absolute viscosity for phase 1

μ_2 absolute viscosity for phase 2

μ_m mixture absolute viscosity

X_{vv} Martinelli parameter for viscous-viscous flow, $X_{vv}^2 \equiv \dfrac{Q_1/\mu_1}{Q_2/\mu_2}$

(x,y,z) rectangular Cartesian coordinates

χ mass quality, $\chi \equiv \dfrac{\rho_2 Q_2}{\rho_1 Q_1 + \rho_2 Q_2}$

NOMENCLATURE

Appendix A

A_c	cross-sectional area of rectangular duct
$A_1'(n)$	coefficient defined by equation (26)
$A_2'(n)$	coefficient defined by equation (27)
2a	width of the rectangular duct
b_1	depth of the less viscous phase 1
b_2	depth of the more viscous phase 2
2b	height of the rectangular duct
$B_1'(n)$	coefficient defined by equation (28)
$B_2'(n)$	coefficient defined by equation (29)
ch	hyperbolic cosine function
D_H	hydraulic diameter
f_M	Moody friction factor
g_c	dimensional conversion factor = 32.174 lb_m-ft/lb_f-sec^2
h	location of the interface with respect to the centerline
k_1, k_2	functions defined by equation (9)
m	absolute viscosity ratio, (μ_2/μ_1)
n	variable defined by equation (20)
p	static pressure
Q_1	volumetric flow rate for phase 1
Q_2	volumetric flow rate for phase 2
ρ_1	density for phase 1

ρ_2	density for phase 2
sh	hyperbolic sine function
v_1	local velocity for phase 1 in z-direction
v_2	local velocity for phase 2 in z-direction
μ_1	absolute viscosity for phase 1
μ_2	absolute viscosity for phase 2
(x,y,z)	rectangular Cartesian coordinates
Y_1,Y_2	variables defined by equation (23)

NOMENCLATURE

Appendix B

$A_1(m)$	coefficient defined by equation (36)
$A_2(m)$	coefficient defined by equation (37)
2a	length of the interface
$\bar{\alpha}$	area-averaged void fraction
$B_1(m)$	coefficient defined by equation (22)
$B_2(m)$	coefficient defined by equation (23)
ch	hyperbolic cosine function
ctg	cotangent function
dA_c	elementary cross-sectional area
(ε,Θ)	bi-polar coordinates in Figure 8
g	gravitational constant = 32.174 ft/sec^2
γ	pipe inclination angle
k_1	parameter defined by equation (3)
k_2	parameter defined by equation (4)
m	dummy integration variable
p	static pressure
Q_1	volumetric flow rate for phase 1
Q_2	volumetric flow rate for phase 2
ρ_1	density for phase 1
ρ_2	density for phase 2
r_1,r_2	radial lengths defined in Figure 8

R	pipe radius
sh	hyperbolic sine function
Θ_1, Θ_2	angular measures defined in Figure 8
v_1	axial velocity for phase 1
v_2	axial velocity for phase 2
μ_1	absolute viscosity for phase 1
μ_2	absolute viscosity for phase 2
(x,y)	rectangular Cartesian coordinates
$\xi_1(m)$	function defined by equation (14)
$\xi_2(m)$	function defined by equation (15)

SUMMARY

The purpose of this thesis is threefold. First, the proper definition for the mixture kinematic viscosity, ν_m, will be developed for stratified, horizontal flow systems. Secondly, using this definition for ν_m, an appropriate expression for the two-phase Reynolds number will be derived which is used as the similarity parameter for modeling the friction factor in two-phase, separated flow. And thirdly, a correlation is presented for predicting the volumetric concentration in separated, two-phase flow.

The results of this analysis will show that the two-phase friction factor reduces to the well-known pressure drop correlation applicable to single-phase flow in terms of the Moody friction factor and the Reynolds number defined in this analysis. In addition, the author's void fraction correlation will show that Hewitt's "triangular" relationship for the volume flow rates, overall pressure drop, and the void fraction, does not hold for laminar, horizontal, stratified flows.

The three separated flow systems analyzed are: (1) flow between wide, horizontal parallel plates; (2) flow through horizontal, rectangular ducts; and (3) flow through horizontal, circular pipes. In all three cases, the drift or diffusion flow model is used to establish the correct expression for the mixture viscosity. Experimental data are used to test the validity of this analysis for predicting the frictional pressure drop and void fraction. Excellent agreement is shown between experimental and predicted results.

CHAPTER I

INTRODUCTION

1.1 Significance of the Problem

The frequent occurrence of two-phase, single- and/or two-component flow in pipelines is characteristic of many modern petroleum, chemical, and nuclear systems. Two current problem areas are the ability to accurately predict the pressure losses and the volumetric concentration in these pipelines. One of the flow regimes frequently observed is stratified flow. This type of two-phase flow has been demonstrated experimentally by several investigators [4,5,28, 33] and it is the subject of this work.

1.2 Review of the Literature

A literature search with respect to horizontal, two-phase flow in conduits revealed that a logical and general method for accurately predicting the frictional pressure drop and volumetric concentration does not exist. Numerous good references [3,10,14,19,29,31] containing discussions of horizontal flow correlations point out that most of these correlations are empirical; therefore, they are subject to the limitations of their own data.

Many investigators seem to rely on the work of Lockhart and Martinelli [21] and Martinelli et al. [23] as the classical approach to this problem. The correlation of the latter was established by performing numerous experiments in horizontal, circular pipes covering a wide range of flow rates at atmospheric pressures. The experimental data were separated into four basic groups depending on whether each phase was flowing in the laminar or turbulent state. The parameters Φ_L and Φ_G, defined in the Nomenclature, were determined and plotted against the Martinelli parameter, X, which is a function of input system quantities and fluid properties only. The Martinelli parameter for laminar-laminar flow, X_{VV}, is also defined in the Nomenclature. Their correlations for predicting the frictional pressure drop and the void fraction are shown in Figure 1. Although the Lockhart-Martinelli correlation gives good agreement in a number of cases, it has been shown to be quite inaccurate in the case of stratified fluid flow [2,5,8,11].

Another and more commonly used approach is to treat the two fluids as if they were a homogeneous mixture with appropriately defined mixture properties (i.e. mixture density and mixture viscosity). Herein lies the major problem. How does one define these mixture properties?

Many investigators [1,2,7,9,12,16,18,22,24,25,26] have tried to establish a frictional pressure drop correlation similar to that obtained in single-phase flow (in terms of the Moody friction factor and the fluid Reynolds number) by choosing arbitrary and artificial definitions

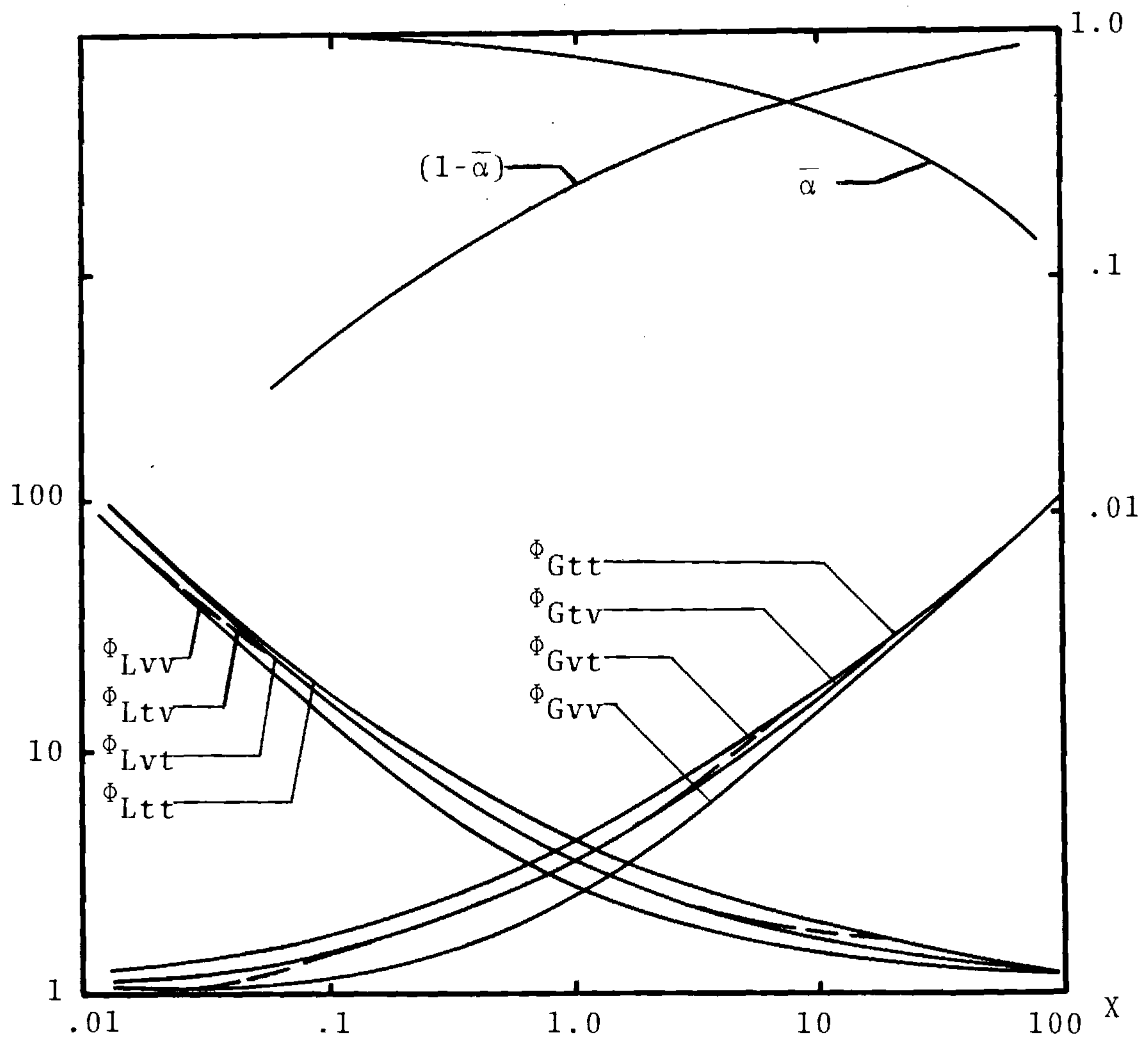

Figure 1. Lockhart-Martinelli Correlation

for the mixture viscosity to use in the definition of the Reynolds number. Numerous definitions for this two-phase viscosity are found in the literature and the researchers all claim that their expressions are the proper definition to use. Seven of the most publicized definitions plus a Russian definition are presented below to illustrate the wide variety from which one has had to choose. They are:

(1) $\mu_m = \mu_1$, (Owens [26], 1962)

(2) $\frac{1}{\mu_m} = \frac{1-\chi}{\mu_1} + \frac{\chi}{\mu_2}$, (Isbin et al. [18], 1957 and McAddams et al. [24], 1962)

(3) $\mu_m = (1-\chi)\mu_1+\chi\mu_2$, (Cicchitti et al. [7], 1960)

(4) $\mu_m = \mu_1^{1-\chi}\mu_2^{\chi}$, (Hagendorn [16], 1965)

(5) $\mu_m = (1-\bar{\alpha})\mu_1+\bar{\alpha}\mu_2$, (Bankoff [1], 1960)

(6) $\mu_m = (1-\beta)\mu_1+\beta\mu_2 C_2$, (Dukler et al. [12], 1954 and Ngyuen and Spedding [25], 1973)

(7) $\frac{1}{\nu_m} = \frac{1-\beta}{\nu_1} + \frac{\beta}{\nu_2}$, (Mamaev et al. [22], 1969)

(8) $\mu_m = \mu_1[1+\chi\frac{v_{fg}}{v_f}]$, (Davidson [9], 1948)

where the mass quality, χ, the volumetric flux concentration, β, and the void fraction, $\bar{\alpha}$, are defined in the Nomenclature. The parameter C_2 is defined in equation (16).

Notice that in every expression but (8), the mixture viscosity reduces to the correct result at the extremes; that is, when

$$\left.\begin{array}{l}\chi \to 0\\ \beta \to 0\\ \overline{\alpha} \to 0\end{array}\right. \equiv \begin{array}{c}\mu_m = \mu_1\\ (\nu_m = \nu_1)\end{array} \tag{9}$$

and when

$$\left.\begin{array}{l}\chi \to 1\\ \beta \to 1\\ \overline{\alpha} \to 1\end{array}\right. \equiv \begin{array}{c}\mu_m = \mu_2\\ (\nu_m = \nu_2)\end{array} \quad . \tag{10}$$

Three of the previous expressions for the mixture viscosity are plotted versus the quality in Figure 2 to point out the large differences one could encounter during any analysis involving a definition for the viscosity depending on his choice of equations (1) through (8). It is easily seen in Figure 2 that the values can differ by a factor of 5 in the worst case!

An entirely different and novel approach to the problem of predicting the frictional pressure drop was undertaken by Dukler, Wicks, and Cleveland [12] in 1964 and rederived by Ngyuen and Spedding [25] in 1973. Dukler et al. introduced and developed a correlation through similarity analysis. Their resulting expressions for the Euler number and the mixture Reynolds number are

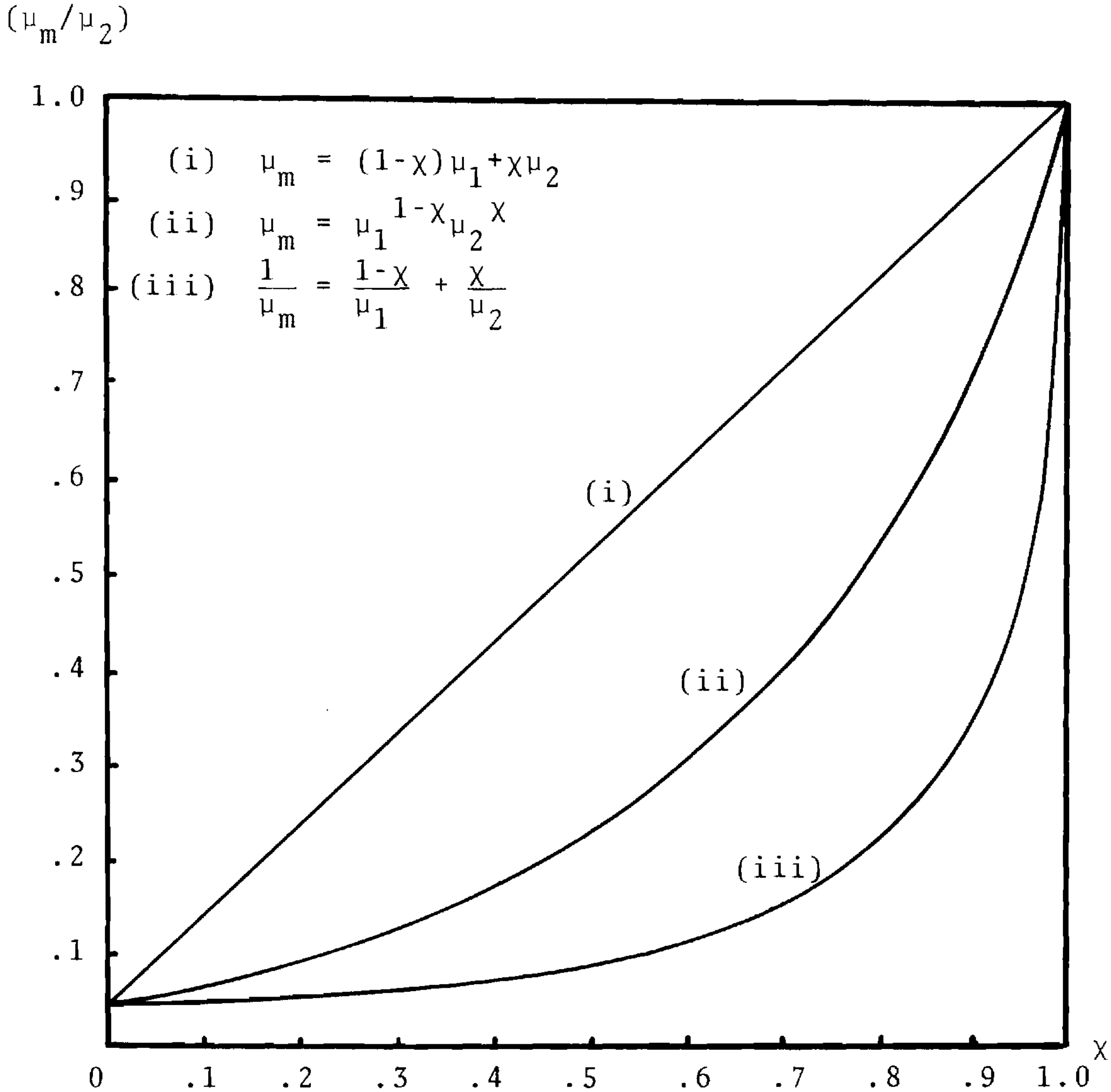

Figure 2. Non-Dimensional Viscosity Ratio versus Quality for $(\mu_2/\mu_1) = 20.1$

$$N_{Eu_{TP}} \equiv 2f_M = \{\frac{(\frac{dp}{\alpha z})}{\frac{j^2}{g_c \ell}}\}[\frac{1}{(1-\beta)\rho_1+\beta\rho_2 C_1}] \tag{11}$$

and

$$N_{Re_{TP}} \equiv \ell j\{\frac{(1-\beta)\rho_1+\beta\rho_2 C_1}{(1-\beta)\mu_1+\beta\mu_2 C_2}\} \quad . \tag{12}$$

As a consequence of this approach, the mixture density, ρ_{TP}, was defined as

$$\rho_{TP} = (1-\beta)\rho_1+\beta\rho_2 C_1 \tag{13}$$

and the mixture viscosity, μ_{TP}, as

$$\mu_{TP} = (1-\beta)\mu_1+\beta\mu_2 C_2 \quad , \tag{14}$$

where the constants C_1 and C_2 are given by

$$C_1 \equiv (\frac{\overline{v}_L}{\overline{v}_G})^2 (\frac{\frac{dv_G}{dz}}{\frac{dv_L}{dz}}) (\frac{v_G}{\overline{v}_G}) [\frac{R_G \overline{R}_L}{\overline{R}_G R_L}] \tag{15}$$

and

$$C_2 \equiv \left(\frac{\overline{v}_L}{\overline{v}_G}\right)\left(\frac{\frac{d^2 v_G}{dn^2}}{\frac{d^2 v_L}{dn^2}}\right)\left[\frac{R_G \overline{R}_L}{\overline{R}_G R_L}\right] \quad . \tag{16}$$

Dukler et al. considered four special cases and made various assumptions in each case to evaluate C_1 and C_2. The two more important cases of interest are the case of flow without "slip" and the case of flow with "slip". In both cases, C_1 and C_2 were assumed to be equal to one.

In Chapter II a brief discussion on the separated flow models (i.e. the two-fluid model and the diffusion or drift model) will show why Dukler's et al. method, as well as the methods of many other investigators who used the homogeneous model approach, are not consistent with these models.

In 1967, Yu [33] did analytical and experimental research on the two-phase frictional pressure drop in laminar, stratified flow in horizontal conduits of varying cross section. In his analysis he introduces the concept of an apparent mixture viscosity which is very similar to the author's expression for flow in rectangular ducts in Chapter IV. However, he did not use this definition to propose a correlation for predicting the frictional pressure drop, nor did he propose a method for predicting the void fraction.

1.3 Purpose

The purpose of this thesis is threefold: (1) to develop the correct definition for the mixture kinematic viscosity, ν_m, for stratified flow systems; (2) to derive an appropriate expression for the mixture Reynolds number which can be used as a similarity parameter for modeling the friction factor in two-phase flow; and (3) to present a correlation for predicting the void fraction in horizontal, separated flow.

The results of this analysis will show that when the Reynolds number similarity group defined in this analysis is used, the two-phase friction factor reduces to the well-known Moody friction factor applicable to single-phase flow systems. Thus, the Moody friction factor in both two-phase and single-phase flow can be correlated on the same diagram. This confirms that the Reynolds number, as defined in this analysis, is the correct similarity group to be used in frictional pressure drop models.

Furthermore, the void fraction correlation as a result of this analysis will show that the "triangular" relationship claimed by Hewitt [17] does not hold for separated, two-phase flow. Hewitt bases his "triangular" relationship on three parameters: the individual volume flow rates, the overall pressure drop, and the void fraction. He claims that in order to calculate the void fraction, a knowledge of both the volume flow rates and the overall pressure drop must be known. In other words, according to Hewitt, to predict any one of the three previously mentioned parameters, one must know the other two parameters.

Experimental data are used to check the validity of both the pressure drop and void fraction correlations.

CHAPTER II

FLOW MODEL FORMULATION

2.1 General

The numerous analyses based on the area-averaged separated flow model can be divided into two basic groups. One is the two-fluid model which is formulated by considering each phase separately, whereas the second is the diffusion or drift model which is formulated by considering the entire mixture. It is this latter flow model which will be the basis of the analyses in Chapters III, IV, and V to develop pressure drop and void fraction correlations for horizontal, separated flow.

Before discussing the drift model, a brief discussion of the two-fluid model is included to point out the major differences in these two models.

2.2 Two-Fluid Model

The two-fluid model is formulated by considering each phase separately. Therefore, this formulation is expressed in terms of six field equations: two continuity equations, two momentum equations, and two energy equations.

This model will yield satisfactory results whenever the two mixture components are weakly coupled, that is when equalization of velocities does not occur [20]. This can be expected whenever there is a large difference between the densities and the velocities of the two components.

Thus, the model will be applicable to problems concerned with the dynamics of the interface and other interactions between the two phases. Since any formulation based on this model is represented in terms of six field equations, a mathematical analysis may be quite difficult; thus, it is not an effective model for system dynamics analyses or for determining mixture properties.

2.3 Diffusion or Drift Model

In contrast to the two-fluid model, the diffusion or drift model is formulated by considering the entire mixture. Therefore, the resulting formulation is expressed in terms of four field equations: three for the mixture plus the void propagation equation for one of the phases [34]. As pointed out by [20] the drift model follows the similar well-established approach used to analyze the dynamic behavior of chemically reacting binary mixtures. It is therefore applicable whenever the two mixture components are closely coupled, that is, whenever they interact so that their differences between the velocities and the other properties are small. Hence, attention is focused on the relative motion rather than the motion of the individual phases. And the field equations must be based on the baricenter, or center of mass, of the mixture.

This last requirement that the conservation equations be expressed in terms of the baricenter is where so many investigators' formulations have been wrong. Although the many traditional formulations were based on the three conservation equations, they did not express these equations in terms of the baricenter. Thus, one important consequence from this is that the mixture properties were not properly defined! In fact, various authors were forced to introduce no less than four definitions for the mixture density [20]. And note that there are many more expressions for the mixture viscosity similar to the eight expressions in Chapter I.

Therefore, in the following chapters, the author will show the correct and consistent approach to use in developing a pressure drop correlation based on this drift model.

CHAPTER III

STRATIFIED, LAMINAR FLOW BETWEEN WIDE, HORIZONTAL PARALLEL PLATES

3.1 Governing Equations

The two-phase frictional pressure drop will be analyzed analytically for the case of stratified, laminar flow between wide, horizontal parallel plates. The flow model is depicted in Figure 3. The basic differential equation governing the laminar, horizontal, fully-developed flow of an incompressible Newtonian fluid is

$$0 = -\frac{dp}{dz} + \mu\left(\frac{d^2v}{dy^2}\right) \tag{1}$$

Thus, for phase 1 and phase 2, respectively, one has

$$0 = -\frac{dp}{dz} + \mu_1\left(\frac{d^2v_1}{dy^2}\right) \tag{2}$$

and

$$0 = -\frac{dp}{dz} + \mu_2\left(\frac{d^2v_2}{dy^2}\right) \tag{3}$$

or rearranging equations (2) and (3), one obtains

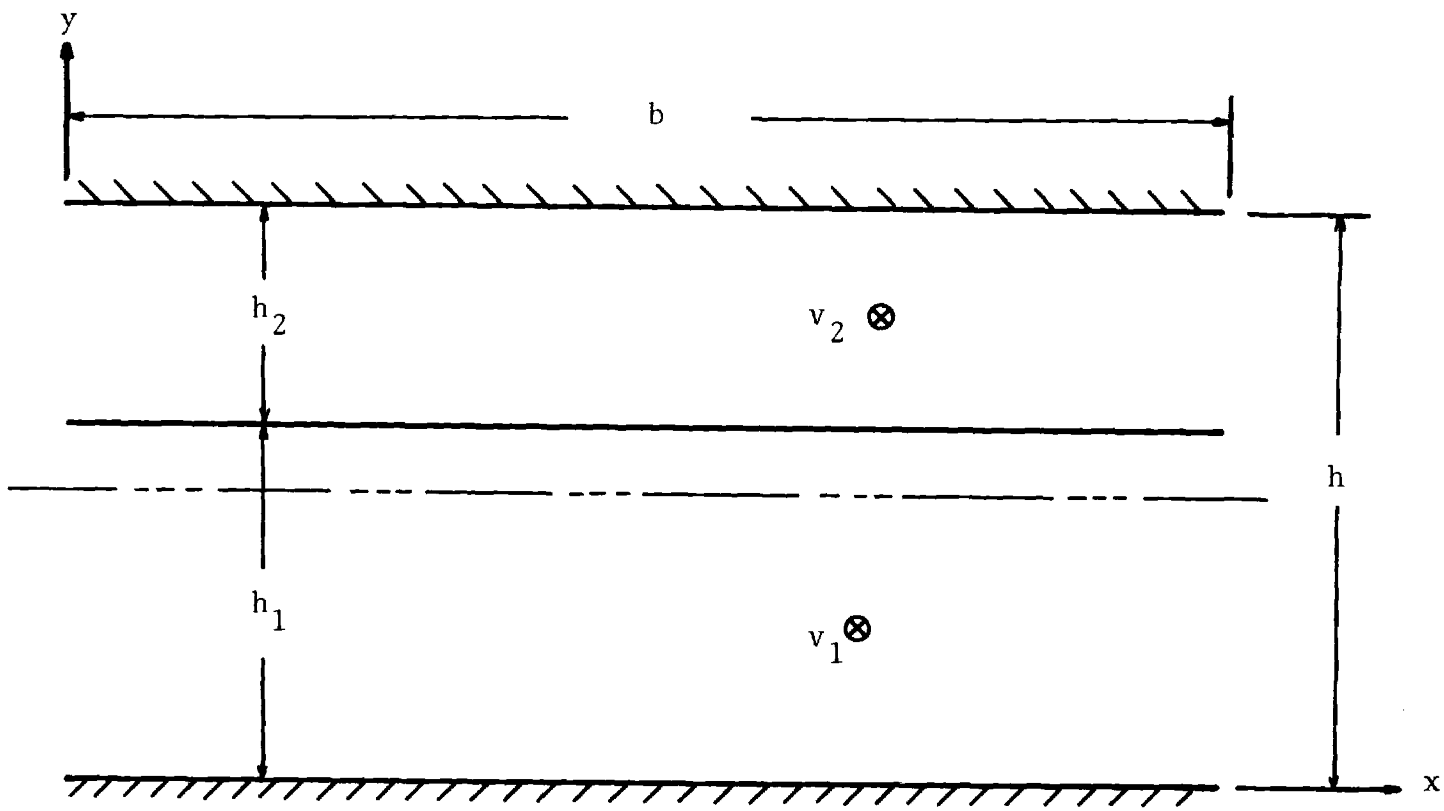

Figure 3. Separated Flow Model for Wide, Horizontal Parallel Plates

$$\frac{d^2 v_1}{dy^2} = \frac{2}{\mu_1} k \tag{4}$$

and

$$\frac{d^2 v_2}{dy^2} = \frac{2}{\mu_2} k \tag{5}$$

where

$$k \equiv \frac{1}{2}\left(\frac{dp}{dz}\right) \quad . \tag{6}$$

The solutions to equations (4) and (5) yield the velocity distribution for each phase, respectively [2,22,32]. Note that the velocity distribution for phase 1 in Whitaker [32] contains an error. The area-averaged velocity for each phase is obtained by integrating the solutions to equations (4) and (5) over their respective depths, h_1 and h_2. Thus, the average velocities for phase 1 and phase 2, respectively, become [22]:

$$\overline{v}_1 = - \frac{h^2}{2} k(1-\overline{\alpha})\left[\frac{(1-\overline{\alpha})}{3\mu_1} + \frac{\overline{\alpha}}{(1-\overline{\alpha})\mu_2+\overline{\alpha}\mu_1}\right] \tag{7}$$

and

$$\bar{v}_2 = -\frac{h^2}{2}k\bar{\alpha}\left[\frac{\bar{\alpha}}{3\mu_2} + \frac{(1-\bar{\alpha})}{(1-\bar{\alpha})\mu_2+\bar{\alpha}\mu_1}\right] \tag{8}$$

where $\bar{\alpha}$ is defined to be the area-averaged void fraction per unit depth; i.e.

$$\begin{aligned} \bar{\alpha} &\equiv \frac{h_2}{h}, \\ 1-\bar{\alpha} &\equiv \frac{h_1}{h}. \end{aligned} \tag{9}$$

<u>3.2 Velocity for the Center of Volume, j</u>

The superficial velocity for phase 1 and phase 2, respectively, is defined as

$$j_1 \equiv (1-\bar{\alpha})\bar{v}_1, \; j_2 \equiv \bar{\alpha}\,\bar{v}_2 . \tag{10}$$

Substitution of equation (9) into equation (10) gives

$$j_1 = -\frac{h^2(1-\bar{\alpha})^2k}{2}\left[\frac{(1-\bar{\alpha})}{3\mu_1} + \frac{\bar{\alpha}}{(1-\bar{\alpha})\mu_2+\alpha\mu_1}\right] \tag{11}$$

and

$$j_2 = -\frac{h^2\bar{\alpha}^2k}{2}\left[\frac{\bar{\alpha}}{3\mu_2} + \frac{(1-\bar{\alpha})}{(1-\bar{\alpha})\mu_2+\bar{\alpha}\mu_1}\right] . \tag{12}$$

The velocity for the center of volume, j, is obtained by adding the superficial velocity for phase 1 and the superficial velocity for phase 2; thus, j becomes

$$j \equiv j_1 + j_2 = -\frac{h^2 k}{6}\left[\frac{(1-\bar{\alpha})^3}{\mu_1} + \frac{\bar{\alpha}^3}{\mu_2} + \frac{3\bar{\alpha}(1-\bar{\alpha})}{(1-\bar{\alpha})\mu_2 + \bar{\alpha}\mu_1}\right] \qquad (13)$$

or substituting for k defined in equation (6), one gets

$$j = -\frac{h^2}{12}\left(\frac{dp}{dz}\right)\left[\frac{(1-\bar{\alpha})^3}{\mu_1} + \frac{\bar{\alpha}^3}{\mu_2} + \frac{3\bar{\alpha}(1-\bar{\alpha})}{(1-\bar{\alpha})\mu_2 + \bar{\alpha}\mu_1}\right] . \qquad (14)$$

3.3 Relative Velocity, v_r

The relative velocity, v_r, is defined as the difference between the average velocity for phase 2 and the average velocity for phase 1; i.e.

$$v_r \equiv \bar{v}_2 - \bar{v}_1 . \qquad (15)$$

Substitution for $\bar{v}_2$ and $\bar{v}_1$ defined in equations (7) and (8) into equation (15) gives

$$v_r = -\frac{h^2}{6}k\left[\frac{\bar{\alpha}^2}{\mu_2} - \frac{(1-\bar{\alpha})^2}{\mu_1}\right] \qquad (16)$$

or substituting for k from equation (6), v_r becomes

$$v_r = -\frac{h^2}{12}\left(\frac{dp}{dz}\right)\left[\frac{\bar{\alpha}^2}{\mu_2}-\frac{(1-\bar{\alpha})^2}{\mu_1}\right] \quad . \tag{17}$$

3.4 Velocity for the Center of Mass, v_m

Zuber and Dougherty [34] have shown that the velocity for the baricenter or the center of mass can be computed by

$$v_m \equiv j-\bar{\alpha}(1-\bar{\alpha})\left[\frac{\rho_1-\rho_2}{\rho_m}\right]v_r \tag{18}$$

Therefore, the defining equation for v_m becomes

$$\rho_m v_m \equiv -\frac{h^2}{12}\left(\frac{dp}{dz}\right)\left[\frac{(1-\bar{\alpha})^3}{\nu_1}+\frac{\bar{\alpha}^3}{\nu_2}+\frac{3\bar{\alpha}(1-\bar{\alpha})\rho_m}{(1-\bar{\alpha})\mu_2+\bar{\alpha}\mu_1}\right] \tag{19}$$

after substituting equations (14) and (17) into equation (18).

Notice that in equation (19) the expression inside the brackets must have the units of a kinematic viscosity. Hence, one can define the mixture kinematic viscosity based on the diffusion model, ν_m, as

$$\frac{1}{\nu_m} \equiv \frac{(1-\bar{\alpha})^3}{\nu_1}+\frac{\bar{\alpha}^3}{\nu_2}+\frac{3\bar{\alpha}(1-\bar{\alpha})\rho_m}{(1-\bar{\alpha})\mu_2+\bar{\alpha}\mu_1} \quad . \tag{20}$$

Equation (20) can be expressed as

$$\frac{1}{\nu_m} = \frac{(1-\bar{\alpha})}{\nu_1}+\frac{\bar{\alpha}}{\nu_2}+I\{\bar{\alpha},\ \text{properties}\} \tag{21}$$

where the function, I, which accounts for the interaction between the two phases, becomes

$$I \equiv -\bar{\alpha}(1-\bar{\alpha})\left[\frac{\mu_2-\mu_1}{(1-\bar{\alpha})\mu_2+\bar{\alpha}\mu_1}\right]\left\{\frac{(1-\bar{\alpha})(2-\bar{\alpha})}{\nu_1}-\frac{\bar{\alpha}(1+\bar{\alpha})}{\nu_2}\right\} - \frac{\bar{\alpha}(1-\bar{\alpha})(2\bar{\alpha}-1)(\rho_1-\rho_2)}{(1-\bar{\alpha})\mu_2+\bar{\alpha}\mu_1} \quad . \tag{22}$$

The absolute mixture viscosity, μ_m, can then be computed from

$$\mu_m \equiv \rho_m \nu_m \tag{23}$$

where the mixture density, ρ_m, is defined as

$$\rho_m \equiv (1-\bar{\alpha})\rho_1+\bar{\alpha}\rho_2 \quad . \tag{24}$$

From an electrical analog, the kinematic mixture viscosity defined in equations (21) and (22) can be thought of as the sum of two "resistances" acting in parallel (i.e. $\frac{(1-\bar{\alpha})}{\nu_1}$ and $\frac{\bar{\alpha}}{\nu_2}$) plus an interaction term, I, due to both "resistances." It is important to note that in all other expressions for the mixture viscosity [1,2,7,9,12,16,18,22,24, 25,26] this interaction term has not been included. It is readily seen in equation (22) that the interaction expression is negligible whenever the void fraction, $\bar{\alpha}$, is very close to zero or one, and whenever the difference between the absolute viscosities of the two fluids is small. All other cases must be determined from experiment.

3.5 Moody Friction Factor, f_M

By considering a force balance on the flow system, one can always write

$$A_c \Delta p \equiv \tau_\omega P_\omega L \tag{25}$$

or

$$\tau_\omega \equiv \left(\frac{\Delta p}{L}\right)\left(\frac{A_c}{P_\omega}\right) \tag{26}$$

where P_ω is the wetted perimeter. By definition, the wall shear stress, τ_ω, can be expressed in terms of the Moody friction factor, f_M, as

$$\tau_\omega \equiv \frac{f_M}{8}\rho_m v_m^{\;2} \quad . \tag{27}$$

Substitution of equation (27) into equation (26) gives

$$f_M = \frac{8}{\rho_m v_m^{\;2}}\left(\frac{\Delta p}{L}\right)\left(\frac{A_c}{P_\omega}\right) \quad . \tag{28}$$

Rewriting equation (19) as

$$\rho_m v_m \nu_m = \frac{h^2}{12}\left(-\frac{dp}{dz}\right) \equiv \frac{h^2}{12}\left(\frac{\Delta p}{L}\right) \tag{29}$$

and substituting equation (29) into equation (28), one gets

$$f_M = \frac{96}{h^2}\left(\frac{A_c}{P_\omega}\right)\frac{\nu_m}{v_m} \quad . \tag{30}$$

Multiplication of the RHS of equation (30) by one (i.e. D_H/D_H, where D_H is the hydraulic diameter defined to be equal four times the cross-sectional area divided by the wetted perimeter) results in the following expression:

$$f_M = \frac{384}{h^2}\left(\frac{A_c}{P_\omega}\right)^2\frac{1}{Re_H} \quad . \tag{31}$$

From Figure 3, one can write

$$A_c = bh, \; P_\omega = 2b \tag{32}$$

and substituting equation (32) into equation (31) gives the following expression for the two-phase Moody friction factor, f_M,:

$$f_M = 96/Re_H \tag{33}$$

where the mixture Reynolds number based on the hydraulic diameter, Re_H, is defined as

$$Re_H \equiv \frac{v_m D_H}{\nu_m} . \tag{34}$$

Notice that equation (33) is identical to the equation used for the case of single-phase flow through wide, horizontal parallel plates when correlating the single-phase friction factor with the fluid Reynolds number. Thus, by appropriately defining the two-phase mixture kinematic viscosity as in equation (16), the two-phase flow problem reduces to a "pseudo-homogeneous" flow with constant properties.

3.6 Void Fraction Correlation

Recalling the definition of j_1 and j_2 in equations (11) and (12), respectively, one can form the ratio, j_2/j_1; i.e.

$$\frac{j_2}{j_1} = \frac{Q_2/A_c}{Q_1/A_c} = \frac{Q_2}{Q_1} = \frac{\bar{\alpha}^2\left[\frac{\bar{\alpha}}{3\mu_2} + \frac{(1-\bar{\alpha})}{(1-\bar{\alpha})\mu_2+\bar{\alpha}\mu_1}\right]}{(1-\bar{\alpha})^2\left[\frac{(1-\alpha)}{3\mu_1} + \frac{\alpha}{(1-\bar{\alpha})\mu_2+\bar{\alpha}\mu_1}\right]} \tag{35}$$

or, in terms of the "slip", $\bar{v}_2/\bar{v}_1$, one obtains

$$S \equiv \frac{\bar{v}_2}{\bar{v}_1} = \frac{j_2/\bar{\alpha}}{j_1/(1-\bar{\alpha})} = \frac{\bar{\alpha}[\frac{\bar{\alpha}}{3\mu_2} + \frac{(1-\bar{\alpha})}{(1-\bar{\alpha})\mu_2+\bar{\alpha}\mu_1}]}{(1-\bar{\alpha})[\frac{(1-\bar{\alpha})}{3\mu_1}+\frac{\bar{\alpha}}{(1-\bar{\alpha})\mu_2+\bar{\alpha}\mu_1}]} \tag{36}$$

or, in terms of the "flowing" volumetric concentration, β, one gets the following expression:

$$\beta \equiv \frac{Q_2}{Q_1+Q_2} = \frac{j_2}{j_1+j_2} = \frac{\bar{\alpha}^2[\frac{\bar{\alpha}}{3\mu_2}+\frac{(1-\bar{\alpha})}{(1-\bar{\alpha})\mu_2+\bar{\alpha}\mu_1}]}{\frac{(1-\bar{\alpha})^3}{3\mu_1}+\frac{\bar{\alpha}^3}{3\mu_2}+\frac{\bar{\alpha}(1-\bar{\alpha})}{(1-\bar{\alpha})\mu_2+\bar{\alpha}\mu_1}} \; . \tag{37}$$

After algebraically manipulating equations (35), (36), and (37), an expression of the following form can be obtained:

$$A_0+A_1\bar{\alpha}+A_2\bar{\alpha}^2+A_3\bar{\alpha}^3+A_4\bar{\alpha}^4 \equiv 0 \tag{38}$$

where the coefficients, A_i's, are given in equations (39), (40), and (41) corresponding to the previous three different ratios, j_2/j_1, $\bar{v}_2/\bar{v}_1$; and β. They are:

$$\begin{aligned} A_0 &= (\frac{\mu_2}{\mu_1})^2(\frac{Q_2}{Q_1}) \\ A_1 &= -\;4(\frac{\mu_2}{\mu_1})[\frac{\mu_2}{\mu_1}-1](\frac{Q_2}{Q_1}) \end{aligned} \tag{39}$$

$$A_2 = \{3(\frac{\mu_2}{\mu_1})[2(\frac{\mu_2}{\mu_1})(\frac{Q_2}{Q_1})-1]-9(\frac{\mu_2}{\mu_1})(\frac{Q_2}{Q_1})\}$$

$$A_3 = -\{2(\frac{\mu_2}{\mu_1})[2(\frac{\mu_2}{\mu_1})(\frac{Q_2}{Q_1})-1]-6(\frac{\mu_2}{\mu_1})(\frac{Q_2}{Q_1})\} \tag{39}$$

$$A_4 = (\frac{\mu_2}{\mu_1}-1)\{(\frac{\mu_2}{\mu_1})(\frac{Q_2}{Q_1})+1\}$$

$$A_0 = (\frac{\mu_2}{\mu_1})S$$

$$A_1 = \{S[4-3(\frac{\mu_2}{\mu_1})]+3\}$$

$$A_2 = \{S[3(\frac{\mu_2}{\mu_1})-5]+2\} \tag{40}$$

$$A_3 = \{1+S[1-(\frac{\mu_2}{\mu_1})]-\frac{\mu_1}{\mu_2}\}$$

$$A_4 = 0$$

$$A_0 = \frac{1}{3}\beta(\frac{\mu_2}{\mu_1})$$

$$A_1 = -\{\frac{2}{3}\beta[(\frac{\mu_2}{\mu_1})-2]\}$$

$$A_2 = (2\beta-1) \tag{41}$$

$$A_3 = -\{2\beta(\frac{\mu_2}{\mu_1})-\frac{1}{3}(\beta+8)\}$$

$$A_4 = \{\beta(\frac{\mu_2}{\mu_1}) + (\beta-1)(\frac{\mu_1}{\mu_2}) + \frac{1}{3}(2-\beta)$$

It is clearly seen from equations (39), (40), and (41) that the void fraction, $\bar{\alpha}$, can be computed solely from the input volumetric flow rates for each phase and their respective properties. The void fraction does <u>not</u> depend on a knowledge of the pressure drop. Therefore, the "triangular" relationship as claimed by Hewitt [17] does not exist!

CHAPTER IV

STRATIFIED, LAMINAR FLOW THROUGH HORIZONTAL, RECTANGULAR DUCTS

4.1 General

The two-phase frictional pressure drop for stratified, laminar flow through horizontal, rectangular ducts will be analyzed analytically and then tested with the available experimental data. The flow model is depicted in Figure 4. The exact analytical solution for the velocity distribution for each phase and their subsequent volume flow rates have been derived by Charles and Lilleleht [5] and Yu [33]. It should be noted that the Fourier coefficients A^*_{in} and B^*_{in} in Yu's analysis are incorrectly printed.

4.2 Velocity for the Center of Mass, v_m

The theoretical volume flow rates for phase 1 and phase 2, respectively, have been derived by [5] and are presented in Appendix A, equations (35) and (36). They are:

$$Q_1 = \frac{128a^4}{\pi^5} \sum_{i=o}^{\infty} \left(\frac{1}{2i+1}\right)^5 [A_1'(n)\{1-ch(nb_1)\}+B_1'(n)sh(nb_1)] - \frac{2}{3}k_1 a^3 b_1 \tag{1}$$

and

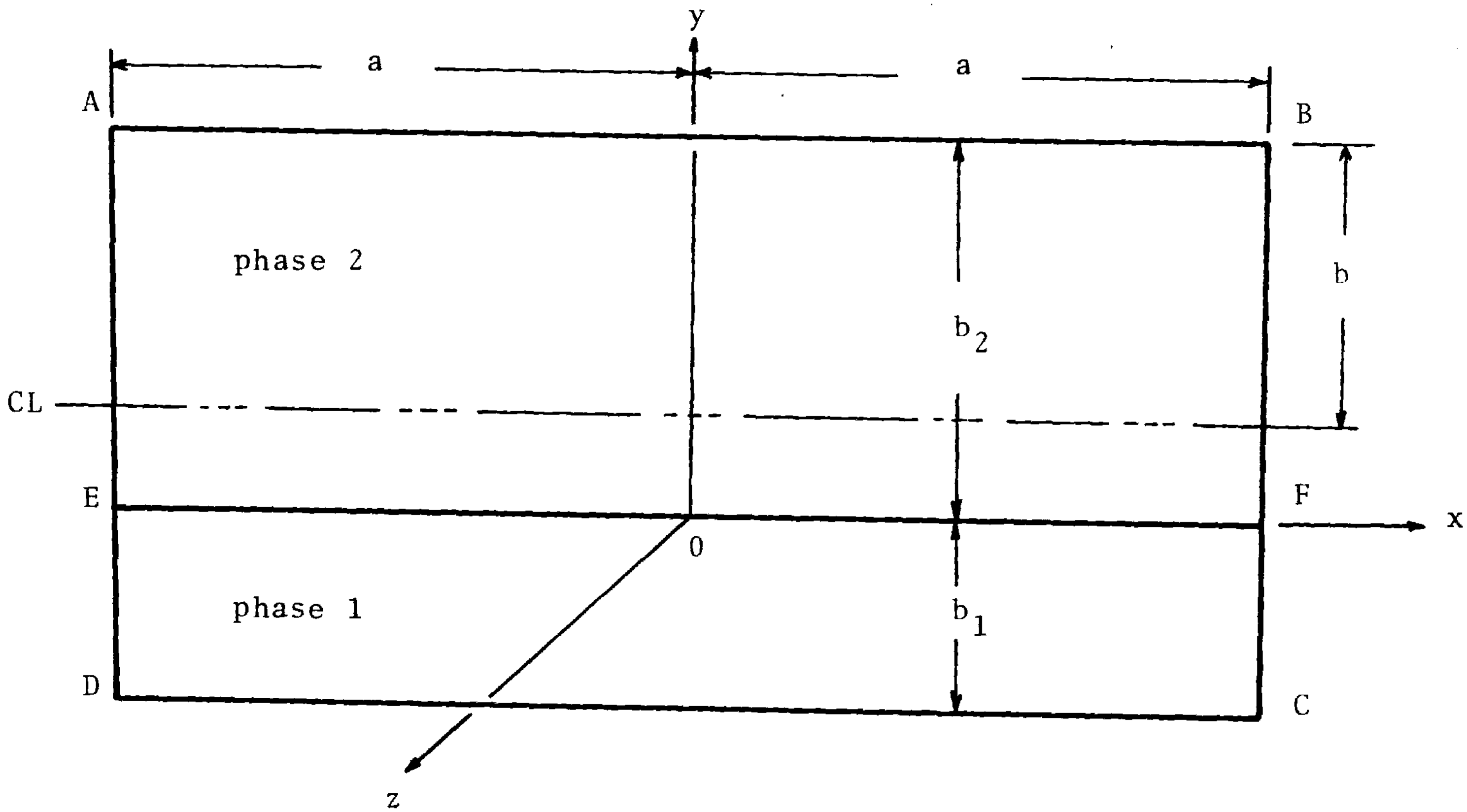

Figure 4. Separated Flow Model for Horizontal, Rectangular Ducts

$$Q_2 = \frac{128a^4}{\pi^5} \sum_{i=o}^{\infty} \left(\frac{1}{2i+1}\right)^5 [A_2'(n)\{ch(nb_2)-1\}+B_2'(n)sh(nb_2)] \tag{2}$$
$$- \frac{2}{3}k_2a^3b_2 \ .$$

Equations (1) and (2) can be rewritten as

$$Q_1 = -\frac{2}{3}k_1ab^3\{(\frac{a}{b})^2 2(1-\bar{\alpha})-\frac{6}{a^2b^3}\sum_n^{\infty}[\frac{1}{n^5}\frac{f_1(n)}{k_1}]\} \tag{3}$$

and

$$Q_2 = -\frac{2}{3}k_2ab^3\{(\frac{a}{b})^2 2\bar{\alpha}-\frac{6}{a^2b^3}\sum_n^{\infty}[\frac{1}{n^5}\frac{f_2(n)}{k_2}]\} \tag{4}$$

where the functions $f_1(n)$ and $f_2(n)$ are defined to be

$$f_1(n) \equiv A_1'(n)\{1-ch(nb_1)\}+B_1'(n)sh(nb_1) \tag{5}$$

and

$$f_2(n) \equiv A_2'(n)[ch(nb_2)-1]+B_2'(n)sh(nb_2) \ . \tag{6}$$

The functions $A_1'(n)$, $A_2'(n)$, $B_1'(n)$, and $B_2'(n)$ are defined in Appendix A, equations (26), (27), (28), and (29), respectively.

From Figure 4, one can write

$$b_1 = 2b(1-\bar{\alpha}), \; b_2 = 2b\bar{\alpha} \tag{7}$$

and dividing the expressions defined in equations (1) and (2) by the cross-sectional area, A_c, which is equal to 4ab, one gets the superficial velocities for phase 1 and phase 2, respectively, as

$$j_1 \equiv \frac{Q_1}{A_c} = -\frac{1}{3}k_1 b^2\{(\frac{a}{b})^2(1-\bar{\alpha})-\frac{3}{a^2b^3}\sum_n^\infty \frac{1}{n^5}f_1(n)\} \tag{8}$$

and

$$j_2 \equiv \frac{Q_2}{A_c} = -\frac{1}{3}k_2 b^2\{(\frac{a}{b})^2\bar{\alpha}-\frac{3}{a^2b^3}\sum_n^\infty \frac{1}{n^5}f_2(n)\} \quad . \tag{9}$$

The defining equation for the velocity for the center of mass can be obtained from

$$G \equiv \rho_m v_m = G_1+G_2 = \rho_1 j_1+\rho_2 j_2 \quad . \tag{10}$$

Thus, after substitution of equations (8) and (9) into equation (10), one obtains

$$\rho_m v_m = -\frac{1}{3}g_c(\frac{dp}{dz})b^2[\frac{F_1'}{\nu_1}+\frac{F_2'}{\nu_2}] \tag{11}$$

where the functions F_1' and F_2' are defined to be

$$F_1' \equiv \left(\frac{a}{b}\right)^2(1-\overline{\alpha})-\frac{3}{a^2b^3}\sum_n^{\infty}\frac{1}{n^5}f_1(n) \tag{12}$$

and

$$F_2' \equiv \left(\frac{a}{b}\right)^2\overline{\alpha}-\frac{3}{a^2b^3}\sum_n^{\infty}\frac{1}{n^5}f_2(n) \quad . \tag{13}$$

From equations (12) and (13) it is seen that the functions F_1' and F_2' depend on both the void fraction, $\overline{\alpha}$, and the aspect ratio, a/b. The author chooses to express the functions defined in equations (12) and (13) as

$$F_1' = F\,F_1 \tag{14}$$

and

$$F_2' = F\,F_2 \tag{15}$$

where the function F (see Appendix A, equation (31)) is defined to be

$$F \equiv 1 - \frac{192b}{\pi^5 a}\sum_{n=1,3,5\ldots}^{\infty}\left[\frac{1}{n^5}\tanh\left(\frac{n\pi a}{2b}\right)\right] \quad . \tag{16}$$

Now, rewriting equation (11) as

$$\rho_m v_m = -\frac{1}{3} g_c \left(\frac{dp}{dz}\right) F b^2 \left[\frac{F_1}{\nu_1} + \frac{F_2}{\nu_2}\right] \tag{17}$$

one can choose to define the mixture kinematic viscosity for the two-phase flow through horizontal, rectangular ducts as

$$\frac{1}{\nu_m} \equiv \frac{F_1}{\nu_1} + \frac{F_2}{\nu_2} \quad . \tag{18}$$

Equation (18) is in a deceivingly compact form, and it appears as though no interaction term results similar to that obtained in Chapter III for the case of flow through horizontal parallel plates. However, this is not the case. An expression for the mixture kinematic viscosity, ν_m, can be obtained after some lengthy algebraic manipulations in a form similar to the one for parallel plates. The result is

$$\frac{1}{\nu_m} = \frac{1-\bar{\alpha}}{\nu_1} + \frac{\bar{\alpha}}{\nu_2} - \frac{3}{a^4 b}\left(\frac{1}{\rho_m}\right) \sum_n^{\infty} \left(\frac{1}{n^5}\left[\frac{f_1}{\nu_1} + \frac{f_2}{\nu_2}\right]\right) \quad . \tag{19}$$

As before, the mixture kinematic viscosity can be thought of as the sum of two "resistances" acting in parallel plus an interaction term.

4.3 Moody Friction Factor, f_M

Recall from Chapter III, equation (28) that the Moody friction factor is defined as

$$f_M \equiv \frac{8}{\rho_m v_m^2}\left(\frac{\Delta p}{L}\right)\left(\frac{A_c}{P_\omega}\right) \quad . \tag{20}$$

Rewriting equation (17) as

$$\left(-g_c\frac{dp}{dz}\right) = \frac{3\rho_m v_m \nu_m}{F\ b^2} \equiv \frac{\Delta p}{L} \tag{21}$$

and substituting equation (21) into equation (20) results in

$$f_M = \frac{24}{F}\left(\frac{1}{b^2}\right)\left(\frac{A_c}{P_\omega}\right)\frac{\nu_m}{v_m} \quad . \tag{22}$$

Similarly, by multiplying the RHS of equation (22) by one (i.e. D_H/D_H) and simplifying, one obtains f_M as

$$f_M = \frac{96}{F}\left(\frac{A_c}{P_\omega}\right)^2\left(\frac{1}{b^2}\right)\frac{1}{Re_H} \tag{23}$$

where the mixture Reynolds number based on the hydraulic diameter, Re_H, is

$$Re_H \equiv \frac{v_m D_H}{\nu_m} \quad . \tag{24}$$

Now, from Figure 4, one can write

$$A_c = 4ab,\ P_\omega = 4(a+b) \tag{25}$$

and substitution of equation (25) into equation (23) gives

$$f_M = \frac{96}{F}\left[\frac{(\frac{a}{b})}{1+(\frac{a}{b})}\right]^2 \frac{1}{Re_H} \tag{26}$$

where a/b is the aspect ratio. Equation (26) will be checked with experimental data in Section 4.5.

4.4 Void Fraction Correlation

Due to the nature of the expressions defined in equations (1) and (2), one cannot explicitly solve for the void fraction, $\bar{\alpha}$, by forming any of the ratios (j_2/j_1), $(\bar{v}_2/\bar{v}_1)$, or β. Although the problem is complicated by the fact that the volume flow rates for each phase are dependent on the system geometry and the void fraction, the infinite series in equations (1) and (2) are in no way a deterrent to the practical use of these theoretical expressions. These series converge very rapidly; hence, only 4-10 terms were needed to obtain an answer accurate to within 1/10,000th absolute error. All machine computations were done on the UNIVAC 1108 at the Rich Computer Center on the Georgia Tech campus.

One simple but effective method which was used by the author for predicting the void fraction is described here.

The functions F_1 and F_2 are computed as a function of the void fraction, $\bar{\alpha}$, for a particular aspect ratio, a/b, and for constant fluid properties. The void fraction is incremented in steps of 0.05 covering the range from zero to one. Then, the ratio β, which is the "flowing" volumetric concentration defined to be equal to $Q_2/(Q_1+Q_2)$, is formed for each void fraction from zero to one. Thus, β becomes

$$\beta(\alpha) \equiv \frac{Q_2}{Q_1+Q_2} = \frac{F_2/\mu_2}{F_1/\mu_1+F_2/\mu_2} \tag{27}$$

or rearranging, one gets

$$\beta(\alpha) = \frac{F_2(\alpha)}{(\frac{\mu_2}{\mu_1})F_1(\alpha)+F_2(\alpha)} \quad . \tag{28}$$

Therefore, for any selected aspect ratio, a/b, and constant viscosity ratio, (μ_2/μ_1), the void fraction, $\bar{\alpha}$, can be determined from equation (28) by knowing the input volume flow rates for each phase and then computing the "flowing" volumetric concentration, β. It does not require a knowledge of the pressure drop; therefore, as before, the "triangular" relationship claimed by Hewitt does not exist!

The author has chosen to correlate $\bar{\alpha}$ versus β because upon inspection of the ratio F_2/F_1 (or F_1/F_2), one can easily see that its value ranges from zero to infinity (or infinity to zero). This is not a physically appealing nor a convenient range over which to interpolate any function. The increment on the void fraction of 0.05 is small enough so that interpolation using equation (28) is good to four decimal places.

4.5 Experimental Verification

A search through the two-phase literature for complete sets of experimental data subject to the earlier assumptions of Section 4.1 yielded only the one data set of Hao-Sheng Yu [33] with which to test the validity of this analysis.

Yu performed experiments with a light paraffin oil and water in a 25 foot long rectangular duct of a/b = 2.0. Measurements were made on the local pressure, interface shape, flow rates, and fluid temperatures. With this data, the Moody friction factor defined in equation (20) was plotted versus the two-phase mixture Reynolds number defined in equation (24). The result is shown in Figure 5. The solid line in this figure is the theoretical result predicted by equation (23); that is,

$$f_M \cong 62.19213\ Re_H^{-1} \qquad (29)$$

where the function F is equal to 0.68605 for an a/b = 2.0.

As before, notice that equation (29) is identical to

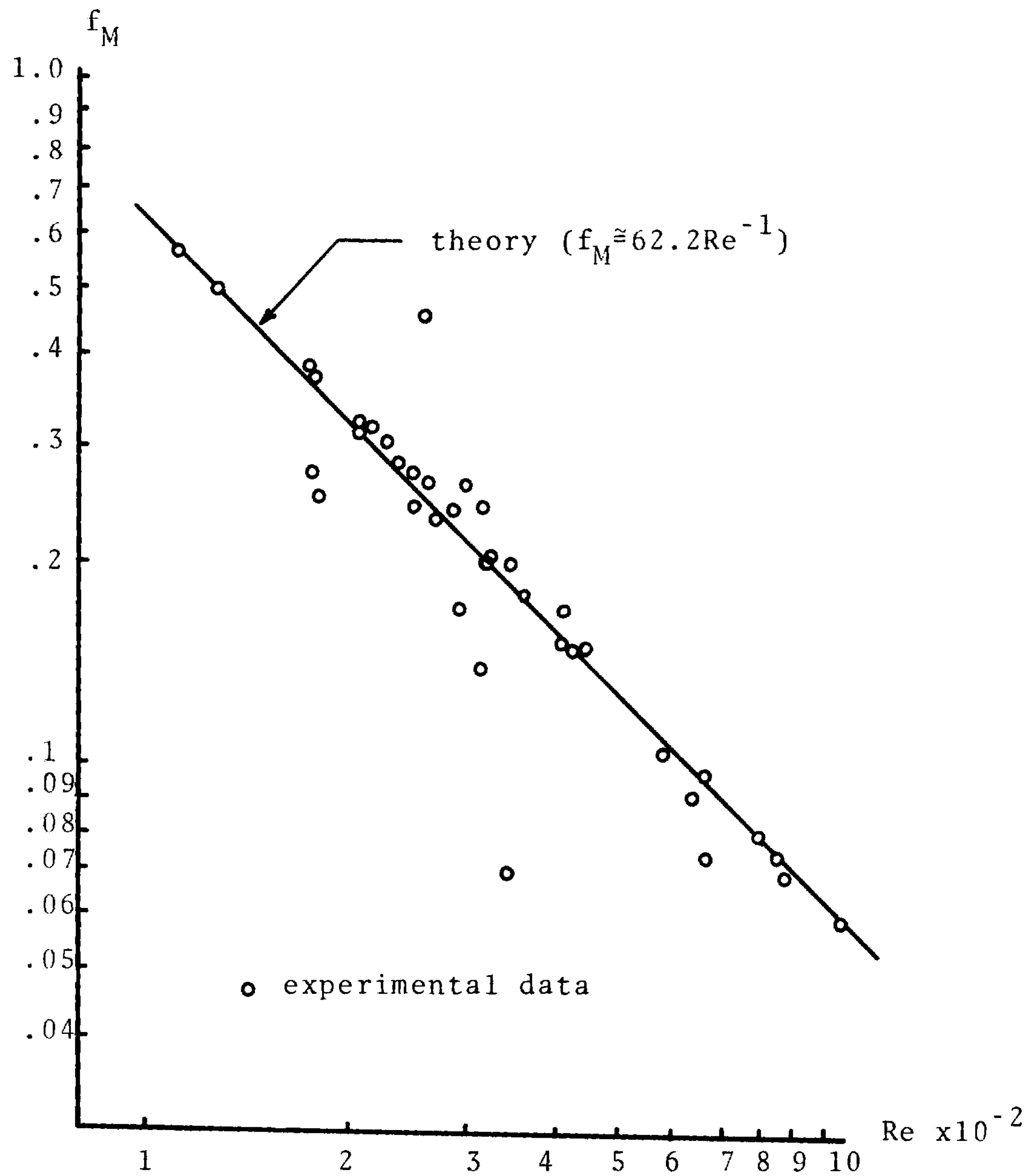

Figure 5. Two-Phase Moody Friction Factor versus Mixture Reynolds Number for Horizontal, Rectangular Ducts of a/b = 2.0

the single-phase expression for predicting the friction factor as a function of the Reynolds number. Thus, by appropriately defining the two-phase mixture kinematic viscosity in equation (18), the two-phase flow problem reduces to a "pseudo-homogeneous" single-phase flow one.

Figure 6 is a plot of the predicted void fraction, $\bar{\alpha}$, versus the "flowing" volumetric concentration, β, defined in equation (28) for an a/b = 2.0 by the author's theory (solid line) and by the Lockhart-Martinelli correlation (dotted line). Notice that the experimental data are in excellent agreement with the author's theory.

Figure 7 is a plot of the two-phase Moody friction factor, f_M, versus the mixture Reynolds number using the author's theoretical value for $\bar{\alpha}$ from Figure 6 to evaluate the kinematic mixture viscosity, ν_m, instead of Yu's experimentally determined value. Notice that the resulting pressure drop correlation in Figure 7 is better than the one in Figure 6.

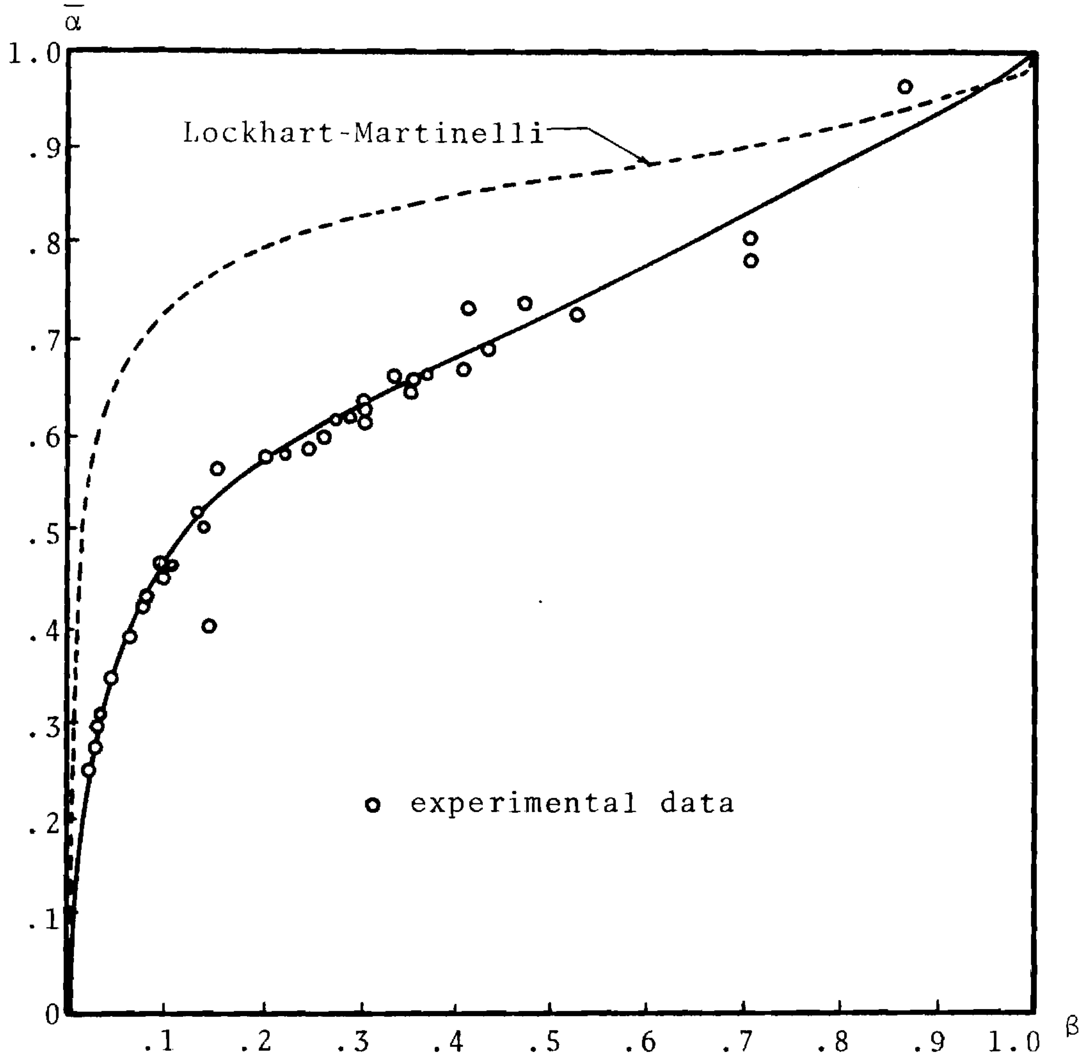

Figure 6. Void Fraction versus "Flowing" Volumetric Concentration for Horizontal, Rectangular Ducts of a/b = 2.0 and (μ_2/μ_1) = 28.8

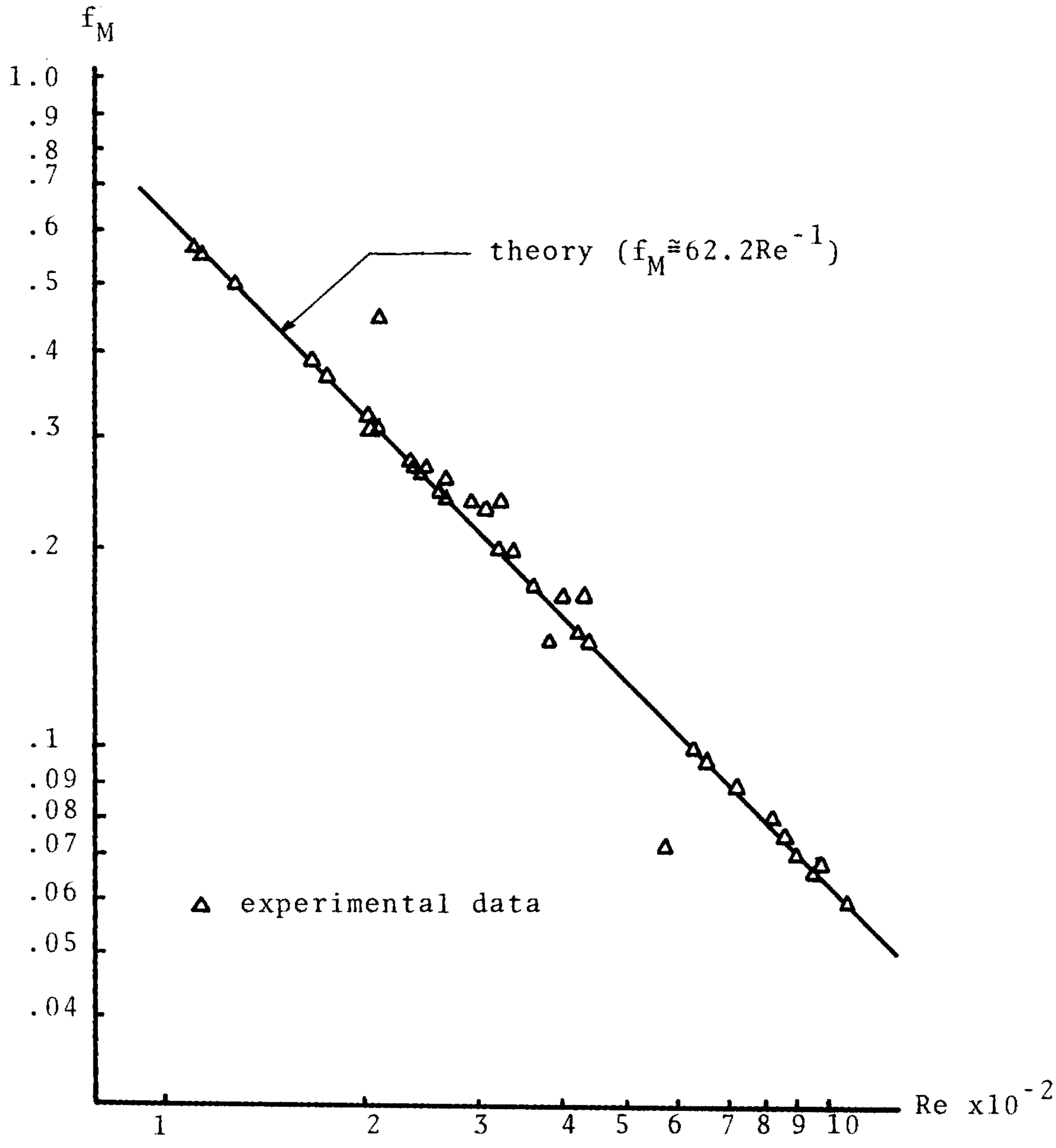

Figure 7. Two-Phase Moody Friction Factor versus Mixture Reynolds Number for Horizontal, Rectangular Ducts of a/b = 2.0 with a Theoretical Value for $\bar{\alpha}$

CHAPTER V

STRATIFIED, LAMINAR FLOW THROUGH HORIZONTAL, CIRCULAR PIPES

5.1 General

The two-phase frictional pressure drop for stratified, laminar flow through horizontal, circular pipes will be analyzed analytically and then tested with the available experimental data. The flow model is shown in Figure 8. The exact analytical solution for the velocity distribution for the two phases and their corresponding volume flow rates has been derived by Mamaev et al. [22]. Their analysis is presented in Appendix B for reference.

5.2 Velocity for the Center of Volume, j

The theoretical volume flow rates for the two phases have been derived by [22] and are presented in Appendix B, equations (54) and (55). They are

$$Q_1 = -\frac{\pi R^4}{8\mu_1}\left(\frac{dp}{dz}\right)F_1 \tag{1}$$

and

$$Q_2 = -\frac{\pi R^4}{8\mu_2}\left(\frac{dp}{dz}\right)F_2 \tag{2}$$

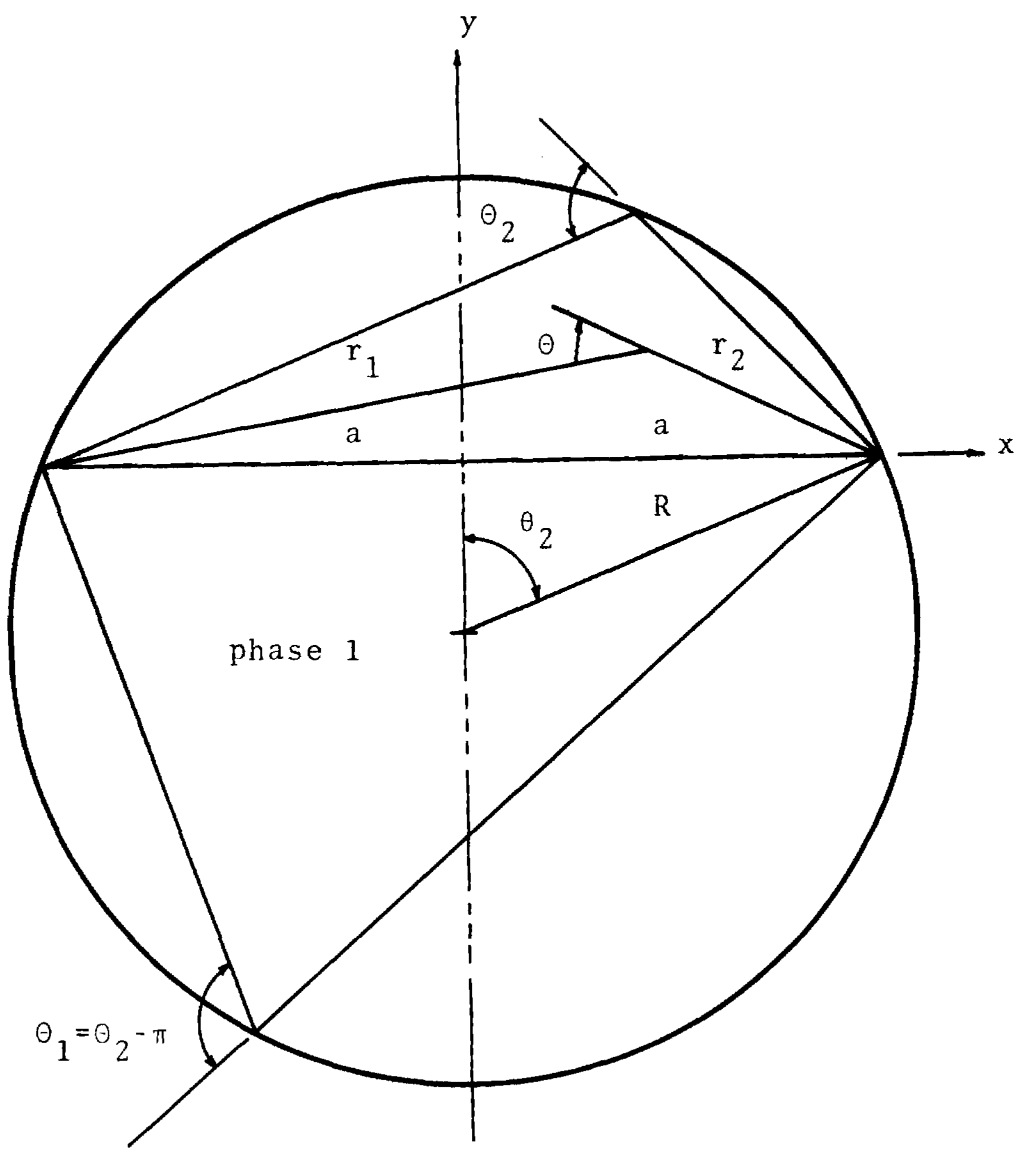

Figure 8. Separated Flow Model for Horizontal, Circular Pipes

where the functions F_1 and F_2, defined in Appendix B, equations (56) and (57), are

$$F_1 \equiv -\frac{1}{\pi}\{\Theta_1-\frac{1}{6}(3+2\sin^2\Theta_2)\sin2\Theta_2\}-2\sin^4\Theta_2 \times$$
$$\times \int_o^\infty [ctg\Theta_1 sh(m\Theta_1)-mch(m\Theta_1)]\frac{mA_1(m)}{sh(m\pi)}dm \tag{3}$$

and

$$F_2 \equiv \frac{1}{\pi}\{\Theta_2-\frac{1}{6}(3+2\sin^2\Theta_2)\sin2\Theta_2\}+2\sin^4\Theta_2 \times$$
$$\times \int_o^\infty [ctg\Theta_2 ch(m\Theta_2)-msh(m\Theta_2)]\frac{mA_2(m)}{sh(m\pi)}dm \quad . \tag{4}$$

The functions $A_1(m)$ and $A_2(m)$, also defined in Appendix B, equations (36) and (37), are

$$A_1(m) = \frac{8}{sh(m\pi)}[\frac{mch(m\Theta_2)(\dot{\mu}_2-\dot{k}_2)-ctg\Theta_2 sh(m\Theta_2)(1-\dot{k}_2)}{(1-\dot{\mu}_2)sh[m(\pi-2\Theta_2)]-(1+\dot{\mu}_2)sh(m\pi)}] \tag{5}$$

and

$$A_2(m) = \frac{8}{sh(m\pi)}[\frac{mch(m\Theta_1)(\dot{k}_1-\dot{\mu}_1)-ctg\Theta_2 sh(m\Theta_1)(\dot{k}_1-1)}{(\dot{\mu}_1-1)sh(m(\pi-2\Theta_2)]-(1+\dot{\mu}_1)sh(m\pi)}] \quad . \tag{6}$$

Adding equations (1) and (2) and then dividing by the cross-sectional area, A_c, gives an expression for the velocity for the center of volume, j, as

$$j = j_1+j_2 = \frac{Q_1+Q_2}{A_c} = -\frac{R^2(\frac{dp}{dz})}{8}\{\frac{1-\bar{\alpha}}{\mu_1}+\frac{\bar{\alpha}}{\mu_2}+\frac{\sin^2\Theta_2\sin 2\Theta_2}{3\pi}(\frac{1}{\mu_1}-\frac{1}{\mu_2}) + + (\frac{I_1}{\mu_1}+\frac{I_2}{\mu_2})\} \tag{7}$$

where the integral terms, I_1 and I_2, are defined to be

$$I_1 \equiv -2\sin^4\Theta_2 \int_o^\infty [ctg\Theta_1 sh(m\Theta_1)-mch(m\Theta_1)]\frac{mA_1(m)}{sh(m\pi)}dm \tag{8}$$

and

$$I_2 \equiv 2\sin^4\Theta_2 \int_o^\infty [ctg\Theta_2 ch(m\Theta_2)-msh(m\Theta_2)]\frac{mA_2(m)}{sh(m\pi)}dm \;. \tag{9}$$

Rewriting j in terms of the functions F_1 and F_2, one obtains

$$j = -\frac{R^2(\frac{dp}{dz})}{8}[\frac{F_1}{\mu_1}+\frac{F_2}{\mu_2}] \;. \tag{10}$$

5.3 Relative Velocity, v_r

The average velocity for each phase can be computed as

$$\bar{v}_1 \equiv \frac{Q_1}{A_1} = -\frac{R^2(\frac{dp}{dz})}{8\mu_1}[1+\frac{\sin^2\Theta_2 \sin 2\Theta_2}{3\pi(1-\bar{\alpha})}+\frac{I_1}{(1-\bar{\alpha})}] \tag{11}$$

and

$$\bar{v}_2 \equiv \frac{Q_2}{A_2} = -\frac{R^2(\frac{dp}{dz})}{8\mu_2}[1-\frac{\sin^2\Theta_2 \sin 2\Theta_2}{3\pi\bar{\alpha}}+\frac{I_2}{\bar{\alpha}}] \tag{12}$$

or expressing the average velocities in terms of F_1 and F_2, one can obtain

$$\bar{v}_1 = -\frac{R^2(\frac{dp}{dz})}{8\mu_1}\,\frac{F_1}{(1-\bar{\alpha})} \tag{13}$$

and

$$\bar{v}_2 = -\frac{R^2(\frac{dp}{dz})}{8\mu_2}\,\frac{F_2}{\bar{\alpha}}\ . \tag{14}$$

Thus, the relative velocity, v_r, is obtained by subtracting equation (12) from equation (11); i.e.

$$v_r \equiv \bar{v}_2-\bar{v}_1 = -\frac{R^2(\frac{dp}{dz})}{8}[\frac{1}{\mu_2}-\frac{1}{\mu_1}-\frac{\sin^2\Theta_2 \sin 2\Theta_2}{3\pi}(\frac{1}{(1-\bar{\alpha})\mu_1}+\frac{1}{\bar{\alpha}\mu_2}) + \frac{I_2}{\bar{\alpha}\mu_2}-\frac{I_1}{(1-\bar{\alpha})\mu_1} \tag{15}$$

or using the definitions in equations (13) and (14), one gets

$$\bar{v}_r = -\frac{R^2(\frac{dp}{dz})}{8}\left[\frac{F_2}{\bar{\alpha}\mu_2}-\frac{F_1}{(1-\bar{\alpha})\mu_1}\right] \quad . \tag{16}$$

5.4 Velocity for the Center of Mass, v_m

As in Chapter III, the defining equation for the velocity for the center of mass, v_m, is

$$v_m \equiv j-\bar{\alpha}(1-\bar{\alpha})(\frac{\rho_1-\rho_2}{\rho_m})v_r \quad . \tag{17}$$

Substitution of equations (7) and (15) into equation (17) results in

$$v_m = -\frac{R^2(\frac{dp}{dz})}{8}(\frac{1}{\rho_m})\left[\frac{1-\bar{\alpha}}{\nu_1}+\frac{\bar{\alpha}}{\nu_2}+\frac{\sin^2\Theta_2\sin2\Theta_2}{3\pi}(\frac{1}{\nu_1}-\frac{1}{\nu_2}) + \right.$$
$$\left. + (\frac{I_1}{\nu_1}+\frac{I_2}{\nu_2})\right] \tag{18}$$

or

$$v_m = -\frac{R^2(\frac{dp}{dz})}{8}(\frac{1}{\rho_m})\left[\frac{F_1}{\nu_1}+\frac{F_2}{\nu_2}\right] \tag{19}$$

after substituting equations (10) and (16) into equation (17).

It is readily seen from equations (18) and (19) that the expression inside the brackets has the units of a kinematic viscosity. Therefore, one can define the two-phase mixture kinematic viscosity, ν_m, as

$$\frac{1}{\nu_m} \equiv \frac{1-\bar{\alpha}}{\nu_1}+\frac{\bar{\alpha}}{\nu_2}+\frac{\sin^2\theta_2\sin2\theta_2}{3\pi}\left(\frac{1}{\nu_1}-\frac{1}{\nu_2}\right)+\left(\frac{I_1}{\nu_1}+\frac{I_2}{\nu_2}\right) \tag{20}$$

or, in terms of the functions F_1 and F_2, as

$$\frac{1}{\nu_m} \equiv \frac{F_1}{\nu_1}+\frac{F_2}{\nu_2} \quad . \tag{21}$$

As with the other two stratified flow cases, the kinematic mixture viscosity can be thought of as the sum of two "resistances" acting in parallel plus an interaction term, I, where this interaction term for horizontal, circular pipes becomes

$$I \equiv \frac{\sin^2\Theta_2\sin2\Theta_2}{3\pi}\left(\frac{1}{\nu_1}-\frac{1}{\nu_2}\right)+\left(\frac{I_1}{\nu_1}+\frac{I_2}{\nu_2}\right) \quad . \tag{22}$$

5.5 Moody Friction Factor, f_M

Recall that the Moody friction factor can be defined as

$$f_M = \frac{8}{\rho_m v_m^2}\left(\frac{\Delta p}{L}\right)\left(\frac{A_c}{P_\omega}\right) \tag{23}$$

or (expressing it in terms of the hydraulic diameter) as

$$f_M = \frac{2}{\rho_m v_m^2}\left(\frac{\Delta p}{L}\right) D_H \quad . \tag{24}$$

Rewriting equation (19) as

$$-\frac{dp}{dz} = \frac{8\rho_m v_m \nu_m}{R^2} \equiv \frac{\Delta p}{L} \tag{25}$$

and substituting equation (24) into equation (23) yields the following expression for f_M:

$$f_M = \frac{16\nu_m D_H}{v_m R^2} = \frac{16\nu_m D_H}{v_m\left(\frac{D^2}{4}\right)} \quad . \tag{26}$$

But, the hydraulic diameter for a circular pipe is identical to the pipe diameter; thus, equation (26) becomes

$$f_M = \frac{64\nu_m}{v_m D} = 64 Re_D^{-1} \quad . \tag{27}$$

This resulting equation is seen to be identical to the equation used in single-phase flow. Therefore, by appropriately defining the two-phase mixture kinematic viscosity, ν_m, once again, the two-phase flow problem reduces to a "pseudo-homogeneous" single-phase problem. The validity of this analysis and equation (27) is checked with experimental data in Section 5.7.

5.6 Void Fraction Correlation

The procedure for predicting the void fraction, $\bar{\alpha}$, in stratified flow through horizontal, circular pipes is the same that was used in Chapter IV. It is not repeated here. This method for predicting the void fraction is tested with experimental data in Section 5.7.

5.7 Experimental Verification

The only available set of experimental data subject to the author's previous assumptions is that of Russell, Hodson, and Govier [28]. Russell et al. performed experiments with a fairly viscous oil and water in a 0.806 inch I.D. horizontal, circular pipe. The Moody friction factor was plotted versus the two-phase mixture Reynolds number. The result is shown in Figure 9. The solid line in this figure is the theoretical result predicted by equation (27). The limited experimental data are in fair agreement with the author's theory.

Figure 10 is a plot of the predicted void fraction

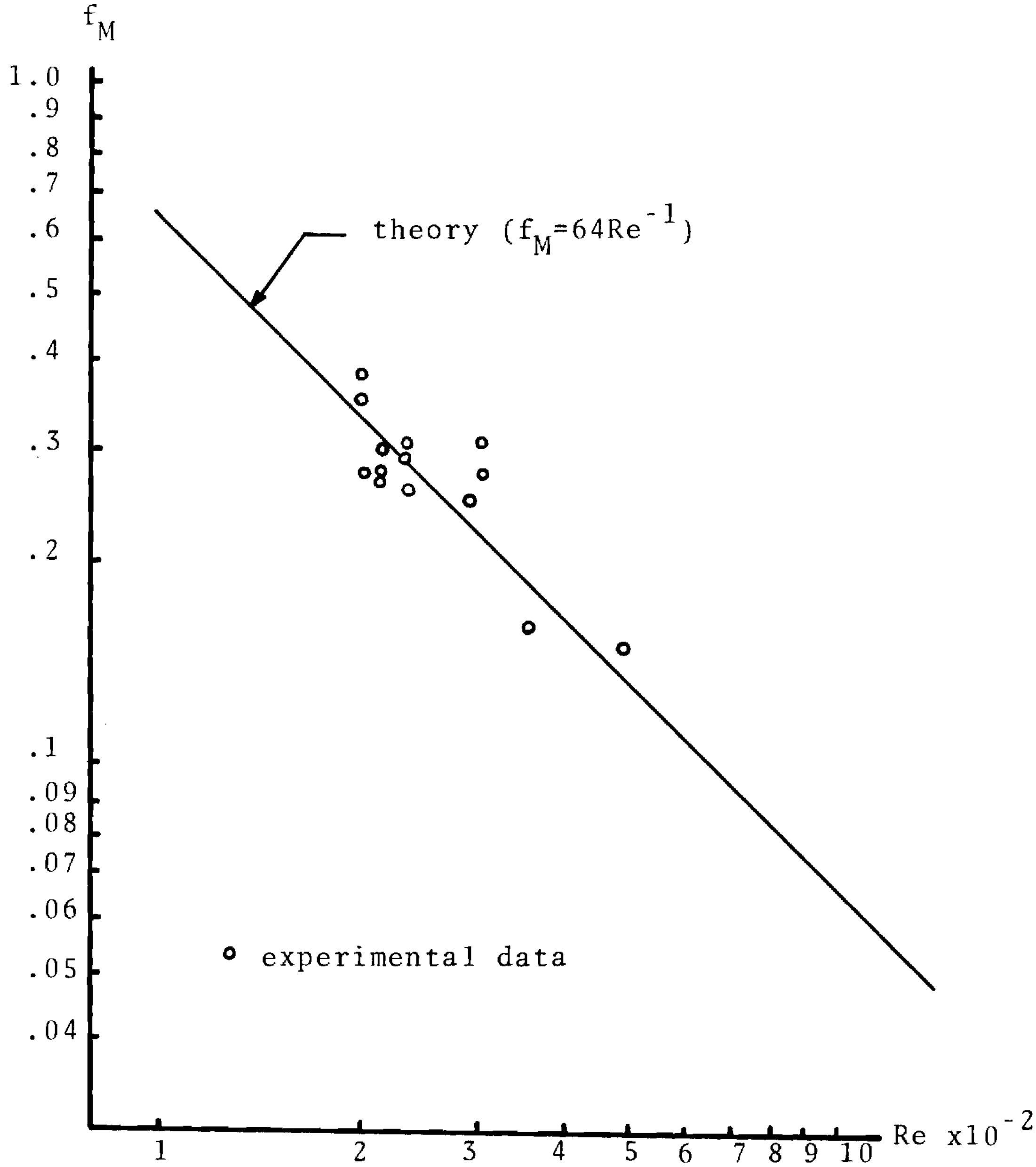

Figure 9. Two-Phase Moody Friction Factor versus Mixture Reynolds Number for Horizontal, Circular Pipes

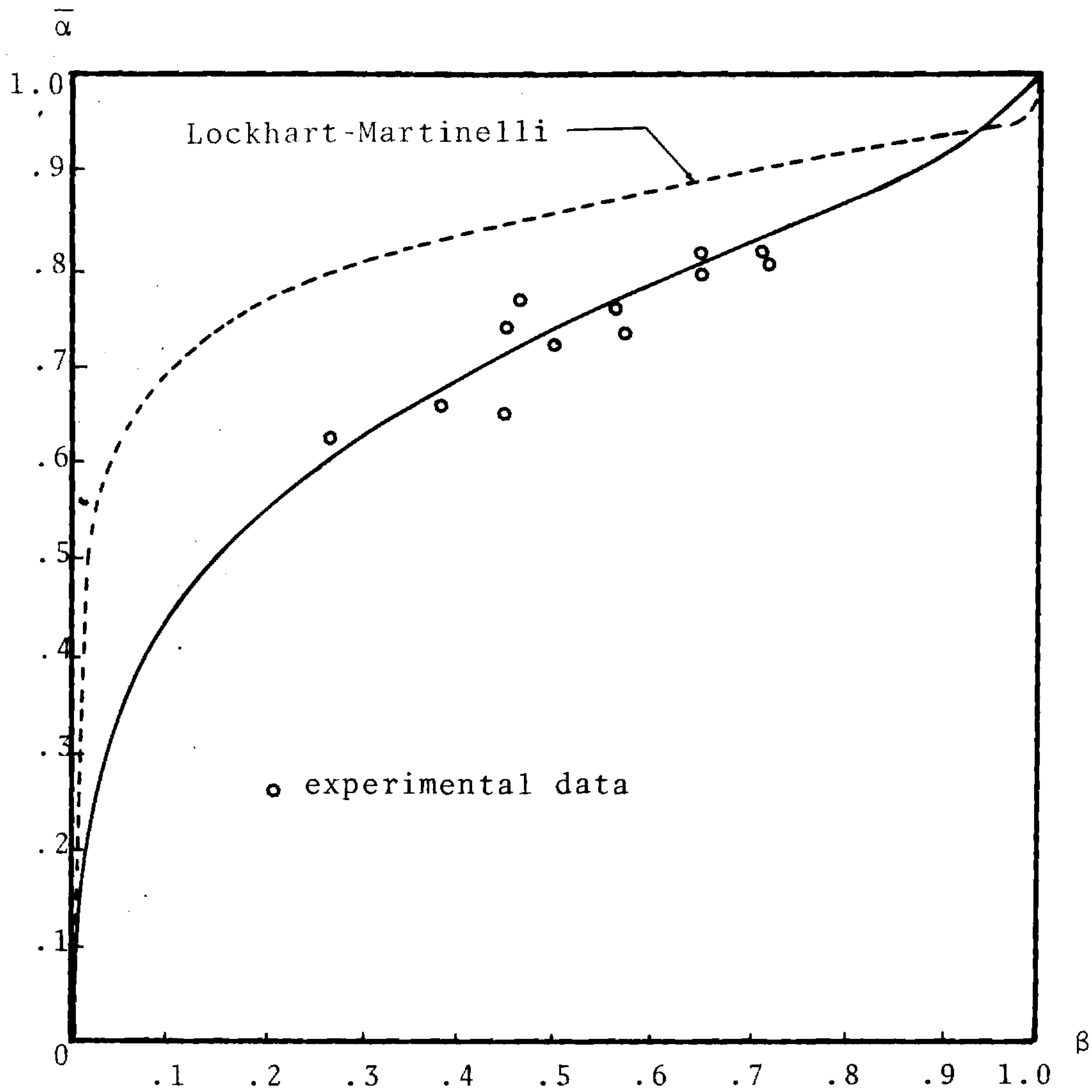

Figure 10. Void Fraction versus "Flowing" Volumetric Concentration for Horizontal, Circular Pipes with $(\mu_2/\mu_1) = 20.1$

versus the "flowing" volumetric concentration by the author's theory (solid line) and by the Lockhart-Martinelli correlation (dotted line). Notice again that the experimental are in better agreement with the author's correlation. Using the author's correlation for $\bar{\alpha}$ in the expression for the mixture kinematic viscosity defined in equation (21), a plot of f_M versus the Re was obtained. The result is shown in Figure 11.

Figure 12 shows the effect of this interaction term, I, in the expression for ν_m. Notice the significant differences between the curves for the second and third definitions in this figure. In the worst case, they can differ by as much as a factor of 5!

Figure 13 is a plot of the average void fraction, $\bar{\alpha}$, versus β for various viscosity ratios (μ_2/μ_1) ranging from 0.001 to 1000. This plot clearly shows that $\bar{\alpha}$ can be determined <u>solely</u> from a knowledge of input system quantities and fluid properties.

Figure 14 is a plot of the functions used in computing ν_m, $F_1(\alpha)$ and $F_2(\alpha)$ versus the void fraction for selected constant viscosity ratios, $\dot{\mu}_2$. These functions are defined in equations (3) and (4) of Section 5.2. The experimental data used correspond to a $\dot{\mu}_2 \simeq 20.1$.

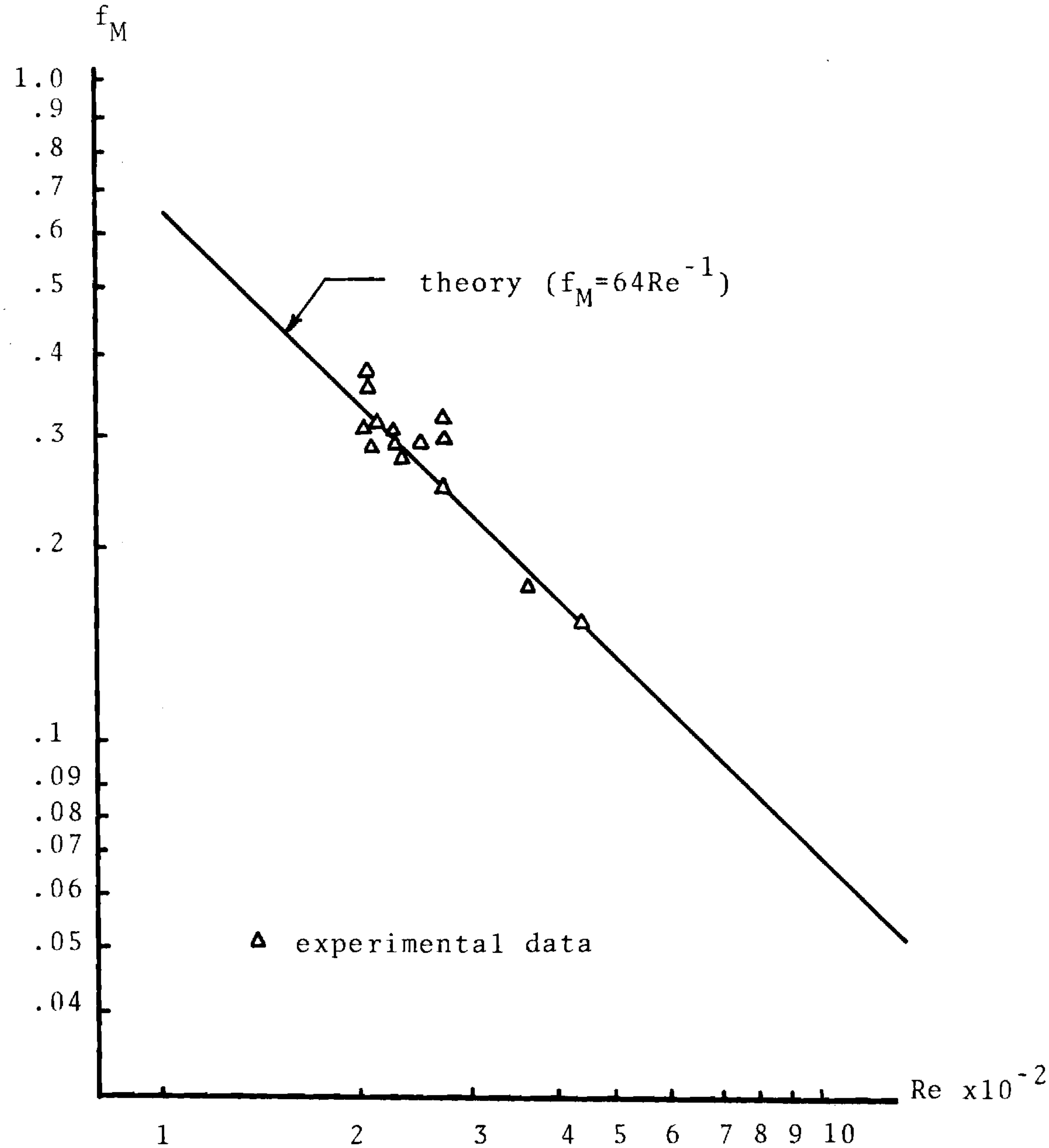

Figure 11. Two-Phase Moody Friction Factor versus Mixture Reynolds Number for Horizontal, Circular Pipes with Theoretical Value for $\bar{\alpha}$

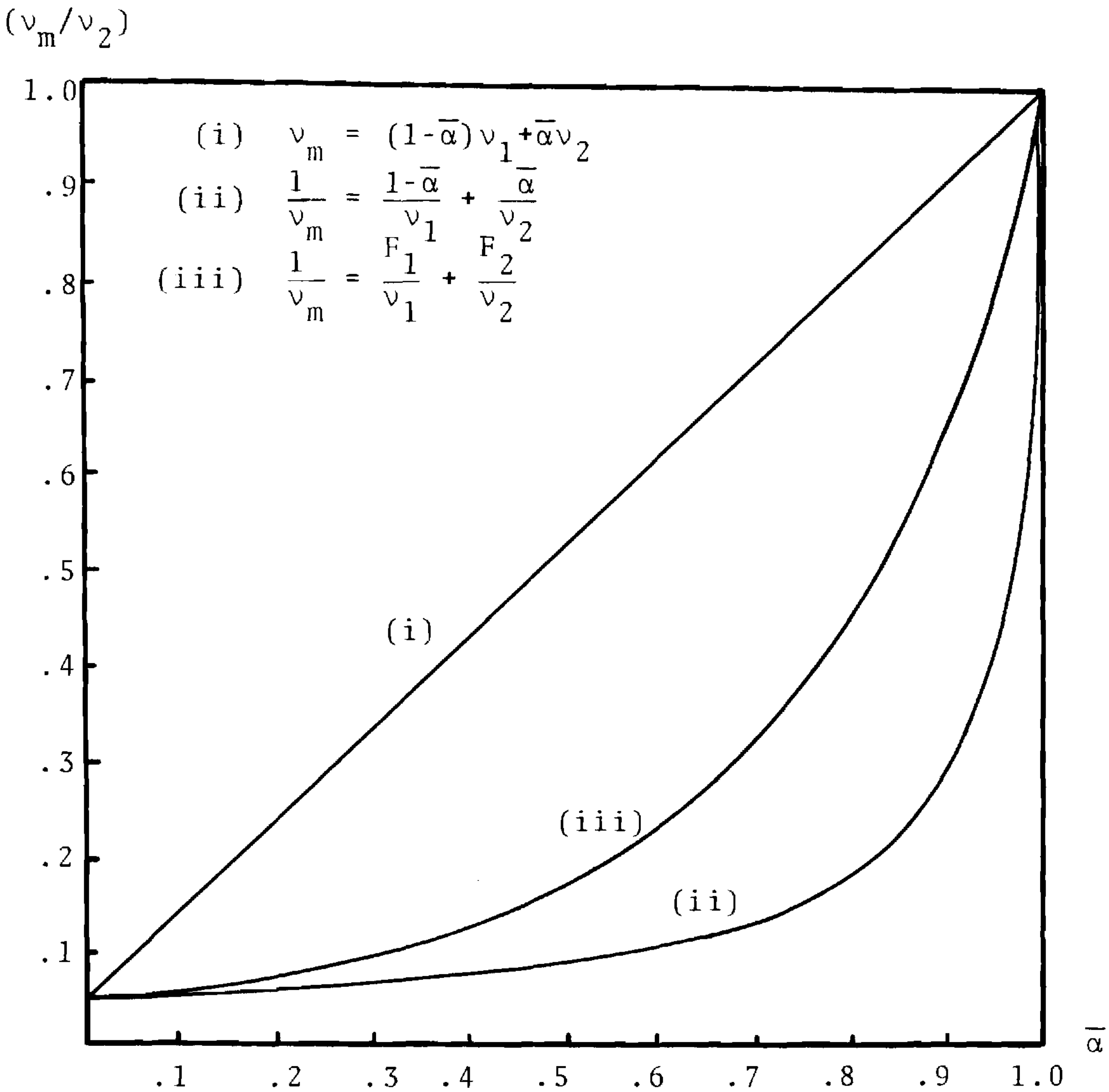

Figure 12. Non-Dimensional Kinematic Mixture Viscosity versus Void Fraction for Horizontal, Circular Pipes with $(\mu_2/\mu_1) = 20.1$ and $(\rho_2/\rho_1) = .834$

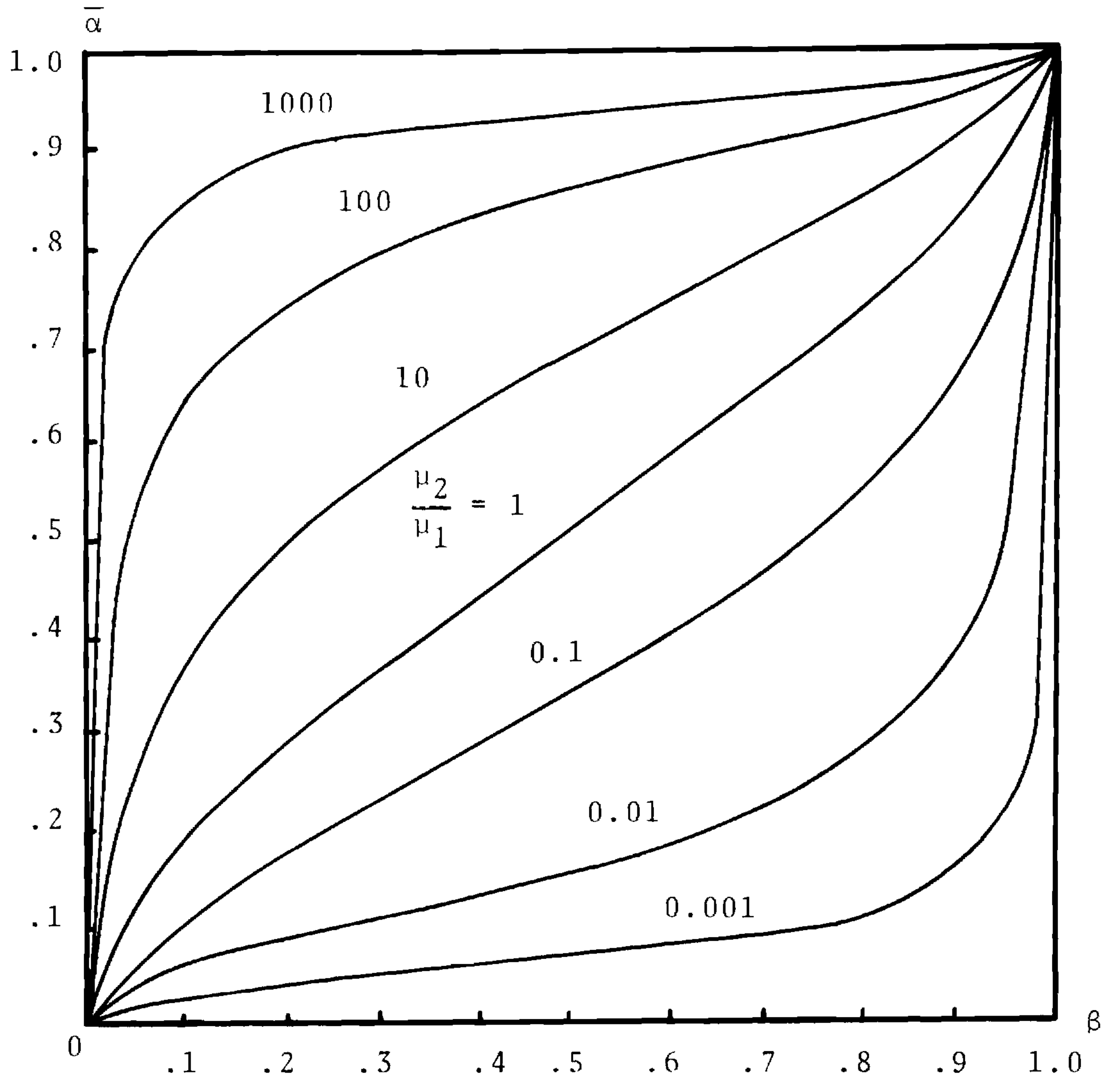

Figure 13. Average Void Fraction versus "Flowing" Volumetric Concentration for Horizontal, Circular Pipes for Various Viscosity Ratios, (μ_2/μ_1) = constant

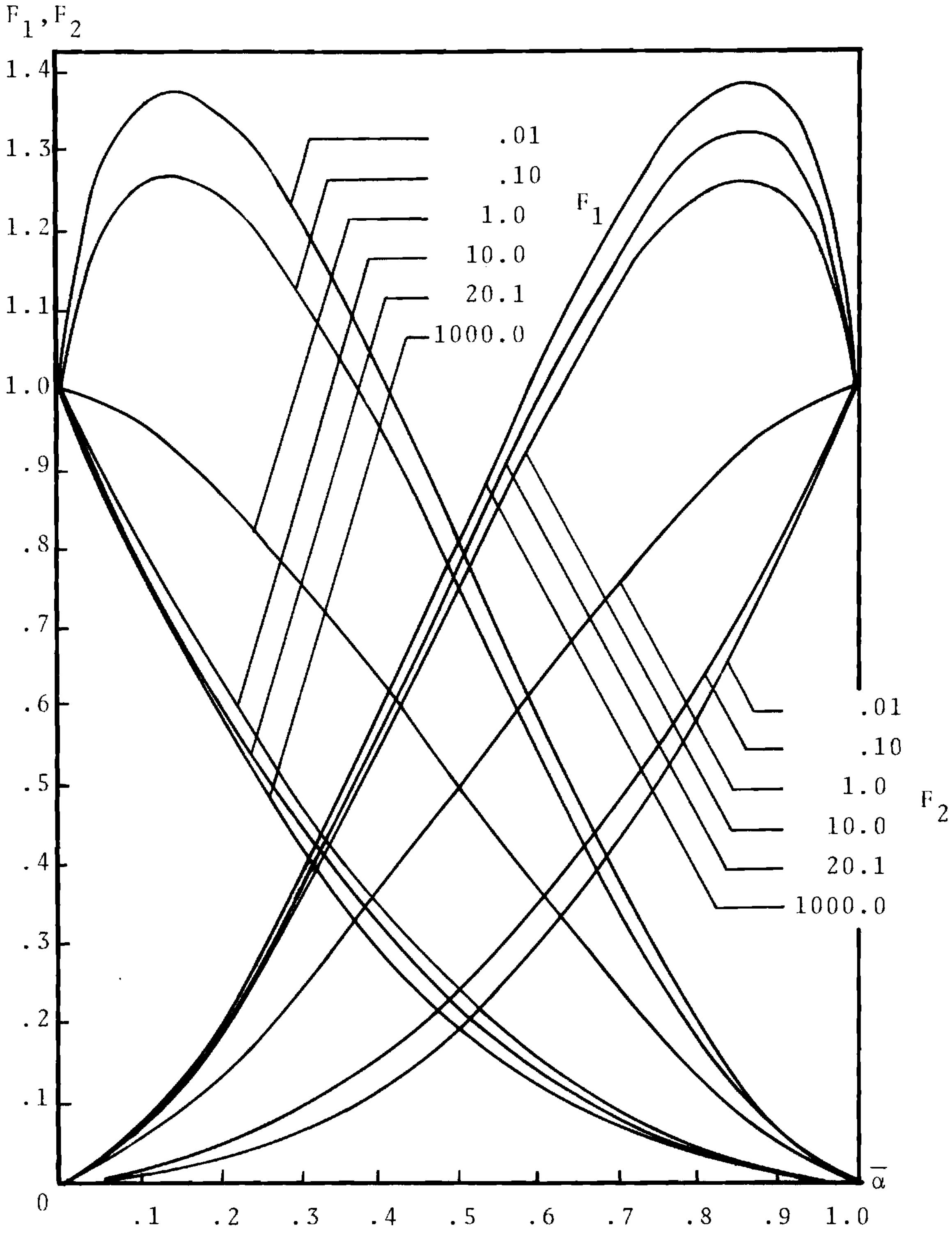

Figure 14. Functions F_1 and F_2 versus the Void Fraction for Selected Constant Viscosity Ratios, $\dot{\mu}_2$

CHAPTER VI

CONCLUSIONS

The following conclusions are made by the author as a result of the previous analyses:

(1) The diffusion or drift flow model is the proper model to use for predicting the two-phase, frictional pressure drop for the horizontal, stratified flow of two Newtonian fluids with a flat interface.

(2) As a direct consequence from using the drift model, the velocity for the two-phase mixture must be defined in terms of the baricenter instead of the center of volume; this results in the proper definition for the mixture kinematic viscosity.

(3) The mixture kinematic viscosity, ν_m, can be thought of as the sum of two "resistances" acting in parallel plus an interaction term which can be neglected under special conditions.

(4) The mixture kinematic viscosity together with the baricenter velocity and the hydraulic diameter define the Reynolds number for separated, two-phase flow.

(5) Using this Reynolds number as a similarity parameter, the frictional pressure drop for separated, two-phase flow can be correlated in terms of the standard Moody friction factor.

(6) Thus, the results of this analysis show that the correlation for frictional pressure drop in single- and two-phase flow are identical if the two-phase Reynolds number, defined in this analysis, is used as the similarity parameter.

(7) In addition to the frictional pressure drop correlation, the analysis developed in this thesis yields an expression for the void fraction in terms of known input parameters, that is, flow rates, duct geometry, and fluid properties.

(8) And finally, as a result of the author's analysis, it can be concluded that the "triangular" relationship claimed by Hewitt [17] does not hold since both the frictional pressure drop and the void fraction can be computed <u>simultaneously</u> given the input parameters (i.e., flow rates, duct geometry, and fluid properties of the individual phases or components.

APPENDICES

APPENDIX A

SEPARATED FLOW IN A RECTANGULAR CONDUIT [5]

Charles and Lilleleht [5] have derived expressions for both the velocity distribution and the volumetric flow rates for the co-current laminar, stratified flow of two immiscible, Newtonian fluids in horizontal, rectangular conduits. Their analysis is presented in this Appendix.

The flow model is depicted in Figure 4. The flow is assumed to be fully developed and the interface between the fluid layers is assumed to be smooth and horizontal. The conduit is represented by ABCD and the interface by EF. Fluid 2 flows above fluid 1, the depth being b_1 and b_2, respectively. The width of the duct is 2a. The (x,y,z) coordinate system has the origin at 0 with the x-axis coincident with the interface and the flow in the z-direction.

The basic differential equation governing the flow of both phases is

$$\frac{\partial^2 v}{\partial x^2} + \frac{\partial^2 v}{\partial y^2} = \frac{g_c}{\mu}\left(\frac{\partial p}{\partial z}\right) \tag{1}$$

which may be written for each phase as

$$\frac{\partial^2 v_j}{\partial x^2} + \frac{\partial^2 v_j}{\partial y^2} = \frac{g_c}{\mu_j}\left(\frac{\partial p}{\partial z}\right), \; j=1,2 \tag{2}$$

where v is the local velocity which is a function of both x and y. The boundary conditions, which are similar to those used in the previous studies [6,8] of stratified flow in a circular pipe, are:

$$v_1=0 \text{ when } x=\pm a, \; -b_1 \leq y \leq 0 \tag{3}$$

$$v_1=0 \text{ when } -a \leq x \leq a, \; y=-b_1 \tag{4}$$

$$v_2=0 \text{ when } x=\pm a, \; 0 \leq y \leq b_2 \tag{5}$$

$$v_2=0 \text{ when } -a \leq x \leq a, \; y=b_2 \tag{6}$$

$$v_1=v_2 \qquad \text{when } -a \leq x \leq a \tag{7}$$

$$\mu_1\left(\frac{\partial v_1}{\partial y}\right)=\mu_2\left(\frac{\partial v_2}{\partial y}\right) \qquad y=0 \tag{8}$$

Let
$$k_j \equiv \frac{g_c\left(\frac{\partial p}{\partial z}\right)}{\mu_j} \tag{9}$$

and
$$m \equiv \frac{\mu_2}{\mu_1} \tag{10}$$

If a variable V_j is defined by the relationship

$$v_j \equiv V_j + \frac{k_j}{2}(x^2-a^2) \qquad (11)$$

then substitution for v_j into the differential equation (2) gives

$$\frac{\partial^2 V_j}{\partial x^2} + \frac{\partial^2 V_j}{\partial y^2} \equiv 0 \qquad . \qquad (12)$$

The boundary conditions defined in equations (3) through (8) now become

$$V_1=0 \text{ when } x=\pm a,\ -b_1\leq y\leq 0 \qquad (13)$$

$$V_1=-\frac{k_1}{2}(x^2-a^2) \text{ when } -a\leq x\leq a,\ y=-b_1 \qquad (14)$$

$$V_2=0 \text{ when } x=\pm a,\ 0\leq y\leq b_2 \qquad (15)$$

$$V_2=-\frac{k_2}{2}(x^2-a^2) \text{ when } -a\leq x\leq a,\ y=b_2 \qquad (16)$$

$$V_2-V_1 = \frac{1}{2}(k_1-k_2)(x^2-a^2) \qquad -a\leq x\leq a \qquad (17)$$

$$\frac{\partial V_1}{\partial y}-m\frac{\partial V_2}{\partial y} = 0 \qquad y=0 \qquad (18)$$

Boundary conditions (13) and (15) give $V_j = 0$ when $x = \pm a$ and are satisfied by terms of the form

$$Y_j \cos\left[\frac{(2i+1)\pi}{2a}\right] \tag{19}$$

where Y_j is a function of y only and i is an integer. Let

$$n \equiv \frac{(2i+1)\pi}{2a} \tag{20}$$

and substitute

$$V_j = Y_j \cos(nx) \tag{21}$$

into equation (12); thus one gets

$$\frac{\partial^2 Y_j}{\partial y^2} - n^2 Y_j = 0 \tag{22}$$

from which it follows that

$$Y_j = A_j(n)\mathrm{sh}(ny) + B_j(n)\mathrm{ch}(ny) \tag{23}$$

in which $A_j(n)$ and $B_j(n)$ are functions of n and, therefore, of i but not of x and y. The solution may therefore be written in the form

$$V_j = \sum_{i=o}^{\infty} [A_j(n)\mathrm{sh}(ny) + B_j(n)\mathrm{ch}(ny)]\cos(nx) \tag{24}$$

which may be considered as a cosine Fourier series, the two coefficients being functions of y. Two of the six boundary conditions have been used. Four remain, therefore, for the evaluation of $A_j(n)$ and $B_j(n)$, $j = 1,2$.

Hence, by using the boundary conditions defined in equations (14), (16), (17) and (18) in conjunction with equation (24), the velocity distribution is obtained as

$$v_j = \frac{16a^2}{\pi^3} \sum_{i=o}^{\infty} \frac{(-1)^i}{(2i+1)^3} [A_j'(n)\,sh(ny) + B_j'(n)\,ch(ny)]\cos(nx) + \\ + \frac{k_j}{2}(x^2 - a^2) \tag{25}$$

where the coefficients $A_j'(n)$ and $B_j'(n)$ for $j = 1,2$ become

$$A_1'(n) = mA_2'(n) \tag{26}$$

$$A_2'(n) = \frac{k_2 ch(nb_1) - k_1 ch(nb_2) + (k_1 - k_2) ch(nb_1) ch(nb_2)}{ch(nb_1) sh(nb_2) + m sh(nb_1) ch(nb_2)} \tag{27}$$

$$B_1'(n) = \frac{k_1 sh(nb_2) + mk_2 sh(nb_1) + m(k_1 - k_2) sh(nb_1) ch(nb_2)}{ch(nb_1) sh(nb_2) + m sh(nb_1) ch(nb_2)} \tag{28}$$

and

$$B_2'(n) = \frac{mk_2 sh(nb_1) + k_1 sh(nb_2) - (k_1 - k_2) sh(nb_2) ch(nb_1)}{ch(nb_1) sh(nb_2) + m sh(nb_1) ch(nb_2)} \tag{29}$$

A limiting case is of interest: if m = 1 and, therefore, $k_1 = k_2$, then the fluids 1 and 2 are identical as far as the problem is concerned. If, in addition, $b_1 = b_2 = b$, then the x-axis lies equidistant between the top and bottom of the conduit. With these substitutions, equation (25) reduces to the expression derived by Cornish (8) for the velocity distribution in single-phase flow given below as

$$v = -\frac{16b^2 g_c}{\pi^3 \mu}\left(\frac{\partial p}{\partial z}\right) \sum_{n=1,3\ldots}^{\infty} \left[\frac{(-1)^{\frac{n-1}{2}}}{n^3}\left(\frac{\operatorname{ch}\left(\frac{n\pi x}{2b}\right)}{\operatorname{ch}\left(\frac{n\pi a}{2b}\right)}\right)\right]\cos\left(\frac{n\pi x}{2b}\right) - \frac{g_c}{2\mu}\left(\frac{\partial p}{\partial z}\right)(b^2 - y^2) \tag{30}$$

and for the volumetric flux, Q, as

$$Q = -\frac{4}{3}\,\frac{ab^3 g_c}{\mu}\left(\frac{\partial p}{\partial z}\right)\left\{1 - \frac{192b}{\pi^5 a}\sum_{n=1,3\ldots}^{\infty}\left[\frac{1}{n^5}\tanh\left(\frac{n\pi a}{2b}\right)\right]\right\} \tag{31}$$

or

$$Q = -\frac{4}{3}\,\frac{a^3 b\; g_c}{\mu}\left(\frac{\partial p}{\partial z}\right)F\ . \tag{32}$$

Cornish considered a conduit of width 2a and depth 2b and he located the origin of his coordinates at the axis of the conduit, with the x-axis horizontal, the y-axis vertical, and the flow in the z-direction.

The volumetric flow rates, Q_1, and Q_2, are obtained by evaluating the integrals

$$Q_1 \equiv \int_{-b_1}^{o} \int_{-a}^{+a} v_1 dxdy \tag{33}$$

and

$$Q_2 \equiv \int_{o}^{b_2} \int_{-a}^{+a} v_2 dxdy \tag{34}$$

Substitution for v_1 and v_2 from equation (25) into equations (33) and (34), respectively, gives

$$Q_1 = \frac{128a^4}{\pi^5} \sum_{i=o}^{\infty} \left(\frac{1}{2i+1}\right)^5 [A_1'(n)(1-ch(nb_1))+B_1'(n)sh(nb_1)] - \\ - \frac{2}{3}k_1 a^3 b_1 \tag{35}$$

and

$$Q_2 = \frac{128a^4}{\pi^5} \sum_{i=o}^{\infty} \left(\frac{1}{2i+1}\right)^5 [A_2'(n)(ch(nb_2)-1)+B_2'(n)sh(nb_2)] - \\ - \frac{2}{3}k_2 a^3 b_2 \tag{36}$$

with $A_1'(n)$, $A_2'(n)$, $B_1'(n)$, and $B_2'(n)$ given by equations (26) through (29).

Expressions have been derived in open form for the velocity distribution and the volumetric flow rates for the stratified, laminar flow of two immiscible fluids in a closed rectangular conduit. It is seen from the analysis that the velocity distribution and flow rates can, therefore, be calculated from a knowledge of the physical dimensions of the conduit, the fluid properties, the pressure gradient, and the position of the interface.

APPENDIX B

SEPARATED FLOW IN THE LAMINAR REGIME THROUGH A HORIZONTAL, CIRCULAR PIPE* [22]

The system for the separated flow of two immiscible fluids with a flat interface is shown in Figure 8. Fluid 1 forms the upper layer and has a density less than that of fluid 2. The flow is also assumed to be isothermal, fully developed, with incompressible, Newtonian fluids of constant viscosities flowing in a constant cross-sectional pipe. The basic differential equation governing this type of flow has the same form in both phases; thus, for phase 1 and phase 2, respectively, in rectangular Cartesian coordinates, it becomes

$$\frac{\partial^2 v_1}{\partial x^2} + \frac{\partial^2 v_1}{\partial y^2} = \frac{2k_1}{\mu_1} \tag{1}$$

and

$$\frac{\partial^2 v_2}{\partial x^2} + \frac{\partial^2 v_2}{\partial y^2} = \frac{2k_2}{\mu_2} . \tag{2}$$

---

*It was discovered while examining the original work that many typographical errors were present in the equations. The author, together with his advisor, Dr. Novak Zuber, translated and verified their analysis, and corrected the expressions containing the errors. Their analysis with corrected equations is presented in this Appendix for reference.

The quantities k_1 and k_2 are defined as

$$k_1 \equiv \frac{1}{2}\left(\frac{\partial p}{\partial x} - g\rho_1 \cos\gamma\right) \tag{3}$$

and

$$k_2 \equiv \frac{1}{2}\left(\frac{\partial p}{\partial x} - g\rho_2 \cos\gamma\right) \tag{4}$$

where the angle γ is the pipe inclination angle as measured from the vertical axis. Hence, for horizontal flow, $(\gamma = \frac{\pi}{2})$, the effects due to gravity forces on the flow are zero.

Since the rectangular coordinate system is not a very convenient system to use with this type of flow system geometry, equations (1) and (2) are transformed to the bi-polar coordinate system, (ε,Θ). Referring to Figure 8, the bi-polar coordinate ε is defined to be $\varepsilon = \ln(r_1/r_2)$, and thus, (x,y) can be expressed in terms of (ε,Θ) as

$$x = \frac{a\ \mathrm{sh}(\varepsilon)}{\mathrm{ch}(\varepsilon)+\cos\Theta},\ y = \frac{a\ \sin\Theta}{\mathrm{ch}(\varepsilon)+\cos\Theta}\ . \tag{5}$$

Using these relationships in equation (5), for example:

$$\frac{\partial v}{\partial x} = \frac{\left(\frac{\partial y}{\partial \Theta}\right)\left(\frac{\partial v}{\partial \varepsilon}\right) - \left(\frac{\partial y}{\partial \varepsilon}\right)\left(\frac{\partial v}{\partial \Theta}\right)}{\left(\frac{\partial x}{\partial \varepsilon}\right)\left(\frac{\partial y}{\partial \Theta}\right) - \left(\frac{\partial x}{\partial \Theta}\right)\left(\frac{\partial y}{\partial \varepsilon}\right)}, \tag{6}$$

$$\frac{\partial v}{\partial y} = \frac{(\frac{\partial x}{\partial \varepsilon})(\frac{\partial v}{\partial \Theta}) - (\frac{\partial x}{\partial \Theta})(\frac{\partial v}{\partial \varepsilon})}{(\frac{\partial x}{\partial \varepsilon})(\frac{\partial y}{\partial \Theta}) - (\frac{\partial x}{\partial \Theta})(\frac{\partial y}{\partial \varepsilon})} , \tag{7}$$

equations (1) and (2) can be expressed in terms of (ε,Θ) as

$$\frac{\partial^2 v_1}{\partial \varepsilon^2} + \frac{\partial^2 v_1}{\partial \Theta^2} = \frac{2k_1 a^2}{\mu_1 [ch(\varepsilon)+\cos\Theta]^2} \tag{8}$$

and

$$\frac{\partial^2 v_2}{\partial \varepsilon^2} + \frac{\partial^2 v_2}{\partial \Theta^2} = \frac{2k_2 a^2}{\mu_2 [ch(\varepsilon)+\cos\Theta]^2} \tag{9}$$

The solutions to equations (8) and (9) yield the local velocity distribution for each phase, respectively. Thus, one obtains

$$v_1(\varepsilon,\Theta) = -\frac{k_1 a^2}{2\mu_1}[\xi_1(\varepsilon,\Theta) + \frac{2\cos\Theta}{ch(\varepsilon)+\cos\Theta}] \tag{10}$$

and

$$v_2(\varepsilon,\Theta) = -\frac{k_2 a^2}{2\mu_2}[\xi_2(\varepsilon_1\Theta) + \frac{2\cos\Theta}{ch(\varepsilon)+\cos\Theta}] \tag{11}$$

where the terms $\frac{-k_1 a^2 \cos\Theta}{\mu_1[ch(\varepsilon)+\cos\Theta]}$ and $\frac{-k_2 a^2 \cos\Theta}{\mu_2[ch(\varepsilon)+\cos\Theta]}$ are the particular solutions to equations (8) and (9), respectively, and the functions $\xi_1(\varepsilon,\Theta)$ and $\xi_2(\varepsilon,\Theta)$ are the complementary solutions to the following set of homogeneous equations:

$$\frac{\partial^2 \xi_1}{\partial \varepsilon^2} + \frac{\partial^2 \xi_1}{\partial \Theta^2} \equiv 0 \qquad (12)$$

and

$$\frac{\partial^2 \xi_2}{\partial \varepsilon^2} + \frac{\partial^2 \xi_2}{\partial \Theta^2} \equiv 0 \ . \qquad (13)$$

The functions ξ_1 and ξ_2 can be expressed in terms of Fourier Integrals as

$$\xi_1(\varepsilon,\Theta) = \int_0^\infty \{A_1(m)sh[m(\Theta-\Theta_1)]+B_1(m)sh(m\Theta)\}\cos(m\varepsilon)dm \qquad (14)$$

and

$$\xi_2(\varepsilon_1\Theta) = \int_0^\infty \{A_2(m)sh[m(\Theta-\Theta_2)]+B_2(m)sh(m\Theta)\}\cos(m\varepsilon)dm \qquad (15)$$

where A_1, B_1, A_2, and B_2 are functions of m and are evaluated from the following four boundary conditions:

(i) on the boundary wetted by phase 1, the velocity of phase 1 must be zero; $v_1(\varepsilon,\Theta) = 0$;

(ii) on the boundary ($\Theta = \Theta_2$ = constant) wetted by phase 2, the velocity of phase 2 must be zero; $v_2(\varepsilon,\Theta) = 0$;

(iii) on the interface ($\Theta = 0$), there must be equality of velocities; thus, $v_1(\varepsilon,0) = v_2(\varepsilon,0)$;

(iv) on the interface, there must also be equality of shear stress; thus, $\mu_1(\frac{\partial v_1}{\partial y})_{\Theta=0} = \mu_2(\frac{\partial v_2}{\partial y})_{\Theta=0}$.

Applying the first two boundary conditions to equations (10) and (11) and (14) and (15), one can obtain

$$\int_0^\infty B_1(m)\,\mathrm{sh}(m\Theta_1)\cos(m\varepsilon)\,dm = -\frac{2\cos\Theta_1}{\mathrm{ch}(\varepsilon)+\cos\Theta_1} \tag{16}$$

and

$$\int_0^\infty B_2(m)\,\mathrm{sh}(m\Theta_2)\cos(m\varepsilon)\,dm = -\frac{2\cos\Theta_2}{\mathrm{ch}(\varepsilon)+\cos\Theta_2} \tag{17}$$

where the right hand side (RHS) of equations (16) and (17), respectively, can be expressed as

$$-\frac{2\cos\Theta_1}{\mathrm{ch}(\varepsilon)+\cos\Theta_1} = -4\,\mathrm{ctg}\Theta_1\int_0^\infty \frac{\mathrm{sh}(m\Theta_1)\cos(m\varepsilon)\,dm}{\mathrm{sh}(m\pi)} \tag{18}$$

and

$$-\frac{2\cos\Theta_2}{\mathrm{ch}(\varepsilon)+\cos\Theta_2} = -4\,\mathrm{ctg}\Theta_2\int_0^\infty \frac{\mathrm{sh}(m\Theta_2)\cos(m\varepsilon)\,dm}{\mathrm{sh}(m\pi)}\,. \tag{19}$$

Substituting equations (18) and (19) into equations (16) and (17), respectively, one obtains

$$\int_0^\infty B_1(m)\,sh(m\Theta_1)\cos(m\varepsilon)dm = -\,4ctg\Theta_1 \int_0^\infty \frac{sh(m\Theta_1)\cos(m\varepsilon)dm}{sh(m\pi)} \tag{20}$$

and

$$\int_0^\infty B_2(m)\,sh(m\Theta_2)\cos(m\varepsilon)dm = -\,4ctg\Theta_2 \int_0^\infty \frac{sh(m\Theta_2)\cos(m\varepsilon)dm}{sh(m\pi)} \tag{21}$$

and from equations (20) and (21), the functions $B_1(m)$ and $B_2(m)$ are determined to be

$$B_1(m) = -\,\frac{4ctg\Theta_1}{sh(m\pi)} \tag{22}$$

and

$$B_2(m) = -\,\frac{4ctg\Theta_2}{sh(m\pi)}\ . \tag{23}$$

From the third boundary condition requiring equality of velocities on the interface, one can obtain

$$\frac{k_1}{\mu_1}\left[\frac{2}{1+ch(\varepsilon)} - \int_0^\infty A_1(m)\,sh(m\Theta_1)\cos(m\varepsilon)dm\right] =$$

$$\frac{k_2}{\mu_2}\left[\frac{2}{1+ch(\varepsilon)} - \int_0^\infty A_2(m)\,sh(m\Theta_2)\cos(m\varepsilon)dm\right]\ . \tag{24}$$

Rewriting the first term inside the brackets on the LHS of equation (24) as

$$\frac{2}{1+\mathrm{ch}(\varepsilon)} = 4 \int_{o}^{\infty} \frac{m \cos(m\varepsilon)}{\mathrm{sh}(m\pi)} dm \tag{25}$$

and substituting the RHS of equation (25) back into equation (24), one can obtain the following:

$$\frac{k_1}{\mu_1}\{ \int_{o}^{\infty} \cos(m\varepsilon)[\frac{4m}{\mathrm{sh}(m\pi)} - A_1(m)\mathrm{sh}(m\Theta_1)]dm =$$

$$\frac{k_2}{\mu_2}\{ \int_{o}^{\infty} \cos(m\varepsilon)[\frac{4m}{\mathrm{sh}(m\pi)} - A_2(m)\mathrm{sh}(m\Theta_2)]dm \ . \tag{26}$$

Thus, from equation (26), the following relationship between $A_1(m)$ and $A_2(m)$ becomes

$$\frac{k_1}{\mu_1}[\frac{4m}{\mathrm{sh}(m\pi)} - A_1(m)\mathrm{sh}(m\Theta_1)] = \frac{k_2}{\mu_2}[\frac{4m}{\mathrm{sh}(m\pi)} - A_2(m)\mathrm{sh}(m\Theta_2)] \ . \tag{27}$$

To explicitly solve for $A_1(m)$ and $A_2(m)$, one must apply the remaining boundary condition requiring equality of shear stress on the interface; thus, transforming this boundary condition from rectangular Cartesian coordinates to the bi-polar coordinates results in

$$\mu_1\left(\frac{\partial v_1}{\partial \Theta}\right)_{\Theta=0} = \mu_2\left(\frac{\partial v_2}{\partial \Theta}\right)_{\Theta} = 0 \tag{28}$$

where from equation (5) it is seen that

$$\left(\frac{\partial x}{\partial \Theta}\right)_{\Theta=0} = 0, \quad \left(\frac{\partial y}{\partial \Theta}\right)_{\Theta=0} = 1 \ . \tag{29}$$

Performing the partial differentiation indicated in equation (28) on equations (10) and (11) and evaluating at the interface, one finds that

$$\mu_1\left(\frac{\partial v_1}{\partial \Theta}\right)_{\Theta=0} = -\frac{a^2 k_1}{2}\left(\frac{\partial \xi_1}{\partial \Theta}\right)_{\Theta=0} \tag{30}$$

and

$$\mu_2\left(\frac{\partial v_2}{\partial \Theta}\right)_{\Theta=0} = -\frac{a^2 k_2}{2}\left(\frac{\partial \xi_2}{\partial \Theta}\right)_{\Theta=0} \ . \tag{31}$$

Now, substituting equations (30) and (31) into equation (28) yields

$$k_1\left(\frac{\partial \xi_1}{\partial \Theta}\right)_{\Theta=0} = k_2\left(\frac{\partial \xi_2}{\partial \Theta}\right)_{\Theta=0} \ . \tag{32}$$

Similarly, performing the partial differentiation indicated in equation (32) on the functions ξ_1 and ξ_2 defined in equations (14) and (15), respectively, and then evaluating at the interface, one can obtain

$$\left(\frac{\partial \xi_1}{\partial \Theta}\right)_{\Theta=0} = \int_0^\infty [A_1(m)ch(m\Theta_1)+B_1(m)]m\cos(m\varepsilon)dm \tag{33}$$

and

$$\left(\frac{\partial \xi_2}{\partial \Theta}\right)_{\Theta=0} = \int_0^\infty [A_2(m)ch(m\Theta_2)+B_2(m)]m\cos(m\varepsilon)dm \ . \tag{34}$$

Substituting for the integrals involving $B_1(m)$ and $B_2(m)$ from equations (20) and (21), respectively, into equations (33) and (34), and then substituting this result into equation (32), one gets

$$k_1[A_1(m)ch(m\Theta_1) - \frac{4ctg\Theta_1}{sh(m\pi)}] = k_2[A_2(m)ch(m\Theta_2) - \frac{4ctg\Theta_2}{sh(m\pi)}] \ . \tag{35}$$

By solving equations (27) and (35) simultaneously, the following expressions for the coefficients $A_1(m)$ and $A_2(m)$ are obtained:

$$A_1(m) = \frac{8}{sh(m\pi)}\left[\frac{mch(m\Theta_2)(\dot{\mu}_2-\dot{k}_2)-ctg\Theta_2 sh(m\Theta_2)(1-\dot{k}_2)}{(1-\dot{\mu}_2)sh[m(\pi-2\Theta_2)]-(1+\dot{\mu}_2)sh(m\pi)}\right] \tag{36}$$

and

$$A_2(m) = \frac{8}{sh(m\pi)}\left[\frac{mch(m\Theta_1)(\dot{k}_1-\dot{\mu}_1)-ctg\Theta_2 sh(m\Theta_1)(\dot{k}_1-1)}{(\dot{\mu}_1-1)sh[m(\pi-2\Theta_2)]-(1+\dot{\mu}_1)sh(m\pi)}\right] \ . \tag{37}$$

where, for convenience, one can define

$$\dot{\mu}_1 \equiv \frac{\mu_1}{\mu_2}, \; \dot{\mu}_2 \equiv \frac{\mu_2}{\mu_1} \tag{38}$$

and

$$\dot{k}_1 \equiv \frac{k_1}{k_2}, \; \dot{k}_2 \equiv \frac{k_2}{k_1}. \tag{39}$$

Notice for horizontal flow that $\dot{k}_1 = \dot{k}_2 = 1.0$.

Substituting for $A_1(m)$, $A_2(m)$, $B_1(m)$, and $B_2(m)$ from equations (36), (37), (20), and (21), respectively, the local velocity distribution for phase 1 and phase 2 can be expressed as

$$v_1(\varepsilon,\Theta) = -\frac{a^2 k_1}{\mu_1}\{\frac{\sin(\Theta_2-\Theta)}{[ch(\varepsilon)+\cos\Theta]\sin\Theta_2} + 4\int_0^\infty \frac{[mch(m\Theta_2)(\dot{\mu}_2-\dot{k}_2)-ctg\Theta_2 sh(m\Theta_2)(1-\dot{k}_2)]\cos(m\varepsilon)sh[m(\Theta-\Theta_1)]dm}{[(1-\dot{\mu}_2)sh[m(\pi-2\Theta_2)]-(1+\dot{\mu}_2)sh(m\pi)]sh(m\pi)}\} \tag{40}$$

and

$$v_2(\varepsilon,\Theta) = -\frac{a^2 k_2}{\mu_2}\{\frac{\sin(\Theta_2-\Theta)}{[ch(\varepsilon)+\cos\Theta]\sin\Theta_2} + 4\int_0^\infty \frac{[mch(m\Theta_1)(\dot{k}_1-\dot{\mu}_1)-ctg\Theta_1 sh(m\Theta_1)(\dot{k}_1-1)]\cos(m\varepsilon)sh[m(\Theta-\Theta_2)]dm}{[(\dot{\mu}_1-1)sh[m(\pi-2\Theta_2)]-(1+\dot{\mu}_1)sh(m\pi)]sh(m\pi)}\} \tag{41}$$

Equations (40) and (41) are valid for all $|\Theta|<\pi$.

From the local velocity distributions defined in equations (40) and (41), one can derive the volumetric fluxes for each phase by integrating over an elementary area. The elementary area in bi-polar coordinates is defined as

$$dA_c \equiv (d\ell)_\Theta \; (d\ell)_\varepsilon \tag{42}$$

where $(d\ell)_\Theta$ and $(d\ell)_\varepsilon$ can be written in terms of (x,y) and (ε,Θ) as

$$(d\ell)_\Theta = [(\frac{\partial x}{\partial \varepsilon})^2 + (\frac{\partial y}{\partial \varepsilon})^2]^{1/2} d\varepsilon \tag{43}$$

and

$$(d\ell)_\varepsilon = [(\frac{\partial x}{\partial \Theta})^2 + (\frac{\partial y}{\partial \Theta})^2]^{1/2} d\Theta \; . \tag{44}$$

Thus, substituting for the elementary, dA_c, from equation (42) and performing the indicated differentiation in equations (43) and (44), one obtains Q_1 and Q_2 as

$$Q_1 = a^2 \int_{\Theta_1}^{\circ} d\Theta \int_{-\infty}^{\infty} \frac{v_1(\Theta,\varepsilon)\, d\varepsilon}{[ch(\varepsilon)+\cos\Theta]^2} \tag{45}$$

$$Q_2 = a^2 \int_{o}^{\Theta_2} d\Theta \int_{-\infty}^{\infty} \frac{v_2(\Theta,\varepsilon)d\varepsilon}{[ch(\varepsilon)+\cos\Theta]^2} \quad . \tag{46}$$

After substituting for the local velocity distributions defined in equations (40) and (41), one obtains the following expressions:

$$Q_1 = \frac{a^4 k_1}{\mu_1}\{ \int_{o}^{\Theta_1} \cos\Theta d\Theta \int_{-\infty}^{\infty} \frac{d\varepsilon}{[ch(\varepsilon)+\cos\Theta]^2} -$$

$$- \, ctg\Theta_1 \int_{o}^{\infty} \sin\Theta d\Theta \int_{-\infty}^{\infty} \frac{d\varepsilon}{[ch(\varepsilon)+\cos\Theta]^3} + \tag{47}$$

$$+ \frac{1}{2} \int_{o}^{\infty} A_1(m)dm \int_{o}^{\infty} sh[m(\Theta-\Theta_1)]d\Theta \int_{-\infty}^{\infty} \frac{\cos(m\varepsilon)d\varepsilon}{[ch(\varepsilon)+\cos\Theta]^2}$$

and

$$Q_2 = - \frac{a^4 k_2}{\mu_2}\{ \int_{o}^{\Theta_2} \cos\Theta d\Theta \int_{-\infty}^{\infty} \frac{d\varepsilon}{[ch(\varepsilon)+\cos\Theta]^2} -$$

$$- \, ctg\Theta_2 \int_{o}^{\Theta_2} \sin\Theta d\Theta \int_{-\infty}^{\infty} \frac{d\varepsilon}{[ch(\varepsilon)+\cos\Theta]^3} + \tag{48}$$

$$+ \frac{1}{2} \int_{o}^{\infty} A_2(m)dm \int_{o}^{\infty} sh[m(\Theta-\Theta_2)]d\Theta \int_{-\infty}^{\infty} \frac{\cos(m\varepsilon)d\varepsilon}{[ch(\varepsilon)+\cos\Theta]}\} \quad .$$

Now, integrating equations (47) and (48) with respect to the variable ε gives

$$Q_1 = \frac{a^4 k_1}{\mu_1}\{ \int_0^{\Theta_1} [\Theta(3-2\sin^2\Theta)-3\sin\Theta\cos\Theta]\frac{\cos\Theta}{\sin^5\Theta}d\Theta -$$

$$- \operatorname{ctg}\Theta_1 \int_0^{\Theta_1} [\Theta(3-2\sin^2\Theta)-3\sin\Theta\cos\Theta]\frac{d\Theta}{\sin^4\Theta} + \tag{49}$$

$$+ \pi \int_0^{\infty} \frac{A_1(m)}{\operatorname{sh}(m\pi)}dm \int_0^{\Theta_1} \frac{\operatorname{sh}[m(\Theta-\Theta_1)]}{\sin^3\Theta}[m\operatorname{ch}(m\Theta)\sin\Theta-\operatorname{sh}(m\Theta)\cos\Theta]d\Theta\}$$

and

$$Q_2 = - \frac{a^4 k_2}{\mu_2}\{ \int_0^{\Theta_2} [\Theta(3-2\sin^2\Theta)-3\sin\Theta\cos\Theta]\frac{\cos\Theta}{\sin^5\Theta}d\Theta -$$

$$- \operatorname{ctg}\Theta_2 \int_0^{\Theta_2} [\Theta(3-2\sin^2\Theta-3\sin\Theta\cos\Theta]\frac{d\Theta}{\sin^4\Theta} + \tag{50}$$

$$+ \pi \int_0^{\infty} \frac{A_2(m)dm}{\operatorname{sh}(m\pi)} \int_0^{\Theta_2} \frac{\operatorname{sh}[m(\Theta-\Theta_2)]}{\sin^3\Theta}[m\operatorname{ch}(m\Theta)\sin\Theta-\operatorname{sh}(m\Theta)\cos\Theta]d\Theta\}$$

Integrating these equations with respect to the variable Θ yields the following expressions for the volumetric fluxes, Q_1 and Q_2, respectively, as

$$Q_1 = \frac{a^4 k_1}{\mu_1} \{\frac{1}{4}[\frac{\Theta_1(1-3ctg^2\Theta_1)}{\sin^2\Theta_1} + ctg\Theta_1(1+3ctg^2\Theta_1)] -$$

$$- \frac{ctg\Theta_1}{\sin^2\Theta_1}(1-\Theta_1 ctg\Theta_1) + \frac{1}{3}ctg\Theta_1 + \tag{51}$$

$$+ \frac{\pi}{2}\int_0^\infty \frac{A_1(m)}{sh(m\pi)}[msh(m\Theta_1)ctg\Theta_1 - m^2 ch(m\Theta_1)]dm\}$$

and

$$Q_2 = - \frac{a^4 k_2}{\mu_2} \{\frac{1}{4}[\frac{\Theta_2(1-3ctg^2\Theta_2)}{\sin^2\Theta_2} + ctg\Theta_2(1+3ctg^2\Theta_2)] -$$

$$- \frac{ctg\Theta_2}{\sin^2\Theta_2}(1-\Theta_2 ctg\Theta_2) + \frac{1}{3}ctg\Theta_2 + \tag{52}$$

$$+ \frac{\pi}{2}\int_0^\infty \frac{A_2(m)}{sh(m\pi)}[msh(m\Theta_2)ctg\Theta_2 - m^2 ch(m\Theta_2)]dm\} .$$

From Figure 8, one can write

$$a = R\sin\Theta_2 \tag{53}$$

and substituting for k_1 and k_2 from equations (3) and (4) into equations (51) and (52), respectively, one can express the volumetric fluxes, Q_1 and Q_2, as

$$Q_1 = -\frac{\pi R^4}{8\mu_1}\left\{\frac{dp}{dx} - g\rho_1\cos\gamma\right\}F_1 \tag{54}$$

and

$$Q_2 = -\frac{\pi R^4}{8\mu_2}\left\{\frac{dp}{dx} - g\rho_2\cos\gamma\right\}F_2 \tag{55}$$

where the functions F_1 and F_2 are expressed as follows:

$$\begin{aligned} F_1 \equiv & -\frac{1}{\pi}[\Theta_1 - \frac{1}{6}\{3+2\sin^2\Theta_2\}\sin 2\Theta_2] - 2\sin^4\Theta_2 \times \\ & \times \int_0^\infty [\mathrm{ctg}\Theta_1 \mathrm{sh}(m\Theta_1) - m\,\mathrm{ch}(m\Theta_1)]\frac{mA_1(m)}{\mathrm{sh}(m\pi)}dm \end{aligned} \tag{56}$$

and

$$\begin{aligned} F_2 \equiv & \frac{1}{\pi}[\Theta_2 - \frac{1}{6}\{3+2\sin^2\Theta_2\}\sin 2\Theta_2 + 2\sin^4\Theta_2 \times \\ & \times \int_0^\infty [\mathrm{ctg}\Theta_2 \mathrm{sh}(m\Theta_2) - m\,\mathrm{ch}(m\Theta_2)]\frac{mA_2(m)}{\mathrm{sh}(m\pi)}dm \ . \end{aligned} \tag{57}$$

From the system geometry, the ratio of the area occupied by phase 1 to the total area of the pipe and the ratio of the area occupied by phase 2 to the total area of the pipe can be written as

$$\frac{A_1}{A_T} \equiv (1-\bar{\alpha}) = -\frac{1}{2\pi}[2\Theta_1 - \sin 2\Theta_1] \tag{58}$$

and

$$\frac{A_2}{A_T} \equiv \bar{\alpha} = \frac{1}{2\pi}[2\Theta_2 - \sin 2\Theta_2] \tag{59}$$

Consider the following special cases:

(i) When $\bar{\alpha} = 0$, $\Theta_1 = -\pi$, $\Theta_2 = 0$; then

$$F_1 = 1.0, \; F_2 = 0 \tag{60}$$

(ii) When $\bar{\alpha} = 1$, $\Theta_1 = 0$, $\Theta_2 = \pi$; then

$$F_1 = 0, \; F_2 = 1.0 \tag{61}$$

(iii) When $\bar{\alpha} = 0.5$, $\Theta_1 = \Theta_2 = -\pi/2$; then

$$(F_1)_{\bar{\alpha}=.5} = \frac{1}{2}\left[1 + \frac{32(\dot{k}_2 - \dot{\mu}_2)}{1+\dot{\mu}_2} \int_0^\infty \frac{m^3 ch^2(\frac{m\pi}{2})\, dm}{sh^3(m\pi)}\right] \tag{62}$$

and

$$(F_2)_{\bar{\alpha}=.5} = \frac{1}{2}\left[1 - \frac{32(\dot{k}_2 - \dot{\mu}_2)}{\dot{k}_2(1+\dot{\mu}_2)} \int_0^\infty \frac{m^3 ch^2(\frac{m\pi}{2})\, dm}{sh^3(m\pi)}\right] . \tag{63}$$

Evaluating the integral terms in equations (62) and (63), one obtains

$$(F_1)_{\bar{\alpha}=.5} = \frac{1}{2}[1 + \frac{(\dot{k}_2-\dot{\mu}_2)}{1+\dot{\mu}_2}(\frac{16-\pi^2}{\pi^2})] \tag{64}$$

and

$$(F_2)_{\bar{\alpha}=.5} = \frac{1}{2}[1 - \frac{(\dot{k}_2-\dot{\mu}_2)}{\dot{k}_2(1+\dot{\mu}_2)}(\frac{16-\pi^2}{\pi^2})] \ . \tag{65}$$

Therefore, when the flow is horizontal ($\dot{k}_1 = \dot{k}_2 = 1.0$), one gets the following result which is valid for all viscosity ratios, $\dot{\mu}_2$:

$$(F_1)_{\bar{\alpha}=.5} + (F_2)_{\bar{\alpha}=.5} = 1 \tag{66}$$

BIBLIOGRAPHY

1. Bankoff, S. G., *Transactions ASME*, 82, 265, 1960.

2. Brodkey, R. S., The Phenomena of Fluid Motions, Addison-Wesley Publishing Company, 1967, pages 457-494.

3. Brown, K. E., Gas Lift Theory and Practice, Prentice-Hall, Inc., 1967, pages 99-165.

4. Charles, M. E., Govier, G. W., and Hodson, G. W., "The Horizontal Pipeline Flow of Equal Density Oil-Water Mixtures," *The Canadian Journal of Chemical Engineering*, February, 1961, pages 27-36.

5. Charles, M. E. and Lilleleht, L. U., "Co-Current Stratified Laminar Flow of Two Immiscible Liquids in a Rectangular Conduit," *The Canadian Journal of Chemical Engineering*, June, 1965, pages 110-116.

6. Charles, M. E. and Redberger, P. J., "The Reduction of Pressure Gradients in Oil Pipelines by the Addition of Water: Numerical Analysis of Stratified Flow," *The Canadian Journal of Chemical Engineering*, April, 1962, pages 70-75.

7. Cicchitti, A., Lombardi, C., Silvestri, M., Soldaini, G., and Zavattarelli, "Two-Phase Cooling Experiments - Pressure Drop, Heat Transfer, and Burnout Measurements," *Energia Nucleare*, 7(6), 1960, pages 407-425.

8. Cornish, R. J., "Flow in a Pipe of Rectangular Cross-Section," *Royal Society Proceedings*, 1929, pages 691-700.

9. Davidson, W. F., "Studies of Heat Transmission Through Boiler Tubing at Pressures from 500-3300 Pounds," *Transactions ASME*, 70, 1948, page 695.

10. DeGance, A. E. and Atherton, R. W., "Horizontal Flow Correlations," *Chemical Engineering*, July, 1970, pages 95-103.

11. Dukler, A. E., Wicks, M., and Cleveland, R. G., "Frictional Pressure Drop in Two-Phase Flow - Part A: A Comparison of Existing Correlations for Pressure Loss and Holdup," *The American Institute of Chemical Engineering Journal*, October, 1964, pages 38-65.

12. Dukler, A. E., Wicks, M., and Cleveland, R. G., "Frictional Pressure Drop in Two-Phase Flow - Part B: An Approach Through Similarity Analysis," *The American Institute of Chemical Engineering Journal*, January, 1964, pages 44-51.

13. Gemmell, A. R. and Epstein, N., "Numerical Analysis of Stratified Laminar Flow of Two Immiscible Newtonian Liquids in a Circular Pipe," *The Canadian Journal of Chemical Engineering*, October, 1962, pages 215-224.

14. Govier, G. W. and Aziz, K., The Flow of Complex Mixtures in Pipes, Van-Nostrand Reinhold Company, 1972, pages 503-616.

15. Govier, G. W. and Omer, M. M., "The Horizontal Pipeline Flow of Air-Water Mixtures," *The Canadian Journal of Chemical Engineering*, June, 1962, pages 93-104.

16. Hagendorn, A. R. and Brown, K. E., "Experimental Study of Pressure Gradients Occuring During Continuous Two-Phase Flow in Small Diameter Vertical Conduits, *Transactions ASME*, 17, April, 1965, pages 136-147.

17. Hewitt, G. F. and Hall Taylor, N. S., Annular Two-Phase Flow, Pergamon Press, 1970, pages 60-81.

18. Isbin, H. S., Moy, J. E., and DaCruz, A. J. R., "Two-Phase Steam-Water Critical Flow," *The American Institute of Chemical Engineering Journal*, 3, 1957, page 361.

19. Kasturi, G., Stepanek, J., and Holland, F. A., "A Review of Two-Phase Flow Literature," *British Chemical Engineering*, April/May, 1971, pages 333-336 and 511-514.

20. Kocamustafaogullari, G., "Thermo-Fluid Dynamics of Separated Two-Phase Flow," Ph.D. Thesis, Georgia Institute of Technology, December, 1971.

21. Lockhart, R. W. and Martinelli, R. C., "Proposed Correlation of Data for Isothermal Two-Phase, Two-Component Flow in Pipes," *Chemical Engineering Process*, January, 1949, pages 39-48.

22. Mamaev, V. A., Odisharian, G. E., Semenov, N. I., and Tochigin, A. A., Hydrodynamics of Gas-Liquid Mixtures in Pipes, Nedra, Moscow, 1969, pages 40-51.

23. Martinelli, R. G., Boelter, M. K., Taylor, T. H. M., Thomsen, E. G., and Morrin, E. H., "Isothermal Pressure Drop for Two-Phase, Two-Component Flow in a Horizontal Pipe," *Transactions ASME*, February, 1944, pages 134-151.

24. McAddams, W. H., Woods, W. K., and Heroma, C. C., "Vaporization Inside Horizontal Tubes - II - Benezene-Oil Mixtures," *Transactions ASME*, 64, 1942, page 193.

25. Ngyuen, V. T. and Spedding, P. L., "Two-Phase Flow: The Concept of Similarity and Equivalent Transport Properties of Fluids," *The American Institute of Chemical Engineering Journal*, 19, 3, May, 1973, pages 652-661.

26. Owens, W. L., "Two-Phase Pressure Gradient," *International Developments in Heat Transfer, Part II*, 1962.

27. Russell, T. W. F. and Charles, M. E., "The Effect of the Less Viscous Liquid in the Laminar Flow of Two Immiscible Liquids," *The Canadian Journal of Chemical Engineering*, February, 1959, pages 18-24.

28. Russell, T. W. F., Hodson, G. W., and Govier, G. W., "Horizontal Pipeline Flow of Mixtures of Oil and Water," *The Canadian Journal of Chemical Engineering*, February, 1959, pages 9-17.

29. Stepanek, J. B. and Kasturi, G., "Two-Phase Flow III: Parameters for Void Fraction and Pressure Drop Correlations," *Chemical Engineering Science*, February, 1972, pages 1881-1891.

30. Tong, L. S., Boiling Heat Transfer and Two-Phase Flow, John Wiley and Sons, Inc., 1965, pages 47-110.

31. Wallis, G. B., One-Dimensional Two-Phase Flow, McGraw-Hill Book Company, 1969, pages 43-105.

32. Whitaker, S., Introduction to Fluid Mechanics, Academic Press, 1968, pages 173-177.

33. Yu, Hao-Sheng, "Stratified Flow in Horizontal Ducts," Ph.D. Thesis, University of Minnesota, 1967.

34. Zuber, N., private communications, 1972-1973.

WAVE PROPAGATION AND CHOKING IN TWO-PHASE TWO-COMPONENT FLOW

A THESIS

Presented to

The Faculty of the Division of Graduate

Studies and Research

By

Dennis R. Liles

In Partial Fulfillment

of the Requirements for the Degree

Doctor of Philosophy

in the School of Mechanical Engineering

Georgia Institute of Technology

December, 1974

WAVE PROPAGATION AND CHOKING IN TWO-PHASE TWO-COMPONENT FLOW

Approved:

Ward O. Winer

W. Winer, Chairman

G. Colwell

G. Colwell

P. Durbetaki

P. Durbetaki

Geo M T Rentzepis

G. Rentzepis

S Shelton

S. Shelton

Date approved by Chairman: 11 October 1974

To Laura and Daniel

ACKNOWLEDGMENTS

The author wishes to express his deep sense of gratitude to the chairman of his committee, Dr. Ward Winer, for his assistance in completing this work. In addition thanks are extended to Drs. G. Colwell, P. Durbetaki, G. Rentzepis, and S. Shelton for their interest and constructive suggestions.

Special thanks are extended to Dr. Novak Zuber, who introduced the author to the area of two-phase flow and suggested the present problem. The appreciation of Dr. Zuber's guidance and encouragement is amplified by the fact that this support remained even after Dr. Zuber's responsibilities precluded the continuation of his role as the author's advisor.

The author would also like to thank the Air Force Office of Scientific Research for its financial assistance (Grant No. 70-1853) which helped make this work possible.

Finally, the author would like to thank not only all of his friends and colleagues, but also his patient wife Laura, for the support which they showed during the progress of this task.

TABLE OF CONTENTS

TABLE OF CONTENTS (Concluded)

LIST OF TABLES

LIST OF ILLUSTRATIONS

NOMENCLATURE

LATIN

A	area
a_{ij}	array coefficients defined in Appendix B
$cov(\psi, \Phi)$	$< \psi \cdot \Phi > - < \psi > \cdot < \Phi >$
C	leading edge pressure pulse velocity
c_p	specific heat at constant pressure
D_e	inside pipe diameter
G	mass flux $(\rho_m V_m)$
g	acceleration due to gravity
I.E.	interfacial energy term due to surface tension
i	enthalpy
j_k	volumetric flux of k-th phase weighed by the total cross sectional area
j	volumetric flux of the mixture weighed by the total cross sectional area
k	wave number, Boltzmann's constant, or isentropic coefficient
$\bar{k}$	unit vector in z direction
$\bar{n}$	unit normal vector
p	pressure
q	heat flux
S	slip ratio $(\frac{V_2}{V_1})$
s	entropy
T	temperature

NOMENCLATURE (Continued)

t	time
V_{kj}	drift velocity of k-th phase with respect to the center of volume of the mixture
V_{km}	drift velocity of k-th phase with respect to the center of mass of the mixture
V_k	mass averaged velocity of k-th phase
V_m	mixture velocity as applied to the center of gravity of the mixture
v	specific volume
z	spatial coordinate

<u>GREEK</u>

α	volume concentration of lighter phase
$\bar{\delta}$	Kronecker delta
θ_{mom}	stress tensor due to surface tension at interface
$\bar{\bar{\pi}}_D$	diffusion stress tensor
ρ	density
σ	surface tension
$\bar{\bar{\tau}}$	viscous stress tensor
τ_w	wall shear
$\dot{\Phi}_{mir}$	irreversible increase of thermal energy
$\dot{\Phi}_{pmr}$	reversible increase of thermal energy
χ	quality
Γ_{ki}	mass formation rate of k-th phase weighed by the total mixture volume

NOMENCLATURE (Concluded)

Subscripts

e	thermodynamic equilibrium
f	liquid phase
g	gas phase
H	homogeneous
i	interface
m	mixture
o	part of function with no derivatives in it
s	constant entropy
tc	total cross section
w	wall
z	component in z direction

Averages

< >	mass weighed average
<< >>	average with respect to cross sectional area of fluid

SUMMARY

The problem of wave propagation and choking has been examined analytically for gas-liquid flows. A drift-flux (mixture) model is employed and the solution is provided by the method of characteristics.

The main thrust of the research is to produce a model which can predict the critical flux in two-component gas-liquid flows in conduits. The characteristics of the set of equations are examined and compared with speed of sound data and conclusions are drawn between the conditions at the critical point and the speed of pressure pulses in the system. While the main emphasis of the research is on two-component flows some one-component work is presented.

CHAPTER I

INTRODUCTION

The purpose of this research is to produce a unified approach to wave propagation and choking in two-phase (gas-liquid) flow using a diffusional or drift model. The solution of the equations is by the method of characteristics with the main emphasis on two-component mixtures.

1. Significance of the Problem

Transient phenomena are often observed both in nature and in engineering systems. In many cases a knowledge of how rapidly pulses travel through the system is a prerequisite to being able to describe the transient behavior of the system. Thus in fluid flows a knowledge of the propagation of pressure pulses in the fluid is often required.

Additionally, in some flow systems, it is observed that lowering the downstream back pressure does not increase the flow rate through the systems. This is referred to as choking and is very important for the design of nuclear reactor safety systems, refrigeration devices, chemical process units, pipe lines, etc.

The relationship between longitudinal pressure pulse propagation and choking is well understood in single phase flow [1] since choking occurs when some point in the flow is at the sonic speed and pressure pulses are unable to propagate further upstream. The situation is not so clearly defined in two-phase flow.

Unfortunately, most analyses of choking in two-phase flow have attempted to draw no parallels with wave propagation. This is due both to the incompleteness and incorrectness of the governing differential equations used to describe the phenomenon as well as the inadequacy of the mathematical method of attack.

It is therefore very important that a consistent and complete model be constructed which can describe both wave propagation and choking in two-phase flow. This is important not only to provide the predictive power so necessary for flow system analysis, but also to establish correctly the connection between wave propagation and choking. This investigation concerns itself with the development of such a model.

2. Objectives of the Investigation

The present investigation has the following thesis objectives:

1. To apply a consistent one-dimensional mixture model for two-phase choking flows and wave propagation with an emphasis on two-component mixtures.

2. To compare solutions provided by the model in order to establish connections between choking and wave propagation in two-phase flows.

3. To compare the results predicted by the model to available data.

CHAPTER II

STATE OF THE ART

In single phase flow a direct connection can be made between the classical one-dimensional analyses for wave propagation and steady-state choking (i.e., the choking point occurs when the mean mass velocity equals the velocity of propagation of pressure pulses). In multiphase flow the investigators of choking flows have often not attempted to connect the two phenomena, which is a consequence of the various methods of attack adopted by the investigators. The literature on each subject will therefore be reviewed separately, drawing parallels where possible.

1. Categories of Models

Field Equations

In order to describe a two-phase flow system by a one-dimensional analysis, three broad approaches may be used. The first is to describe the system as a homogeneous single phase analogue with one overall continuity equation, one momentum equation, and one energy or entropy equation.

The second approach is to write a two-fluid model using separate continuity, momentum, and energy equations for each phase [2]. The jump conditions at the interface are also required to define the system properly. It must be noted that some authors use a hybrid model combining, for example, one continuity equation, two momentum equations, and one energy equation [3]. This hybrid approach is however inconsistent. A good listing of the variety of equation groupings used by investigators is found in [4].

The third approach is to use the drift-flux model in which one overall continuity equation, one overall momentum equation, one overall energy equation, and an additional continuity equation for one of the phases, all of which are written with respect to the center of mass of the mixture are employed. This is the approach outlined in this thesis.

Once the field equations have been established, thermodynamic, thermal, interphase transfers, and mechanical constitutive equations are needed to effect closure or, at least, assumptions about those equations. As in the case of field equations, a large variety of different sets of constitutive equations have been used by investigators. One comment should be made; many authors refer to their assumptions of flow evolution as in thermodynamic equilibrium which means that $(\frac{\partial p}{\partial v})_f$ and $(\frac{\partial p}{\partial v})_g$ were evaluated along the saturation line. In fact, a two-phase flow system can only be in thermodynamic equilibrium if not only the pressure and temperature are equal, but if the kinetic and potential energies and surface forces are equal across the interface [5]. This essentially never occurs in practice.

2. Methods of Solution for the Choking Problem

There are four general strategies that have been used in an attempt to solve the choking problem. These are the experimental correlation, direct assumptions about the choking condition, the wave front model, and the determinant method. Each will be covered separately.

Empirical Correlations

This is the oldest method and, of course, does not require the establishment of the proper field equations. Burnell [6] developed an equation for predicting the critical discharge through square-edge orifices:

$$G_{CRITICAL} = \sqrt{2 g_c \rho_f \left(P_{UPSTREAM} - (1 - C_1) P_{SAT}\right)}$$

where C_1 is an empirical constant. Zaloudek [7] examined choking flow in short pipes and found a correlation in the form:

$$G_{CRITICAL} = C_2 \sqrt{2 g_c \rho_f \left(P_{UPSTREAM} - P_{SAT}\right)}$$

C_2 was a correlation constant.

A number of other correlations exist [8,9], but all suffer from the defect inherent in a model which does not utilize proper field equations; that is, a question of the utility of the correlations for other fluids and flow conditions.

Direct Assumptions About Choking

This is a large category embracing quite a varied group of literature. The formulations begin with a highly simplified set of field equations which are often incomplete or incorrect and assumptions about the conditions at the choking point are then made which allow a solution to be found. The difficulty with these approaches is incompleteness and arbitrariness. Full sets of equations are not easily handled by these methods, which often impose arbitrary choking conditions. This raises serious questions about the applicability of the results.

The simplest model is the homogeneous equilibrium model (no slip, thermodynamic equilibrium) resulting in:

$$G^2_{CRITICAL} = -\left(\frac{\partial P}{\partial v}\right)_H$$

where

$$v_H = (1-x)\,v_f + x\,v_g$$

The derivatives of P with respect to v are then evaluated along the saturation curve for single component media or isentropically or isothermally for two-component flows. Unfortunately, while the procedure is simple it is inaccurate, always underestimating the observed critical mass flux. It has been used as a reference for correlations [9]. Reference [10] includes a section on making the necessary calculations.

Many authors have arrived at a similar form for the choking mass flux, i.e.:

$$G^2_{CRITICAL} = -\left(\frac{\partial P}{\partial v}\right)$$

The differences in the models of this form involve the definition of v and the assumptions used in evaluating the partial derivatives. Seldom do the authors try to connect their $(\frac{\partial p}{\partial v})$ with the speed of sound (squared) because of the lack of a formal consistent approach.

Isbin, et al. [9] used a relation

$$v_m = \frac{v_g x^2}{\alpha} + \frac{v_f (1-x)^2}{(1-\alpha)}$$

and the Lockhart-Martinelli correlation for the void fraction to evaluate the choking conditions. Massena [11] employed the modified Armand correlation for void fraction. Both assumed thermodynamic equilibrium. It must be noted that v_m is not the proper mixture specific volume [2].

Faletti and Moulton [12] used a homogeneous approach and supplied a direct functional correlation based on steam table correlations. An interesting part of their experimental work was the use of a surface active agent (detergent) to reduce the surface tension. They noted no significant change in the value of the choking mass flux, although the static pressure at the choking point changed.

Moody [13] wrote energy and continuity equations and claimed at the choking point that $(\frac{\partial G}{\partial S})_p$ and $(\frac{\partial G}{\partial p})_S = 0$. This assumed among other things that the slip ratio S and the pressure are independent which they are not. Moody arrived at an expression for the slip ratio which is identical to Zivi's [14], i.e., $S = \sqrt[3]{\frac{v_g}{v_L}}$. He was then able to solve the equations using the upstream stagnation conditions for the critical mass flux. In a later paper Moody [15] used momentum and energy equations as well as a friction factor to extend this idea. Moody's most recent work is discussed under the wave front model. Unfortunately in no instance does the author present a complete set of mixture field equations as a solid basis from which to start.

Cruver and Moulton [16] wrote overall mass, momentum, mechanical, and total energy equations, and then defined four specific volumes:

Area specific volume:

$$v_a = \left(\frac{1}{A_{Tc}} \int_{A_{Tc}} \rho \, dA \right)^{-1}$$

Momentum specific volume:

$$v_m = \frac{1}{G^2 A_{TC}} \int_{A_{TC}} \rho V^2 \, dA$$

Kinetic energy specific volume:

$$v_{KE} = \left[\frac{1}{G^3 A_{TC}} \int_{A_{TC}} \rho V^3 \, dA \right]^{1/2}$$

Velocity-weighed specific volume:

$$v_V = \frac{1}{G A_{TC}} \int_{A_{TC}} V \, dA$$

They also assumed that the change in mixture entropy (incorrectly defined) was equal to zero.

Fauske [10] using simple momentum and continuity equations and the condition $(\frac{\partial G}{\partial p}) = 0$ arrived at a formulation which included a fixed slip ratio of $\sqrt{\frac{v_g}{v_L}}$. This form corresponded with the experimental data better than most of the past analyses. But Cruver and Moulton [16] showed that this slip ratio did not produce the maximum Fauske thought it did. Fauske in conjunction with Henry [17] later modified his analysis to include interphase transfers and for one component flows at higher pressures a no slip condition at the critical point. Additional assumptions of somewhat dubious accuracy were also needed to effect closure.

Levy [18] evaluated $(\frac{\partial p}{\partial v_m})$ such that ds = 0 at the choking point. However, his equation for the mixture entropy was not correct [2].

A vapor choking model was used by R. V. Smith [19] to obtain a relation for the critical mass flux. He assumed the choking condition occurred when the vapor velocity was at its local sonic value. This completely arbitrary supposition is made less realistic by several of the experimental speed of sound investigations for annular dispersed flow [20] which recorded lower velocities than the speed of sound of the gas.

<u>Wave Front Models</u>

Several models have been formulated which assume a wave front at the critical point. Conservation equations are written across the front and the choking condition is determined.

Moody [21] derived overall continuity, momentum, and energy balances across the wave face along with four mixture specific volumes:

$$v_c = v^* / (\chi + S(1-\chi))$$

$$v_m = v^* \left(\chi + \frac{1-\chi}{\chi}\right)$$

$$v_E = v^{*2} \left(\chi + \frac{1-\chi}{S^2}\right)$$

where

$$v^* = \chi v_g + (1-\chi) S v_f$$

and two mixture enthalpies:

$$i^* = x i_f + (1-x) s i_g$$

$$i = x i_g + (1-x) i_f$$

He arrived at:

$$G^2_{CRITICAL} = -\left(\frac{\partial P}{\partial v_m}\right)$$

where v_m is not the true mixture specific volume. He assumed frozen conditions and either an isentropic change for each phase or homogeneous flow. Moody's results were in reasonable agreement with the data used.

Another wave front model was proposed by D'Arcy [22]. After writing continuity and simplified momentum equations for each phase across the wave, the equations were solved assuming an isentropic change for each phase and frozen flow (no mass transfer). D'Arcy employed the empirical void fraction correlation of Semenov and Kosterin [35] to complete his set of equations. His results showed only fair correspondence with the data.

Determinant Method

Several recent investigators have begun examining choking in two-phase flow by the necessary condition that the determinant of the coefficients of the partial derivatives of the field equations goes to zero at the critical point. Mathematically this is an offshoot of the method of characteristics [23]. The advantages of the procedure are twofold: it is a degenerate case of the wave propagation situation and hence the two phenomena may be investigated easily simultaneously and it is a procedure which allows difficult sets of equations to be handled simultaneously and with relative facility.

Giot and Fritte [24] proposed a two-fluid model (six field equations) and investigated the choking condition. Numerical integration of the equation for several interfacial shear expressions showed only fair agreement with the data. The authors also proposed a mixture model which was not written with respect to the center of mass.

Katto's [25] model included an overall continuity equation, separate momentum equations for each phase, an overall energy equation and an energy equation for the vapor phase. Thermodynamic equilibrium was assumed. The results of the analysis showed fair agreement with data from Faletti, Zaloudek, Fauske, and Moy. This "mixture" model is however not consistent [2] and cannot properly account for nonequilibrium effects.

Ogoasawara [3] wrote an overall continuity equation, two momentum equations, and a total energy equation. This model like Katto's is not complete in the sense that nonequilibrium between the phases cannot be properly accounted for, and in fact, thermodynamic equilibrium was assumed. In addition the equations were not written in a properly integrated mixture form.

Boure, et al. [4] examined a two-fluid model including the appropriate jump conditions. The authors imply that a mixture model is, of necessity, incomplete; which is not true if all of the proper constitutive equations are known. In fact fewer constitutive equations are required for a mixture model than for a two-fluid model, presumably making it easier to use.

An examination is made by the authors into the consequences of assuming different forms for some of the constitutive equations. A very good discussion of single phase choking is presented with some interesting ideas that tend to dispel earlier ideas on isentropic evolution.

3. Methods of Solution of the Wave Propagation Problem

It must be mentioned that the problem of interest is the determination of average wave speeds and not such effects as scattering. Four methods cover the majority of approaches in the literature; the single equation "thermodynamic" model, the wave front model, the linearized plane wave model, and the method of characteristics.

Single Equation "Thermodynamic" Model

Writing a continuity equation and simplified momentum equation for the mixture and assuming a mixture equation of state of the form

$$P = P(\rho_m, q)$$

with constant q, yields upon a small amount of manipulation,

$$c = \sqrt{\left(\frac{\partial P}{\partial \rho_m}\right)_q}$$

with q normally being the entropy s. The form of the equation is identical to the single phase case, as well it should be, due to the obvious and unfortunately incorrect [2] similarities between the single phase and two phase sets of equations used in the derivation. The differences between analyses of this type center on the evaluation of $(\frac{\partial p}{\partial \rho})$ and, except for the case of a quiescent mixture, which is essentially impossible to obtain, the analyses fail to mention what this velocity is with respect to. This is a serious defect when high speed flows with the possibility of choking occur.

The simplest formulation for this model is the homogeneous assumption utilizing an equation of mixture specific volume of the form

$$v_H = (1-x)\, v_f + x\, v_g$$

and either thermodynamic equilibrium or an isentropic assumption ds = 0 and an equation of mixture entropy of the form

$$s = (1-x)\, s_f + x\, s_g$$

Karplus' report [26] is typical of this analysis and his agreement with the data appears reasonable largely because of the large scatter in the data. The homogeneous assumption (i.e., $V_g = V_f$) is never found in practice and will only approximate real behavior in the case of low void fraction bubbly flows.

Grolmes and Fauske [27] employed the correct definition of the mixture density, but then made a homogeneous assumption with either frozen or equilibrium evolution. The frozen, homogeneous model showed good agreement with their data.

Henry, et al. [28] incorporated the slip ratio into the evaluation but since the original equation = $(\frac{\partial p}{\partial \rho})^{\frac{1}{2}}$ is not derived from a complete, consistent set of equations and since the wrong mixture density was used, the results must be viewed with skepticism.

Radovsky [29] considered a phenomenological relationship for the non-equilibrium thermodynamics of a multiphase mixture experiencing a pressure transient, and was able to provide results analogous to the frozen and equilibrium sound speeds of a reacting mixture of gases, including the effects of dispersion.

The Wave Front Model

The basis for the model is the concept of a linear velocity transformation equal in magnitude to the speed of the traveling wave superimposed on the system so that the wave is effectively frozen. As a minimum, continuity and momentum equations are written across the interface and either a differential (wave) or a finite (shock) change in the variables is considered.

Henry, et al. [28] is typical of the formulation using both mixture and separated flow models to describe the flow. Unfortunately, as pointed out in [2], the equations as written are not sufficient to encompass thermal non-equilibrium effects and do not form a properly integrated, properly averaged set of equations. Their formulations however do take into account the various flow regimes and show reasonable correspondence with the data.

D'Arcy [22] used a separated flow model employing continuity and momentum equations for each phase and solved the set by establishing the compatibility condition that the determinant of the coefficients is equal to zero. Except at very low void fractions ($< .1$) and for stratified flow, correspondence with the data was not good. D'Arcy did however indicate reference velocities for the wave motion.

The Linearized Plane Wave Model

This model proceeds by writing separate continuity, momentum, and energy equations (two-fluid model) for each phase along with assumptions about the interphase energy and momentum transport and then linearizing the equations. The standard acoustic assumption that the perturbations can be expressed in the form

$$a e^{i(\omega t - kz)}$$

is applied to the equations and a speed of sound, including dispersive effects, is the result.

The advantages to the method lie in establishing the speed of sound as a function of frequency (dispersion). The disadvantages are that small perturbations only may be considered and explicit relations for the interphase transport normally used only apply to small bubbles. In addition in no instance are the initial equations the true integrated balance conditions over the phases with the associated jump conditions at the interface [2].

Mecredy, et al. [30] calculated the dispersion effects for small bubbles with a low relative velocity or slip (stokes flow). Their high frequency limit corresponded reasonably well with established data.

Hsieh, et al. [31] considered only homogeneous flow and defined an average mixture specific heat and coefficient of heat conduction of dubious accuracy. No comparison with available data was made.

<u>The Method of Characteristics</u>

The method of characteristics is a powerful mathematical tool which is used in the solution of hyperbolic differential equations. To apply the method to two-phase flow wave propagation either a diffusional (mixture) model or separated flow (two-fluid) model is established with the appropriate constitutive conditions and equations of variation. The necessary condition, that the determinant of the coefficients of the partial derivatives is zero is formed, and the characteristic velocities are obtained.

The advantages are that complex sets of equations may be solved simultaneously (albeit numerically), the technique is a direct extension of single phase experience without the necessity to make too many debilitating assumptions, and both the propagation velocities and the velocities with which the wave motion is referenced are obtained.

Several European investigations [4,32] have been published on the method as applied to a separated model. The equations used by Boure, et al. [32] are exact integrated formulations with the appropriate interfacial jump conditions. The work is still in progress and no published comparisons with data exist at present.

It is the purpose of this investigation to apply the method to a diffusional model proposed by Zuber and Koca [2]. Their diffusional model is mathematically less complex than the separated flow system (four equations vs. six) and internally includes the explicit effects of interphase momentum transport and heat transfer.

4. Conclusions

A few final observations should be made on the state of the art of two-phase flow wave propagation and choking. The approach to these problems has often been haphazard and interconnections tenuous. In the case of wave propagation seldom is a flow velocity given as a reference for the propagation. This is a consequence of the fact that the majority of the investigators have not used the method of characteristics as the solution tool. When the method of characteristics was used, it was either with a two fluid model or with an improperly formulated "mixture" model. It is felt that a properly derived set of mixture field equations coupled with a solution by the method of characteristics would provide an advancement in the understanding of the complex phenomena of wave propagation and choking in gas-liquid flow.

CHAPTER III

ANALYSIS: FORMULATION OF THE PROBLEM

The purpose of the analysis is to apply a consistent mixture model to the problems of both choking and wave propagation in gas-liquid mixtures. This chapter discussed the governing set of equations, the assumptions made, and the solution technique by the method of characteristics.

In the present analysis the two-phase flow is represented by a set of four one-dimensional mixture field equations derived by Zuber [33] and Kocamustafaogullari [2]. These equations are time smoothed and space averaged and are written with regard to the true center of mass of the flowing mixture. Reference [2] contains an excellent discussion of the advantages of using such a formulation to describe the system dynamics. This formulation has been successfully applied by Ishii [34] and Saha [35] to the problem of flow stability in a duct with boiling.

The equations in general form (with the assumption of no suction or injection at the flow boundaries) are as follows:

Overall conservation of mass:

$$\frac{\partial \rho_m}{\partial t} + \frac{\partial}{\partial z}(\rho_m V_m) = -\rho_m V_m \frac{d}{dz}(\ln A_{rc}) \qquad (1)$$

Void propagation: (conservation of mass for the vapor phase)

$$\frac{\partial \alpha}{\partial t} + j\frac{\partial \alpha}{\partial z} = -\frac{\partial}{\partial z}(\alpha V_{gj}) + \alpha(1-\alpha)\left[\frac{1}{\rho_f}\frac{D_f \rho_f}{Dt}\right. \tag{2}$$

$$\left. - \frac{1}{\rho_g}\frac{D_g \rho_g}{Dt}\right] + \frac{\rho_m}{\rho_f \rho_g}\Gamma_{gi} - \alpha V_{gj}\frac{d}{dz}(\ln A_{Tc})$$

where:

$$\frac{D_g}{Dt} = \frac{\partial}{\partial t} + V_g \frac{\partial}{\partial z}$$

and

$$\frac{D_f}{Dt} = \frac{\partial}{\partial t} + V_f \frac{\partial}{\partial z}$$

Momentum equation for the mixture:

$$\rho_m \frac{D_m V_m}{Dt} = -\frac{\partial P_m}{\partial z} + \frac{\partial}{\partial z}\pi_D + \rho_m g_z \tag{3}$$

$$-\left[P_m - \mathcal{T}_m + \pi_D + \mathrm{cov}(mom\,T)\right]\frac{d}{dz}(\ln A_{Tc})$$

$$+ \frac{1}{A_{Tc}}\int_{\xi_i} \nabla_s \cdot \bar{\bar{\theta}}_{mom}\frac{dA}{dz} - \frac{\partial}{\partial z}\mathrm{cov}(mom\,T)$$

$$-\frac{1}{A_{Tc}}\sum_{K=1}^{2}\int_{\xi_{KW}}\left\{\left[\left(P_{KW}\,\bar{\bar{\delta}} - \mathcal{T}_{KW}\right)\cdot \vec{n}_{KW}\right]\cdot \vec{k}\right\}\frac{dA}{dz}$$

where

$$\frac{D_m V_m}{Dt} = \frac{\partial V_m}{\partial t} + V_m \frac{\partial V_m}{\partial z}$$

Energy equation for the mixture:

$$
\begin{aligned}
\frac{\partial}{\partial t}(\rho_m i_m) + \frac{\partial}{\partial z}(\rho_m V_m i_m) = & - \frac{\partial q_{mz}}{\partial z} \qquad (4) \\
& + \frac{\partial P_m}{\partial t} + \frac{\partial}{\partial z}(P_m V_m) + \dot{\Phi}_{mR} + \dot{\Phi}_{miR} \\
& - \frac{\partial}{\partial z}\Big\{ \left[(1-\alpha) \rho_f i_f V_{fm} + \alpha \rho_g i_g V_{gm} \right] \\
& - \left[(1-\alpha) P_f V_{fm} + \alpha P_g V_{gm} \right] \Big\} \\
& - \Big\{ \rho_m V_m i_m + \left[(1-\alpha) \rho_f i_f V_{fm} + \alpha \rho_g i_g V_{gm} \right] \\
& - P_m V_m - \left[(1-\alpha) P_f V_{fm} + \alpha P_g V_{gm} \right] \\
& + \mathrm{cov}(ENGT) - \left[(1-\alpha) \mathrm{cov}(P_f \cdot V_f) \right. \\
& \left. + \alpha \, \mathrm{cov}(P_g \cdot V_g) \right] \Big\} \frac{d}{dz}(\ln A_{TC}) - \frac{1}{A_{TC}} \int_{\xi_i} (I.E.) \frac{dA}{dz} \\
& - \frac{1}{A_{TC}} \sum_{K=1}^{2} \int_{\xi_{KW}} \left[\vec{q}_{KW} \cdot \vec{n}_{KW} \right] \frac{dA}{dz} + \frac{\partial}{\partial z}\left[(1-\alpha) \mathrm{cov}(P_f \cdot V_f) + \alpha \, \mathrm{cov}(P_g \cdot V_g) \right]
\end{aligned}
$$

It must be noted that these equations are written in terms of the true velocity of the center of mass

$$
V_m = \frac{(1-\alpha) \rho_f V_f + \alpha \rho_g V_g}{(1-\alpha) \rho_f + \alpha \rho_g}
$$

We will now simplify the equations by assuming:

(a) The velocity, temperature, and pressure profiles are sufficiently flat across each phase (turbulent flow) so that the covariant terms are zero. This may not be a good assumption for choking flows in sharp edge orifices [50] or converging-diverging nozzles [47,48] with a small radius of curvature in the axial direction at the throat. The possibility of using a covariant correlation term to correct for the two-dimensionality of the flow is discussed in the next chapter.

(b) The interfacial source terms are negligible. This implies that the surface tension is not important to the flow dynamics. Under this condition:

$$S_{\xi_i} (I.E.) \frac{dA}{dz} = 0$$

and

$$S_{\xi_i} \nabla_s \cdot \bar{\bar{\Theta}}_{mom} \frac{dA}{dz} = 0$$

(c) Axial conduction is negligible. This means:

$$\frac{\partial q_{mz}}{\partial z} = 0$$

(d) The viscous terms within the fluid are small so that:

$$\tau_m \approx 0$$

and

$$\dot{\Phi}_{miR} \approx 0$$

(e) A uniform pressure exists at any cross section, therefore:

$$P_f = P_g = P_m = P$$

This is a good assumption if the surface tension effects are small, the amplitude of the pressure pulses is small, and the flow geometry is such that the flow is substantially one-dimensional.

In addition, to effect closure, the following equations are needed. These are

The definition of the mixture density

$$\rho_m = (1-\alpha)\,\rho_f + \alpha\,\rho_g \tag{5}$$

with a thermal equation of state for each phase

$$\rho_g = \rho_g(P, T_g) \tag{6}$$

and

$$\rho_f = \rho_f(P, T_f) \tag{7}$$

The definition of the mixture enthalpy

$$i_m = \frac{\alpha \rho_g i_g + (1-\alpha)\rho_f i_f}{\rho_m} \tag{8}$$

with a caloric equation of state for each phase

$$i_g = i_g(p, T_g) \tag{9}$$

and

$$i_f = i_f(p, T_f) \tag{10}$$

Constitutive equation for phase change

$$\Gamma_{gi} = f_1 \tag{11}$$

In the case of a two-component flow $f_1 = 0$, which neglects the effect of dissolved gases in the liquid phase. For one-component flow, one possible model for Γ_g is discussed in Appendix A.

Kinematic constitutive equation for V_{gj} which depends on the flow regime

$$V_{gj} = V_g - j = \frac{(1-\alpha)(S-1)\, V_m}{\left[1 + \frac{\alpha \rho_g}{\rho_m}(S-1)\right]} \tag{12}$$

and either a slip function.

$$S = S(\alpha) \qquad (13a)$$

or

$$V_{gj} = V_{gj}(\rho_f, \rho_g, \sigma, g) \qquad (13b)$$

Definition of V_{fm}

$$V_{fm} = V_f - V_m = -\frac{\alpha}{1-\alpha}\frac{\rho_g}{\rho_m} V_{gj} \qquad (14)$$

Definition of V_{gm}

$$V_{gm} = V_g - V_m = \frac{\rho_f}{\rho_m} V_{gj} \qquad (15)$$

The equation for the drift stress

$$\pi_D = \frac{\alpha}{1-\alpha}\frac{\rho_f \rho_g}{\rho_m} V_{gj}^2 \qquad (16)$$

Definition for the reversible conversion of flow work into thermal energy.

$$\dot{\Phi}_{mR} = -(1-\alpha)\langle\langle P_f \nabla\cdot V_f \rangle\rangle - \alpha\langle\langle P_g \nabla\cdot V_g \rangle\rangle \qquad (17a)$$

where

$$(1-\alpha)\langle\langle \rho_f \nabla\cdot V_f \rangle\rangle = P\left\{ \frac{\partial}{\partial z}\left[(1-\alpha)V_f\right] - (1-\alpha)V_f \frac{d}{dz}(\ln A_{TC}) - \Gamma_{gi}\frac{1}{\rho_g} \right\} \tag{17b}$$

and

$$\alpha\langle\langle \rho_g \nabla\cdot V_g \rangle\rangle = P\left[\frac{\partial}{\partial z}(\alpha V_g) + \alpha V_g \frac{d}{dz}(\ln A_{TC}) + \Gamma_{gi}\frac{1}{\rho_f} \right] \tag{17c}$$

An equation for the wall shear

$$\tau_w = f_3 \tag{18}$$

The relation between V_f, V_m, and V_{gj}

$$V_f = V_m - \frac{\alpha}{1-\alpha}\frac{\rho_g}{\rho_m} V_{gj} \tag{19}$$

The relation between V_g, V_m, and V_{gj}

$$V_g = V_m + \frac{\rho_f}{\rho_m} V_{gj} \tag{20}$$

An equation for the heat transfer at the wall

$$q_w = f_4 \tag{21}$$

Geometrical equations defining

$$\frac{dA}{dz} = f_5 \tag{22}$$

and (for circular geometry)

$$\frac{d}{dz}\left(\ln A_{TC}\right) = \frac{2}{De}\,\frac{dDe}{dz} \tag{23}$$

with De a known function of z.

After the initial simplifications, twenty-four variables remain, ρ_f, ρ_g, ρ_m, V_f, V_g, V_m, V_{gj}, V_{fm}, V_{gm}, P, T_f, T_g, α, q_w, τ_w, $\frac{dA}{dz}$, $\frac{d \ln A_{TC}}{dz}$, j, Γ_{gi}, $\dot{\Phi}_{mR}$, π_D, i_f, i_g, and i_m.

Twenty-three equations (four field, nineteen other) have been enumerated although the specific forms of f_2, f_3, V_{gj}, or S have not been given yet. In addition to the aforementioned quantities an equation of thermodynamic constraint is needed to complete our system.

Two cases are considered: thermal equilibrium

$$T_f = T_g \quad \text{AND} \quad \frac{\partial T_f}{\partial z} = \frac{\partial T_g}{\partial z} \tag{24}$$

and the polytropic case

$$\frac{P}{\rho_g^{m}} = \text{CONSTANT} \tag{25}$$

where n may vary between 1 and k. The effect of these constraints is discussed in the next chapter on results and conclusions.

Since the method of characteristics is to be used as the solution tool, we do not have to specify the exact relation for the wall shear or the heat transfer (f_3 and f_4). Rather, since the available data are for essentially adiabatic systems, we may neglect the wall heat transfer, i.e., $f_4 = 0$.

The wall shear determines the axial <u>location</u> of the choking point, but if the equation for the wall shear has no partial derivatives in it, it does not determine the <u>conditions</u> at the choking point since the method of characteristics examines the requirements for discontinuities of derivatives. Therefore, we need only specify that f_3 have no partial derivatives in it, i.e.:

$$\tau_w = f_3 (P, V_m, V_{gj}, \alpha, - - -) \tag{26}$$

We are still left with the determination of the slip function or V_{gj}. It has been mentioned [45] that a two-fluid model is inherently superior to a diffusion model because the additional two field equations do not require the assumption of a specific slip function (or a function of V_{gj}) or an equation for the thermodynamic evolution of one phase. This is misleading, because two additional constitutive equations, one for the interfacial shear and one for the interfacial heat transfer, are required to complete a two-fluid formulation.

It is felt that it is both easy and reasonable to specify the thermodynamic constraint as opposed to the actual interfacial heat transfer. In addition for several flow situations, particularly in slug and bubbly flow either V_{gj} (in vertical flow) or the slip function (in horizontal flow) is known with better accuracy than the actual interfacial shear. In fact in the same paper [45] that advocated the superiority of the two fluid model over mixture models, three undefined functions existed in the interfacial shear term with an additional two in the interfacial heat transfer relations.

For low velocity bubbly flow in a vertical column, Zuber, et al. [46] showed that the correlation

$$V_{gj} = 1.41 \sqrt[4]{\frac{\sigma g (\rho_f - \rho_g)}{\rho_f^2}} \tag{27}$$

provided a good fit for the data. Since most of the speed of sound data available in bubbly flow were taken at low mass fluxes in a vertical channel, Equation 27 was employed under these conditions in the model.

The majority of the critical flow data involves a type of bubbly flow [50] in horizontal tubes. As the void fraction increases, a transition to an annual wave and annular mist flow develops [49], but at no time has pure annular flow with a flat interface been observed.

For these conditions a slip correlation based on Zuber and Findlay's [46] model is appropriate. The equation that they derived is

$$S = \frac{(1-\alpha)}{\dfrac{1}{C_o + \dfrac{\langle \alpha V_{gj} \rangle}{\langle \alpha \rangle \langle j \rangle}} - \alpha} \tag{28}$$

The effect of $\frac{\langle \alpha V_{gj} \rangle}{\langle \alpha \rangle \langle j \rangle}$ has been shown to be small at high values of the volumetric flux j [46] and this term is therefore neglected. C_o will be a function of the flow regime and pressure at the choking point, but a value in the range $1.1 \leq C_o \leq 1.2$ was shown in the paper by Zuber and Findlay to provide good correspondence with data in bubbly flow.

One difficulty with this correlation is that for a given value of C_o there is some value of the void fraction at which the slip ratio becomes infinite. From a physical standpoint C_o will be a function of void fraction and changes in C_o will occur with flow regime changes. To simplify the computation of the slip ratio the slip was allowed to vary as Equation (28) demands with a given fixed C_o until a value of eighty or ninety percent of this cutoff void fraction was reached. Then the slip condition was frozen at that value for the remainder of the range of void fraction. This procedure provided reasonable agreement with Henry's [50] air-water critical flow-data as shown in Figure 1.

After substitution of the Equations (5-11 and 13-23) back into the field equations, our reduction is complete with the exception of the specific form of V_{gj} and the specific thermodynamic relation between P, T_f, and T_g. Recognizing that these two relations will be inserted at the time of calculation in the computer program, the equations then have dependent variables V_m, α, P, T_f, and are as follows:

Void propagation equation:

$$\left\{\alpha \frac{\partial V_{gj}}{\partial V_m}\right\}\frac{\partial V_m}{\partial z} + \frac{\partial \alpha}{\partial t} + \left\{V_m + \frac{\rho_f}{\rho_m} V_{gj} + \alpha \frac{\partial V_{gj}}{\partial \alpha}\right\}\frac{\partial \alpha}{\partial z} + \left\{\alpha(1-\alpha)\left[\frac{1}{\rho_g}\left(\frac{\partial \rho_g}{\partial P}\right)_{T_g} - \frac{1}{\rho_f}\left(\frac{\partial \rho_f}{\partial P}\right)_{T_f}\right]\right\}\frac{\partial P}{\partial t} \qquad (29)$$

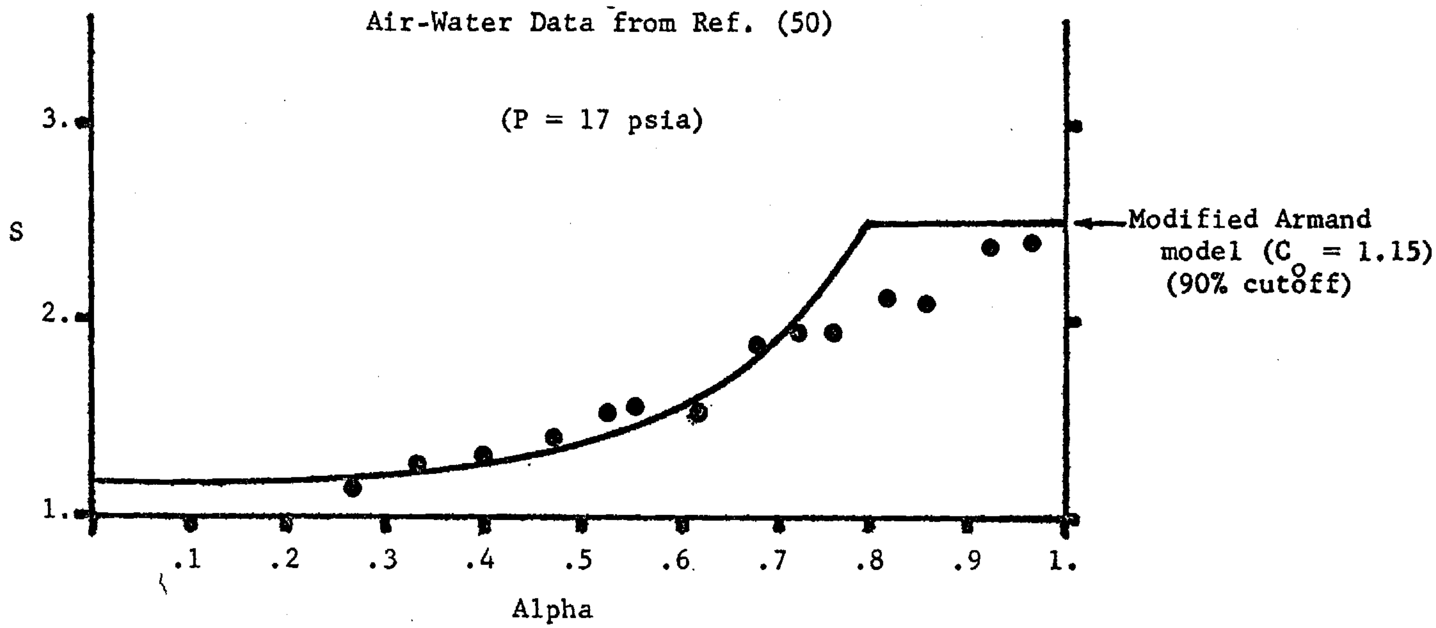

Figure 1. Slip Ratio

$$+ \left\{ \alpha \left[\left(\frac{\partial V_{gj}}{\partial \rho_f}\right)\left(\frac{\partial \rho_f}{\partial P}\right)_{T_f} + \left(\frac{\partial V_{gj}}{\partial \rho_g}\right)\left(\frac{\partial \rho_g}{\partial P}\right)_{T_g} \right] + \frac{\alpha(1-\alpha)}{\rho_g}\left(V_m\right.\right.$$

$$\left.\left. + \frac{\rho_f}{\rho_m} V_{gj}\right)\left(\frac{\partial \rho_g}{\partial P}\right)_{T_g} - \frac{\alpha(1-\alpha)}{\rho_f}\left(V_m - \frac{\alpha}{1-\alpha}\frac{\rho_g}{\rho_m} V_{gj}\right)\left(\frac{\partial \rho_f}{\partial P}\right)_{T_f} \right\} \frac{\partial P}{\partial z}$$

$$+ \left\{ -\frac{\alpha(1-\alpha)}{\rho_f}\left(\frac{\partial \rho_f}{\partial T}\right)_P \right\} \frac{\partial T_f}{\partial t} + \left\{ \alpha \left[\left(\frac{\partial V_{gj}}{\partial \rho_f}\right)\left(\frac{\partial \rho_f}{\partial T}\right)_P \right.\right.$$

$$\left.\left. - \frac{(1-\alpha)}{\rho_f}\left(V_m - \frac{\alpha}{1-\alpha}\frac{\rho_g}{\rho_m} V_{gj}\right)\left(\frac{\partial \rho_f}{\partial T}\right)_P \right] \right\} \frac{\partial T_f}{\partial z}$$

$$+ \left\{ \frac{\alpha(1-\alpha)}{\rho_g}\left(\frac{\partial \rho_g}{\partial T}\right)_P \right\} \frac{\partial T_g}{\partial t} + \left\{ \alpha \left[\left(\frac{\partial V_{gj}}{\partial \rho_g}\right)\left(\frac{\partial \rho_g}{\partial T}\right)_P \right.\right.$$

$$\left.\left. + \frac{(1-\alpha)}{\rho_g}\left(V_m + \frac{\rho_f}{\rho_m} V_{gj}\right)\left(\frac{\partial \rho_g}{\partial T}\right)_P \right] \right\} \frac{\partial T_g}{\partial z}$$

$$= -\alpha V_{gj} \frac{2}{D_e}\frac{d D_e}{d z}$$

Overall continuity equation:

$$\left\{ (1-\alpha)\rho_f + \alpha \rho_g \right\} \frac{\partial V_m}{\partial z} + \left\{ \rho_g - \rho_f \right\} \frac{\partial \alpha}{\partial t} \tag{30}$$

$$+ \left\{ V_m(\rho_g - \rho_f) \right\} \frac{\partial \alpha}{\partial z}$$

$$+ \left\{ (1-\alpha)\left(\frac{\partial \rho_f}{\partial P}\right)_{T_f} + \alpha\left(\frac{\partial \rho_g}{\partial P}\right)_{T_g} \right\} \frac{\partial P}{\partial t}$$

$$+ \left\{ V_m \left[(1-\alpha)\left(\frac{\partial \rho_f}{\partial P}\right)_{T_f} + \alpha\left(\frac{\partial \rho_g}{\partial P}\right)_{T_g} \right] \right\} \frac{\partial P}{\partial z}$$

$$+ \left\{ (1-\alpha)\left(\frac{\partial \rho_f}{\partial T}\right)_P \right\} \frac{\partial T_f}{\partial t} + \left\{ V_m(1-\alpha)\left(\frac{\partial \rho_f}{\partial T}\right)_P \right\} \frac{\partial T_f}{\partial z}$$

$$+\left\{\alpha\left(\frac{\partial\rho_g}{\partial T}\right)_p\right\}\frac{\partial T_g}{\partial t}+\left\{V_m\,\alpha\left(\frac{\partial\rho_g}{\partial T}\right)_p\right\}\frac{\partial T_g}{\partial z}$$

$$=-\left\{\rho_m V_m\frac{2}{D_e}\right\}\frac{dD_e}{dz}$$

Overall momentum equation:

$$\rho_m\frac{\partial V_m}{\partial t}+\left\{\rho_m V_m+\frac{\alpha}{1-\alpha}\frac{\rho_f\rho_g}{\rho_m}2V_{gj}\left(\frac{\partial V_{gj}}{\partial V_m}\right)\right\}\frac{\partial V_m}{\partial z} \tag{31}$$

$$+\left\{\frac{\alpha}{1-\alpha}\frac{\rho_f\rho_g}{\rho_m}V_{gj}^2\left[\frac{1}{\alpha(1-\alpha)}-\frac{\rho_g-\rho_f}{\rho_m}+\frac{2}{V_{gj}}\left(\frac{\partial V_{gj}}{\partial\alpha}\right)\right]\right\}\frac{\partial\alpha}{\partial z}$$

$$+\left\{1+\frac{\alpha}{1-\alpha}\frac{\rho_f\rho_g}{\rho_m}V_{gj}\left[V_{gj}\left(\frac{1}{\rho_f}-\frac{1-\alpha}{\rho_m}\right)\left(\frac{\partial\rho_f}{\partial P}\right)_{T_f}\right.\right.$$

$$+V_{gj}\left(\frac{1}{\rho_g}-\frac{\alpha}{\rho_m}\right)\left(\frac{\partial\rho_g}{\partial P}\right)_{T_g}+2\left(\frac{\partial V_{gj}}{\partial\rho_f}\right)\left(\frac{\partial\rho_f}{\partial P}\right)_{T_f}$$

$$\left.\left.+2\left(\frac{\partial V_{gj}}{\partial\rho_g}\right)\left(\frac{\partial\rho_g}{\partial P}\right)_{T_g}\right]\right\}\frac{\partial P}{\partial z}+\left\{\frac{\alpha}{1-\alpha}\frac{\rho_f\rho_g}{\rho_m}V_{gj}\left[V_{gj}\left(\frac{1}{\rho_f}\right.\right.\right.$$

$$\left.\left.\left.-\frac{1-\alpha}{\rho_m}\right)\left(\frac{\partial\rho_f}{\partial T}\right)_p+2\left(\frac{\partial V_{gj}}{\partial\rho_f}\right)\left(\frac{\partial\rho_f}{\partial T}\right)\right]\right\}\frac{\partial T_f}{\partial z}$$

$$+\left\{\left(\frac{\alpha}{1-\alpha}\right)\frac{\rho_f\rho_g}{\rho_m}V_{gj}\left[V_{gj}\left(\frac{1}{\rho_f}-\frac{\alpha}{\rho_m}\right)\left(\frac{\partial\rho_g}{\partial T}\right)_p\right.\right.$$

$$\left.\left.+2\left(\frac{\partial V_{gj}}{\partial\rho_g}\right)\left(\frac{\partial\rho_g}{\partial T}\right)_p\right]\right\}\frac{\partial T_g}{\partial z}$$

$$=\rho_m g_z+\frac{4}{D_e}\tau_w$$

$$-\left\{P+\frac{\alpha}{1-\alpha}\frac{\rho_f\rho_g}{\rho_m}V_{gj}^2\right\}\frac{2}{D_e}\frac{dD_e}{dz}$$

Overall energy equation:

$$\Big\{(1-\alpha)\,\rho_f i_f + \alpha \rho_g i_g + \frac{\alpha \rho_f \rho_g (i_g - i_f)}{\rho_m}\Big(\frac{\partial V_{gj}}{\partial V_m}\Big)\Big\}\frac{\partial V_m}{\partial z} \qquad (32)$$

$$+ \big\{\rho_g i_g - \rho_f i_f\big\}\frac{\partial \alpha}{\partial t} + \Big\{v_m(\rho_g i_g - \rho_f i_f) + \frac{V_{gj}\,\rho_f^2 \rho_g}{\rho_m^2}(i_g$$

$$- i_f)\Big[1 + \frac{\alpha \rho_m}{V_{gj}\,\rho_f}\Big(\frac{\partial V_{gj}}{\partial \alpha}\Big)\Big]\Big\}\frac{\partial \alpha}{\partial z} + \Big\{(1-\alpha)\Big[\frac{T_f}{\rho_f}\Big(\frac{\partial \rho_f}{\partial T}\Big)_p$$

$$+ i_f\Big(\frac{\partial \rho_f}{\partial P}\Big)_{T_f}\Big] + \alpha\Big[\frac{T_g}{\rho_g}\Big(\frac{\partial \rho_g}{\partial T}\Big)_p + i_g\Big(\frac{\partial \rho_g}{\partial P}\Big)_{T_g}\Big]\Big\}\frac{\partial P}{\partial t}$$

$$+ \Big\{V_m\Big[(1-\alpha)\Big(\frac{T_f}{\rho_f}\Big(\frac{\partial \rho_f}{\partial T}\Big)_p + i_f\Big(\frac{\partial \rho_f}{\partial P}\Big)_{T_f}\Big) + \alpha\Big(\frac{T_g}{\rho_g}\Big(\frac{\partial \rho_g}{\partial T}\Big)_p$$

$$+ i_g\Big(\frac{\partial \rho_g}{\partial P}\Big)_{T_g}\Big)\Big] + \frac{\alpha V_{gj}}{\rho_m}\Big[\frac{T_g \rho_f}{\rho_g}\Big(\frac{\partial \rho_g}{\partial T}\Big)_p - \frac{T_f \rho_g}{\rho_f}\Big(\frac{\partial \rho_f}{\partial T}\Big)_p$$

$$+ (i_g - i_f)\frac{\alpha \rho_g^2}{\rho_m}\Big(\frac{\partial \rho_f}{\partial P}\Big)_T + (i_g - i_f)\Big(\frac{(1-\alpha)\rho_f^2}{\rho_m}\Big)\Big(\frac{\partial \rho_g}{\partial P}\Big)_{T_g}\Big]$$

$$+ \frac{\alpha \rho_f \rho_g}{\rho_m}(i_g - i_f)\Big[\Big(\frac{\partial V_{gj}}{\partial \rho_f}\Big)\Big(\frac{\partial \rho_f}{\partial P}\Big)_T + \Big(\frac{\partial V_{gj}}{\partial \rho_g}\Big)\Big(\frac{\partial \rho_g}{\partial P}\Big)_{T_g}\Big]\Big\}\frac{\partial P}{\partial z}$$

$$+ \Big\{(1-\alpha)\Big[\rho_f c_{pf} + i_f\Big(\frac{\partial \rho_f}{\partial T}\Big)_p\Big]\Big\}\frac{\partial T_f}{\partial t} + \Big\{V_m(1-\alpha)\Big[\rho_f c_{pf}$$

$$+ i_f\Big(\frac{\partial \rho_f}{\partial T}\Big)_p + \frac{\alpha V_{gj}}{\rho_m}\Big[-\rho_f \rho_g c_{pf} + (i_g - i_f)\frac{\alpha \rho_g^2}{\rho_m}\Big(\frac{\partial \rho_f}{\partial T}\Big)_p\Big]$$

$$+ \alpha\frac{\rho_f \rho_g}{\rho_m}(i_g - i_f)\Big(\frac{\partial V_{gj}}{\partial \rho_f}\Big)\Big(\frac{\partial \rho_f}{\partial T}\Big)_p\Big\}\frac{\partial T_f}{\partial z} + \Big\{\alpha\Big[\rho_g c_{pg}$$

$$+ i_g\Big(\frac{\partial \rho_g}{\partial T}\Big)_p\Big]\Big\}\frac{\partial T_g}{\partial t} + \Big\{V_m \alpha\Big[\rho_g c_{pg} + i_g\Big(\frac{\partial \rho_g}{\partial T}\Big)_p\Big]$$

$$+ \frac{\alpha V_{gj}}{\rho_m}\Big[\rho_f \rho_g c_{pg} + (i_g - i_f)\frac{(1-\alpha)\rho_f^2}{\rho_m}\Big(\frac{\partial \rho_g}{\partial T}\Big)_p\Big]$$

$$+ \frac{\alpha \rho_f \rho_g}{\rho_m}(i_g - i_f)\Big(\frac{\partial V_{gj}}{\partial \rho_g}\Big)\Big(\frac{\partial \rho_g}{\partial T}\Big)_p\Big\}\frac{\partial T_g}{\partial z} = -\big\{V_m(1-\alpha)\rho_f i_f$$

$$+ V_m \alpha \rho_g i_g + \frac{\alpha \rho_g \rho_f V_{gj}}{\rho_m}\left(i_g - i_f\right)\Big\} \frac{2}{D_e} \frac{dD_e}{dz}$$

The equations may be non-dimensionalized by using the following parameters:

$$t^* = \frac{tV_o}{L} \qquad z^* = \frac{z}{L}$$

$$P^* = \frac{P}{\rho_{mo} V_o^2} \qquad V_m^* = \frac{V_m}{V_o}$$

$$\alpha^* = \alpha \qquad V_{gj}^* = \frac{V_{gj}}{V_o}$$

$$\rho_m^* = \frac{\rho_m}{\rho_{mo}} \qquad \Delta\rho^* = \frac{\rho_g - \rho_f}{\rho_{mo}}$$

$$\rho_f^* = \frac{\rho_f}{\rho_{mo}} \qquad \rho_g^* = \frac{\rho_g}{\rho_{mo}}$$

$$T_g^* = \frac{T_g}{T_{go}} \qquad T_f^* = \frac{T_f}{T_{fo}}$$

$$\Gamma_{gi}^* = \frac{\Gamma_{gi} L}{V_{mo} \rho_{mo}} \qquad g_z^* = \frac{g_z L}{V_o^2}$$

$$\tau^* = \frac{\tau_w}{\rho_{mo} V_{mo}^2} \qquad i_m^* = \frac{i_m}{V_o^2}$$

$$i_g^* = \frac{i_g}{V_o^2} \qquad i_f^* = \frac{i_f}{V_o^2}$$

$$\Delta i^* = \frac{i_g - i_f}{V_o^2}$$

where V_o, ρ_{mo}, T_{go}, and T_{fo} are any representative velocity, density, length, and temperatures, respectively.

The following dimensionless numbers may be defined:

$$N_{gjm} = \left(\frac{\partial V_{gj}}{\partial V_m}\right) \qquad N_{gjg} = \frac{\rho_{mo}}{V_o}\left(\frac{\partial V_{gj}}{\partial \rho_g}\right)$$

$$N_{gj\alpha} = \frac{1}{V_o}\left(\frac{\partial V_{gj}}{\partial \alpha}\right) \qquad M^2_{Tg} = V_o^2\left(\frac{\partial \rho_g}{\partial P}\right)_{Tg}$$

$$N_{gjf} = \frac{\rho_{mo}}{V_o}\left(\frac{\partial V_{gj}}{\partial \rho_f}\right) \qquad M^2_{Tf} = V_o^2\left(\frac{\partial \rho_f}{\partial P}\right)_{Tf}$$

$$N_{Pg} = \left(\frac{\partial \rho_g}{\partial T}\right)_P \frac{T_{go}}{\rho_{mo}} \qquad N_{Pf} = \left(\frac{\partial \rho_f}{\partial T}\right)_P \frac{T_{fo}}{\rho_{mo}}$$

$$c^*_{pf} = c_{pf}\frac{T_{fo}}{V_o^2} \qquad c^*_{pg} = c_{pg}\frac{T_{go}}{V_o^2}$$

The dimensionless expanded field equations are:

Dimensionless void propagation equation

$$\begin{aligned}
&\alpha^* N_{gjm}\frac{\partial V^*_m}{\partial z^*} + \frac{\partial \alpha^*}{\partial t^*} + \Big\{ V^*_m \frac{\rho^*_f}{\rho^*_m} V^*_{gj} \\
&+ \alpha^* N_{gj\alpha} \Big\} \frac{\partial \alpha^*}{\partial z^*} + \Big\{ \alpha^* \left[N_{gjf} M^2_{Tf} + N_{gjg} M^2_{Tg} \right] \\
&+ \frac{\alpha^*(1-\alpha^*)}{\rho^*_g}\left(V^*_m + \frac{\rho^*_f}{\rho^*_m} V^*_{gj} \right) M^2_{Tg} \\
&+ \frac{\alpha^*(1-\alpha^*)}{\rho^*_f}\left(V^*_m - \frac{\alpha^*}{(1-\alpha^*)}\frac{\rho^*_g}{\rho^*_m} V^*_{gj} \right) M^2_{Tf} \Big\} \frac{\partial P^*}{\partial z^*} \\
&+ \Big\{ \alpha^*(1-\alpha^*)\left[\frac{1}{\rho^*_g} M^2_{Tg} - \frac{1}{\rho^*_f} M^2_{Tf} \right] \Big\} \frac{\partial P^*}{\partial t^*}
\end{aligned} \tag{33}$$

$$- \{ \frac{\alpha^* (1-\alpha^*)}{\rho_f^*} N_{pf} \} \frac{\partial T_f^*}{\partial t^*}$$

$$+ \alpha^* [N_{pf} N_{gjf} - \frac{(1-\alpha^*)}{\rho_f^*} (V_m^*$$

$$- \frac{\alpha^*}{(1-\alpha^*)} \frac{\rho_g^*}{\rho_m^*} V_{gj}^*) N_{pf}] \} \frac{\partial T_f^*}{\partial z^*}$$

$$+ \{ \alpha^* \frac{(1-\alpha^*)}{\rho_g^*} N_{pg} \} \frac{\partial T_g^*}{\partial t^*} + \alpha^* [N_{pg} N_{gjg}$$

$$+ \frac{(1-\alpha^*)}{\rho_g^*} (V_m^* \frac{\rho_f^*}{\rho_m^*} V_{gj}^*) N_{pg}] \} \frac{\partial T_g^*}{\partial z^*}$$

$$= - \alpha^* V_{gj}^* \frac{2}{D_e^*} \frac{dD_e^*}{dz^*} + \frac{\rho_m^*}{\rho_f^* \rho_g^*} \Pi_{gi}^*$$

Dimensionless continuity equation

$$\rho_m^* \frac{\partial V_m^*}{\partial z^*} + \Delta\rho^* \frac{\partial \alpha^*}{\partial t^*} + V_m^* \Delta\rho^* \frac{\partial \alpha^*}{\partial z^*} \qquad (34)$$

$$+ [(1-\alpha^*) M_{Tf}^2 + \alpha^* M_{Tg}^2] \frac{\partial P^*}{\partial t^*}$$

$$+ V_m^* [(1-\alpha^*) M_{Tf}^2 + \alpha^* M_{Tg}^2] \frac{\partial P^*}{\partial z^*}$$

$$+ \{ (1-\alpha^*) N_{pf} \} \frac{\partial T_f^*}{\partial t^*} + \{ V_m^* (1-\alpha^*) N_{pf} \} \frac{\partial T_f^*}{\partial z^*}$$

$$+ \{ \alpha^* N_{pg} \} \frac{\partial T_g^*}{\partial t^*} + \{ V_m^* \alpha^* N_{pg} \} \frac{\partial T_g^*}{\partial z^*}$$

$$= - \rho_m^* V_m^* \frac{2}{D_e^*} \frac{dD_e^*}{dz^*}$$

Dimensionless momentum equation

$$
\begin{aligned}
&\{\rho_m^*\}\frac{\partial V_m^*}{\partial t^*}+\left\{\rho_m^* V_m^*+\frac{\alpha^*}{1-\alpha^*}\frac{\rho_f^*\rho_g^*}{\rho_m^*}2V_{gj}^* N_{gjm}\right\}\frac{\partial V_m^*}{\partial z^*} \qquad (35)\\
&+\left(\frac{\alpha^*}{1-\alpha^*}\right)\frac{\rho_f^*\rho_g^*}{\rho_m^*}V_{gj}^{*2}\left[\frac{1}{\alpha^*(1-\alpha^*)}-\frac{\Delta\rho^*}{\rho_m^*}+\frac{2}{V_{gj}^*}N_{gj\alpha}\right]\frac{\partial \alpha^*}{\partial z^*}\\
&+\left\{1+\frac{\alpha^*}{1-\alpha^*}\frac{\rho_f^*\rho_g^*}{\rho_m^*}V_{gj}^*\left[V_{gj}^*\left(\frac{1}{\rho_f^*}-\frac{(1-\alpha^*)}{\rho_m^*}\right)M_{Tf}^2\right.\right.\\
&+V_{gj}\left(\frac{1}{\rho_g^*}-\frac{\alpha^*}{\rho_m^*}\right)M_{Tg}^2+2N_{gjf}M_{Tf}^2\\
&\left.\left.+2N_{gjg}M_{Tg}^2\right]\right\}\frac{\partial P^*}{\partial z^*}+\left\{\left(\frac{\alpha^*}{1-\alpha^*}\right)\frac{\rho_f^*\rho_g^*}{\rho_m^*}V_{gj}^*\left[V_{gj}^*\left(\frac{1}{\rho_f^*}\right.\right.\right.\\
&\left.\left.\left.-\frac{(1-\alpha^*)}{\rho_m^*}\right)N_{Pf}+2N_{gjf}N_{Pf}\right]\right\}\frac{\partial T_f^*}{\partial z^*}\\
&+\left\{\frac{\alpha^*}{(1-\alpha^*)}\frac{\rho_f^*\rho_g^*}{\rho_m^*}V_{gj}^*\left[V_{gj}^*\left(\frac{1}{\rho_g^*}-\frac{\alpha^*}{\rho_m^*}\right)N_{Pg}\right.\right.\\
&\left.\left.+2N_{gjg}N_{Pg}\right]\right\}\frac{\partial T_g^*}{\partial z^*}=\rho_m^* g_z^*\\
&+\frac{4}{D_e^*}\tau_w^*-\left\{P^*+\right.\\
&\left.\left(\frac{\alpha^*}{1-\alpha^*}\right)\frac{\rho_f^*\rho_g^*}{\rho_m^*}V_{gj}^{*2}\right\}\frac{2}{D_e^*}\frac{dD_e^*}{dz^*}
\end{aligned}
$$

Dimensionless energy equation:

$$
\left\{\rho_m^* i_m^*+\frac{\alpha^*\rho_f^*\rho_g^*}{\rho_m^*}\Delta i^* N_{gjm}\right\}\frac{\partial V_m^*}{\partial z^*} \qquad (36)
$$

$$
+ \left\{ \rho_g^* i_g^* - \rho_f^* i_f^* \right\} \frac{\partial \alpha^*}{\partial t^*} + \left\{ V_m^* \left(\rho_g^* i_g^* \right.\right.
$$

$$
\left.\left. - \rho_f^* i_f^* \right) + \frac{V_{gj}^* \rho_f^{*2} \rho_g^*}{\rho_m^{*2}} \Delta i^* \left[1 + \frac{\alpha^* \rho_m^*}{V_{gj}^* \rho_f^*} N_{gj\alpha} \right] \right\} \frac{\partial \alpha^*}{\partial z^*}
$$

$$
+ \left\{ (1-\alpha^*) \left[\frac{T_f^*}{\rho_f^*} N_{pf} + i_f^* M_{T_f}^2 \right] + \alpha^* \left[\frac{T_g^*}{\rho_g^*} N_{pg} \right.\right.
$$

$$
\left.\left. + i_g^* M_{T_g}^2 \right] \right\} \frac{\partial p^*}{\partial t^*} + \left\{ V_m^* \left[(1-\alpha^*) \left(\frac{T_f^*}{\rho_f^*} N_{pf} \right.\right.\right.
$$

$$
\left.\left. + i_f^* M_{T_f}^2 \right) + \alpha^* \left(\frac{T_g^*}{\rho_g^*} N_{pg} + i_g^* M_{T_g}^2 \right) \right]
$$

$$
+ \frac{\alpha^* V_{gj}^*}{\rho_m^*} \left[\frac{T_g^* \rho_f^*}{\rho_g^*} N_{pg} - \frac{T_f^* \rho_g^*}{\rho_f^*} N_{pf} + \frac{\Delta i^* \alpha^* \rho_g^{*2}}{\rho_m^*} M_{T_f}^2 \right.
$$

$$
\left. + \frac{\Delta i^* (1-\alpha^*) \rho_f^{*2}}{\rho_m^*} M_{T_g}^2 \right] + \frac{\alpha^* \rho_f^* \rho_g^*}{\rho_m^*} \Delta i^* \left[N_{gjf} M_{T_f}^2 \right.
$$

$$
\left.\left. + N_{gjg} M_{T_g}^2 \right] \right\} \frac{\partial p^*}{\partial z^*} + \left\{ (1-\alpha^*) \left[\rho_f^* c_{pf}^* + i_f^* N_{pf} \right] \right\} \frac{\partial T_f^*}{\partial t^*}
$$

$$
+ \left\{ V_m^* (1-\alpha^*) \left[\rho_f^* c_{pf}^* + i_f^* N_{pf} \right] + \frac{\alpha^* V_{gj}^*}{\rho_m^*} \left[- \rho_f^* \rho_g^* c_{pf}^* \right.\right.
$$

$$
\left.\left. + \frac{\Delta i^* \alpha^* \rho_g^{*2}}{\rho_m^*} N_{pf} \right] + \frac{\alpha^* \rho_f^* \rho_g^* \Delta i^*}{\rho_m^*} N_{gjf} N_{pf} \right\} \frac{\partial T_f^*}{\partial z^*}
$$

$$
+ \left\{ \alpha^* \left[\rho_g^* c_{pg}^* + i_g^* N_{pg} \right] \right\} \frac{\partial T_g^*}{\partial t^*} + \left\{ V_m^* \alpha^* \left[\rho_g^* c_{pg}^* \right.\right.
$$

$$
\left. + i_g^* N_{pg} \right] + \frac{\alpha^* V_{gj}^*}{\rho_m^*} \left[\rho_f^* \rho_g^* c_{pg}^* + \frac{\Delta i^* (1-\alpha^*) \rho_f^{*2}}{\rho_m^*} N_{pg} \right]
$$

$$
\left. + \frac{\alpha^* \rho_f^* \rho_g^* \Delta i^*}{\rho_m^*} N_{gjg} N_{pg} \right\} \frac{\partial T_g^*}{\partial z^*} =
$$

$$-\left\{V_m^*(1-\alpha^*)\rho_f^*\, i_f^* + V_m^*\, \alpha^*\, \rho_g^*\, i_g^* + \frac{\alpha^*\, \rho_f^*\, \rho_g^*\, V_{gj}^*}{\rho_m^*}\, \Delta i^*\right\} \frac{2}{D_e^*}\, \frac{dD_e^*}{dz^*}$$

The specific form for V_{gj} and the thermodynamic constraint have of course not been included and are left as separate entities for flexibility.

Equations (33-36) may be simplified in various ways which depend on the fluid properties at the point of interest, the range of void fraction of interest, and the type of phenomena considered (i.e., wave propagation is a transient phenomenon which may occur at low mass fluxes, while the critical flux phenomenon occurs at relatively high mass fluxes). For example, the compressibility of the liquid may be neglected under most conditions, but if alpha is very small ($\alpha \rightarrow 0$) the compressibility becomes important. The complete equations were used for the numerical computation of the choking mass flux and propagation velocities, but a highly simplified analysis of the choking phenomenon will be considered in the next chapter. This was obtained by considering only the first order terms in the void propagation, continuity, and momentum equations.

The formulation of the problem is now complete. The next section considers the solution technique; the method of characteristics.

CHAPTER IV

METHOD OF SOLUTION

The formulation to the problem using the mixture model resulted in a set of four first order differential equations. The solution procedure to determine the local critical conditions and the average propagation speeds will be the method of characteristics.

1. The Method of Characteristics

If a differential equation or set of differential equations with the appropriate boundary conditions is solved, the solution takes the form of an integral surface or series of integral surfaces in a space formed by the variables. If the solution is everywhere analytic, then the Taylor's theorem may be used to extend the solution in a process referred to as analytic continuation. If however, the derivatives are discontinuous, the solution may not be extended across the discontinuities by Taylor's theorem and the solution space is not everywhere analytic.

Strictly analytic integral surfaces are characteristic of steady state equilibrium problems (elliptic differential equations) while those involving propagation phenomena (hyperbolic equations) possess discontinuities in the derivatives. It is to this latter group of problems that attention is now devoted.

The equations which evolve under the conditions described in the preceding chapter are of the first order and it is therefore the conditions under which discontinuities in first derivatives arise which is of interest. The following sections will examine a formal method for determining the characteristics, the application of this procedure to single phase wave propagation and choking, and finally the application to the present problem.

Matrix Method: Consider a set of n first order differential equations with two independent variables z, t

$$
\begin{array}{ccccccccc}
a_{11}\dfrac{\partial X_1}{\partial z} & + & a_{12}\dfrac{\partial X_1}{\partial t} & + & \cdots & + & a_{1n-1}\dfrac{\partial X_n}{\partial z} + a_{1n}\dfrac{\partial X_n}{\partial t} & = & F_1 \\
\vdots & & \vdots & & & & \vdots & & \vdots \\
a_{n1}\dfrac{\partial X_1}{\partial z} & + & a_{n2}\dfrac{\partial X_1}{\partial t} & + & \cdots & + & a_{nn-1}\dfrac{\partial X_n}{\partial z} + a_{nn}\dfrac{\partial X_n}{\partial t} & = & F_n
\end{array}
$$

The equations do not need to be linear, but it is assumed that the a_{ij}'s are not a function of partial derivatives. Then we may write the system in matrix form as:

$$
\begin{bmatrix}
a_{11} & a_{12} \cdots\cdots & a_{1n-1} & a_{1n} \\
\cdot & & \cdot & \cdot \\
\cdot & & \cdot & \cdot \\
\cdot & & \cdot & \cdot \\
a_{n1} & a_{n2} \cdots\cdots & a_{nn-1} & a_{nn} \\
d_z & d_t & 0 & 0 \\
\cdot & \cdot & & \\
\cdot & \cdot & & \\
0 & 0 \cdots\cdots & dz & dt
\end{bmatrix}
\begin{bmatrix}
\dfrac{\partial X_1}{\partial z} \\
\dfrac{\partial X_1}{\partial t} \\
\vdots \\
\\
\dfrac{\partial X_n}{\partial z} \\
\dfrac{\partial X_n}{\partial t}
\end{bmatrix}
=
\begin{bmatrix}
F_1 \\
F_2 \\
\\
F_n \\
dx_1 \\
\\
dx_n
\end{bmatrix}
$$

The second set of n equations represent the equations of variation for the dependent variables and express the fact that

$$dx_m = \frac{\partial X_m}{\partial z}\,dz + \frac{\partial X_m}{\partial t}\,dt$$

To attempt to solve the set of equations for the values of the partial derivatives at a point in space and in time, Cramer's rule could be used. For example:

$$\frac{\partial X_m}{\partial z} = \frac{\begin{vmatrix} a_{11} \cdots\cdots & F_1 & a_{1n} \\ a_{n1} & F_n & a_{nn} \\ dx & dx_1 & \\ 0 & dx_n & dt \end{vmatrix}}{\text{Det } a_{ij}}$$

where Det a_{ij} = the determinant of the coefficients of the partial derivatives. If the value of this determinant is zero, then the $\frac{\partial x_i}{\partial z}$'s and $\frac{\partial x_i}{\partial t}$'s are indeterminant and this condition represents the necessary condition for the propagation of discontinuities in the first derivatives (zeroth order discontinuities).

In order for the derivatives to have a relationship to one another along the propagation paths it is necessary and sufficient that the determinant representing the numerator also be equal to zero. This holds true for the entire set of partial derivatives $\frac{\partial x_i}{\partial z}$ and $\frac{\partial x_i}{\partial t}$. The expansion of the numerators yields sets of ordinary differential equations valid along the characteristic paths.

2. Single Phase Flow: Wave Propagation and Choking

In single phase flow the wave is considered to be a small pressure perturbation which is mathematically represented as a discontinuity in the first derivatives of the dependent variables. Abbott [23] has a good discussion both of the method of characteristics in general and this problem in particular.

The one-dimensional continuity and momentum equations for a pure fluid (in the absence of body forces and shear terms) may be written:

$$\frac{\partial \rho}{\partial t} + V\frac{\partial \rho}{\partial z} + \rho\frac{\partial V}{\partial z} = 0 \qquad (37)$$

$$\rho\frac{\partial V}{\partial t} + \rho V\frac{\partial V}{\partial z} + \frac{\partial P}{\partial z} = 0 \qquad (38)$$

In addition an equation of state is required:

$$P = P(\rho, s) \qquad (39)$$

and the assumption that the process is isentropic

$$ds = 0$$

Expanding (39)

$$dP = \left(\frac{\partial P}{\partial \rho}\right)_s d\rho + \left(\frac{\partial P}{\partial s}\right)_\rho \cancel{ds}^{\,0} \qquad (40)$$

and substituting back into (38) yields

$$\rho \frac{\partial v}{\partial t} + \rho v \frac{\partial v}{\partial z} + \left(\frac{\partial P}{\partial \rho}\right)_s \frac{\partial \rho}{\partial z} \tag{41}$$

(41) along with (37) and the two equations of variation

$$d\rho = \left(\frac{\partial \rho}{\partial z}\right) dz + \left(\frac{\partial \rho}{\partial t}\right) dt \tag{42}$$

$$dv = \left(\frac{\partial v}{\partial z}\right) dz + \left(\frac{\partial v}{\partial t}\right) dt \tag{43}$$

may be written in matrix form

$$\begin{bmatrix} v & 1 & \rho & 0 \\ \left(\frac{\partial P}{\partial \rho}\right)_s & 0 & \rho v & \rho \\ dz & dt & 0 & 0 \\ 0 & 0 & dz & dt \end{bmatrix} \begin{bmatrix} \frac{\partial \rho}{\partial z} \\ \frac{\partial \rho}{\partial t} \\ \frac{\partial v}{\partial z} \\ \frac{\partial v}{\partial t} \end{bmatrix} = \begin{bmatrix} 0 \\ 0 \\ dP \\ dv \end{bmatrix} \tag{44}$$

If the determinant of the left hand array is set equal to zero and expanded the characteristic directions

$$\frac{dz}{dt} = v \pm \sqrt{\left(\frac{\partial P}{\partial \rho}\right)_s}$$

are obtained. Boure, et al. [4] showed that the isentropic assumption is not required per se, and in fact, that the overall flow may not be isentropic to allow the propagation of the discontinuities to be an isentropic evolution. It is also possible to write the continuity, momentum, and energy equations for single phase flow and if internal shear stresses and conduction are ignored, the same result [8] is obtained without the necessity of formally assuming an isentropic process.

The critical condition for single phase flow occurs when the fluid at some point reaches the sonic velocity and pressure pulses can no longer propagate upstream to affect the flow. This may be examined for the steady state case by considering the condition that

$$\begin{vmatrix} V & \rho \\ \left(\frac{\partial P}{\partial \rho}\right)_s & \rho V \end{vmatrix} = 0$$

or

$$V_{CRITICAL} = \sqrt{\left(\frac{\partial P}{\partial \rho}\right)_s}$$

Thus, the method of characteristics provides a bridge between the examination of pressure pulses and critical flow. This technique, well proven in single phase flow, can be extended to the more complex two-phase flow situation.

3. Two-Phase Flow: Wave Propagation and Choking

The employment of the mixture or diffusional model to two-phase flow problems results in a system of four field equations. Four variables: V_m, α, P, and T_f, remain after the constitutive equations are inserted.

The problem then assumes the form

$$
\begin{array}{l}
\text{Void Propagation} \\
\text{Continuity} \\
\text{Momentum} \\
\text{Energy} \\
\\
\\
\\
\\
\end{array}
\begin{bmatrix}
a_{11} & a_{12} & a_{13} & a_{14} & a_{15} & a_{16} & a_{17} & a_{18} \\
a_{21} & a_{22} & a_{23} & a_{24} & a_{25} & a_{26} & a_{27} & a_{28} \\
a_{31} & a_{32} & a_{33} & a_{34} & a_{35} & a_{36} & a_{37} & a_{38} \\
a_{41} & a_{42} & a_{43} & a_{44} & a_{45} & a_{46} & a_{47} & a_{48} \\
dt & dz & 0 & 0 & 0 & 0 & 0 & 0 \\
0 & 0 & dt & dz & 0 & 0 & 0 & 0 \\
0 & 0 & 0 & 0 & dt & dz & 0 & 0 \\
0 & 0 & 0 & 0 & 0 & 0 & dt & dz
\end{bmatrix}
\begin{bmatrix}
\frac{\partial V_m^*}{\partial t^*} \\
\frac{\partial V_m^*}{\partial z^*} \\
\frac{\partial \alpha^*}{\partial t^*} \\
\frac{\partial \alpha^*}{\partial z^*} \\
\frac{\partial P^*}{\partial t^*} \\
\frac{\partial P^*}{\partial z^*} \\
\frac{\partial T_f^*}{\partial t^*} \\
\frac{\partial T_f^*}{\partial z^*}
\end{bmatrix}
=
\begin{bmatrix}
F_1 \\ F_2 \\ F_3 \\ F_4 \\ dv_m \\ d\alpha \\ dp \\ dT_f
\end{bmatrix}
\tag{45}
$$

where the a_{ij}'s are listed in Appendix B and

$$F_1 = \frac{\rho_m^*}{\rho_f^* \rho_g^*} \Gamma_{gio}^* - \alpha^* V_{gj}^* \frac{2}{D_e^*} \frac{dD_e^*}{dz^*}$$

$$F_2 = - \rho_m^* V_m^* \frac{2}{D_e^*} \frac{dD_e^*}{dz^*}$$

$$F_3 = - \left[P_m - \Pi_D \right] \frac{2}{D_e^*} \frac{dD_e^*}{dz^*} + \frac{4}{D_e^*} \tau_{wo}^*$$

$$F_4 = P\,\Gamma_{gio}\,\frac{\Delta\rho^*}{\rho_g^*\,\rho_f^*} - \Big\{\rho_m^*\,V_m^*\,i_m^* + \big[(1-\alpha^*)\rho_f^*\,i_f^*\,V_{fm}^*$$

$$+\alpha^*\rho_g^*\,i_g^*\,V_{gm}^*\big] - \rho_m^*\,V_m^* - \big[(1-\alpha^*)\rho_f^*\,V_{fm}^* + \alpha^*\,\rho_g^*\,V_{gm}^*\big]\Big\}\frac{2}{D_e}\,\frac{dD_e^*}{dz}$$

If the determinant of the coefficient array in (45) is expanded about the last four rows a quartic equation in $\frac{dz^*}{dt^*}$ results. The coefficients of the quartic expression are of course functions of the a_{ij}'s. The roots of the fourth order polynomial are obtained numerically and represent the characteristic directions for the mixture model.

Steady state choking conditions were obtained by considering the reduced array of the coefficients of the spacial derivatives.

$$\begin{vmatrix} a_{12} & a_{14} & a_{16} & a_{18} \\ a_{22} & a_{24} & a_{26} & a_{28} \\ a_{32} & a_{34} & a_{36} & a_{38} \\ a_{42} & a_{44} & a_{46} & a_{48} \end{vmatrix} = 0 \qquad (46)$$

The mixture mass velocity V_m was iterated for a given set of conditions (pressure, temperature, and void fraction) until condition (46) was satisfied.

Although other values of V_m might satisfy (46) (the trivial solution $V_m = 0$ exists if the slip function is used to provide a value of V_{gj}), the procedure used provides the value of V_m and hence G (i.e., $\rho_m V_m$) most representative of the critical condition.

The range of hyperbolicity was also determined by an iteration technique to determine (for a given set of conditions) at what mass flux the characteristic directions became complex. This information is needed if the equations are to be integrated by the method of characteristics since the roots must be real for the method to apply.

4. Program Wave

The determination of the critical mass flux, the characteristic directions, and the range of hyperbolicity was accomplished by a computer program written in Fortran IV for use on a Univac 1108. The program is straightforward and a copy appears in Appendix C. The rather lengthy nature of the main body of Wave was dictated by the desire to incorporate several slip models and thermodynamic constraints into the program. The subroutine Deter generated the values of the four by four determinants needed in the expansion of (45) and (46) and the subroutine Dat provided the thermodynamic information needed. The ideal gas equation of state was used for the calculation of the vapor properties for two-component (air-water) flow. The effect of relative humidity in the gaseous phase was considered. Since single-component (steam-water) flow was to be examined in Appendix A, the properties of steam were included in subroutine Dat. The equations of state for steam and for the liquid were calculated on the basis of the equations appearing in Keenan and Keyes Steam Tables [53].

The actual solution for the roots of the quartic equation, necessary to determine the characteristic directions, was provided by a packaged root finding subroutine which is a part of the computer library for the Univac 1108. This obviated the need to write a separate subroutine to perform this function.

CHAPTER V

RESULTS AND CONCLUSIONS

The results of the analysis are presented in separate sections for wave propagation, choking, and the range of hyperbolicity for two-component (air-water) flow. The section on the results for critical flow also includes a discussion on the relationship between critical flow and pressure pulse propagation in two-component flows.

1. Pressure Pulse Propagation in Two-Component Flow

a. Bubbly Flow

Henry, et al. [28] have taken data on pressure pulse propagation in vertical tubes under bubbly flow conditions. The speeds recorded represent leading edge data and the results presented in this section ignore such effects as dispersion and scattering.

Using Equation (27) for V_{gj}, the four roots representing the characteristic directions are always real under the conditions tested ($0 < \alpha < 1$, 25 psia $\leq P \leq 65$ psia, $T = 70^{o}F$) even when the mass flux inputed is increased well beyond the expected critical flux for a given value of void fraction and pressure.

One root was always the mass averaged velocity of the liquid V_f and one was always the mass averaged velocity of the gas V_g. The other two roots were assumed, from the single phase analogue to represent V_p-C and V_p+C, respectively, where V_p is the velocity relative to which the waves were propagating. C would therefore be the speed of sound.

It was mentioned in the literature review that many of the models used to predict the speed of pressure pulse propagation do not indicate what the fluid reference velocity is. This could prove to be a major flaw if anything other than very low fluid velocities are considered.

For the specific function of V_{gj} used in this model (Equation 27) V_p was exactly (within the accuracy of the root finding program) V_m, the velocity of the center of mass of the mixture. This was true even at low values of V_m and relatively high values of the void fraction where the predicted slip ratio might rise to a value of two, and where $V_f \ll V_m$ so that a clear determination of V_p could be made. In addition the propagation velocity C was independent of V_m.

It must be stated, however, that the model does not require this particular function for V_{gj} to prove effective. If one assumes homogeneous flow (S = 1) or the Armand slip model (with $1 < C_o < 1.2$), the propagation speed results reproduce those obtained with Equation (27) within 4 percent for the range of pressure and void fractions ($\alpha < .5$) tested.

In any event it was determined that the best results over the widest range of α occurred when an isentropic evolution (polytropic exponent $n = k = 1.4$) was assumed for the gaseous phase. Figures 2 through 5 show the correspondence of this drift flux model with the data.

If either a complete thermal equilibrium model ($T_g \equiv T_f$, $\frac{\partial T_g}{\partial z} = \frac{\partial T_f}{\partial z}$, and $\frac{\partial T_g}{\partial t} = \frac{\partial T_f}{\partial t}$) or an isothermal model ($n = 1$) is assumed, the predicted velocities are somewhat below the isentropic values and most of the data (see Tables 1 and 2). However, the advantage of the isentropic condition over the isothermal becomes less apparent at low values of the void fraction and in fact as the bubble size decreases ($\alpha < .05$), the isothermal

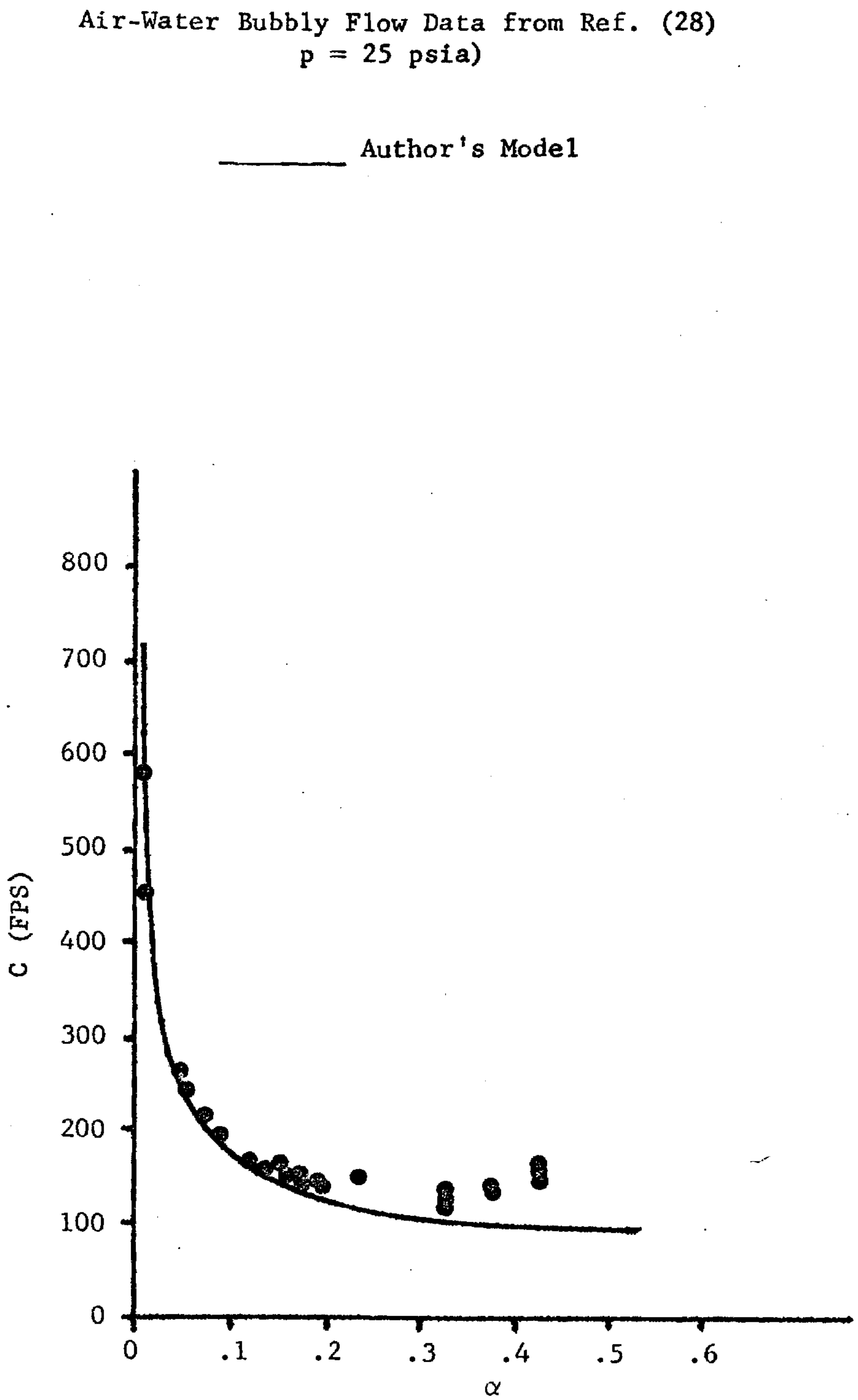

Figure 2. Two-Component Pressure Pulse Speed

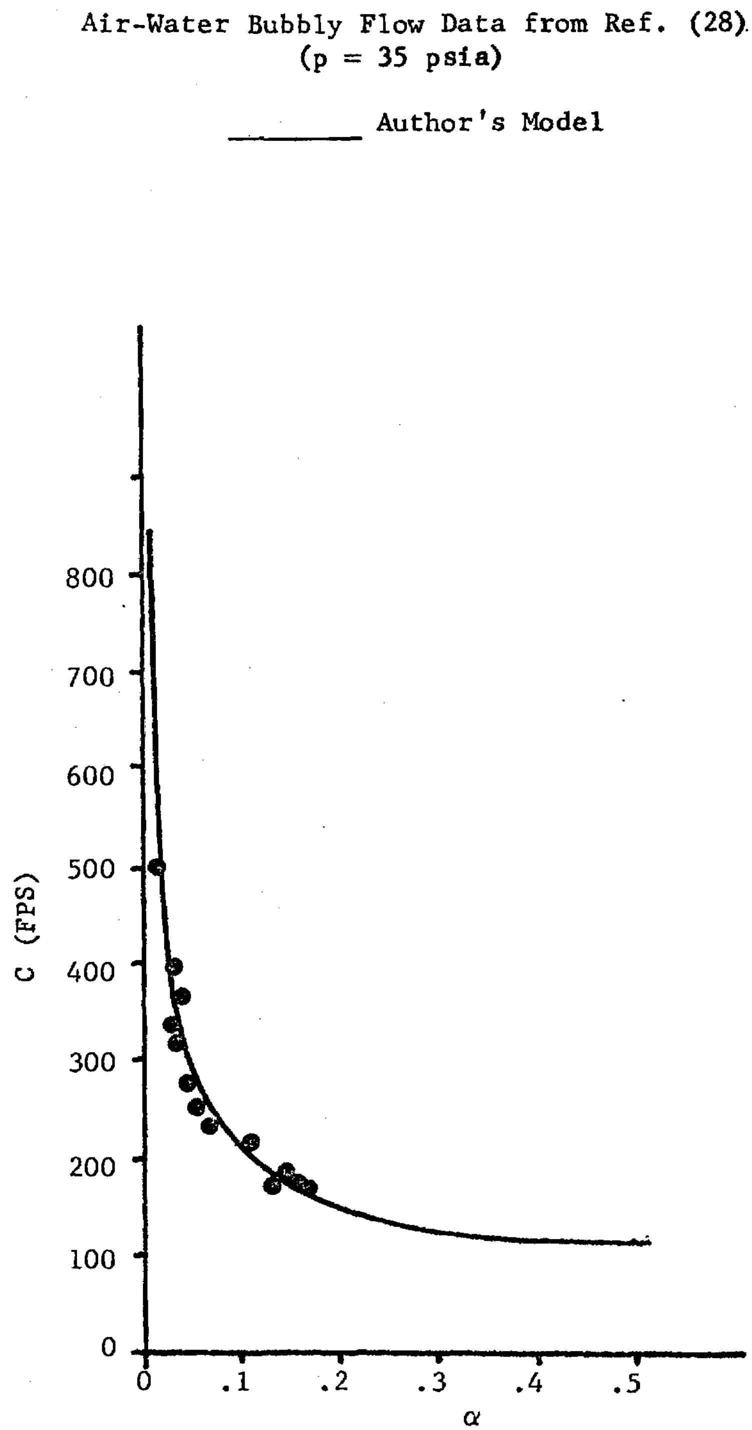

Figure 3. Two-Component Pressure Pulse Speed

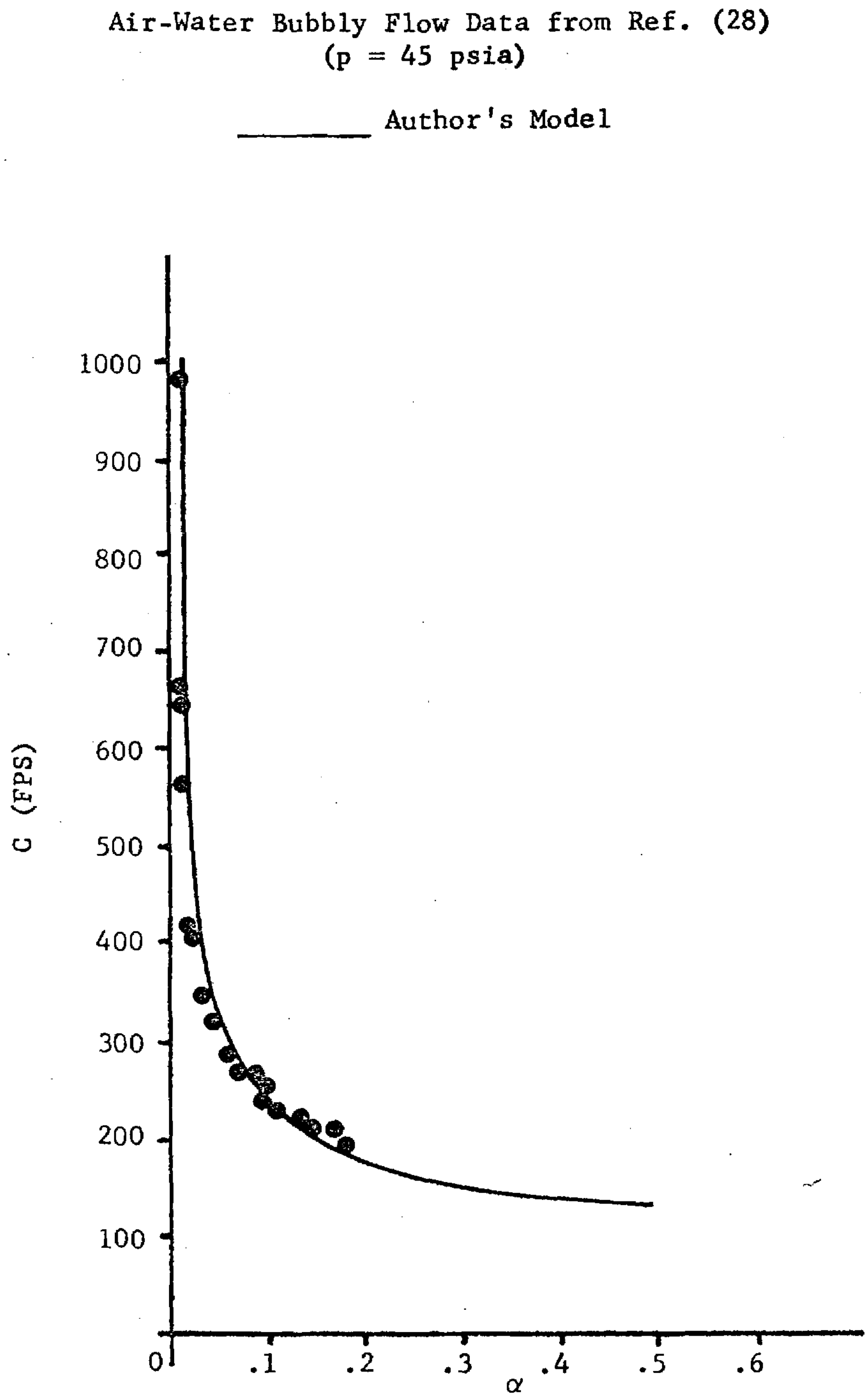

Figure 4. Two-Component Pressure Pulse Speed

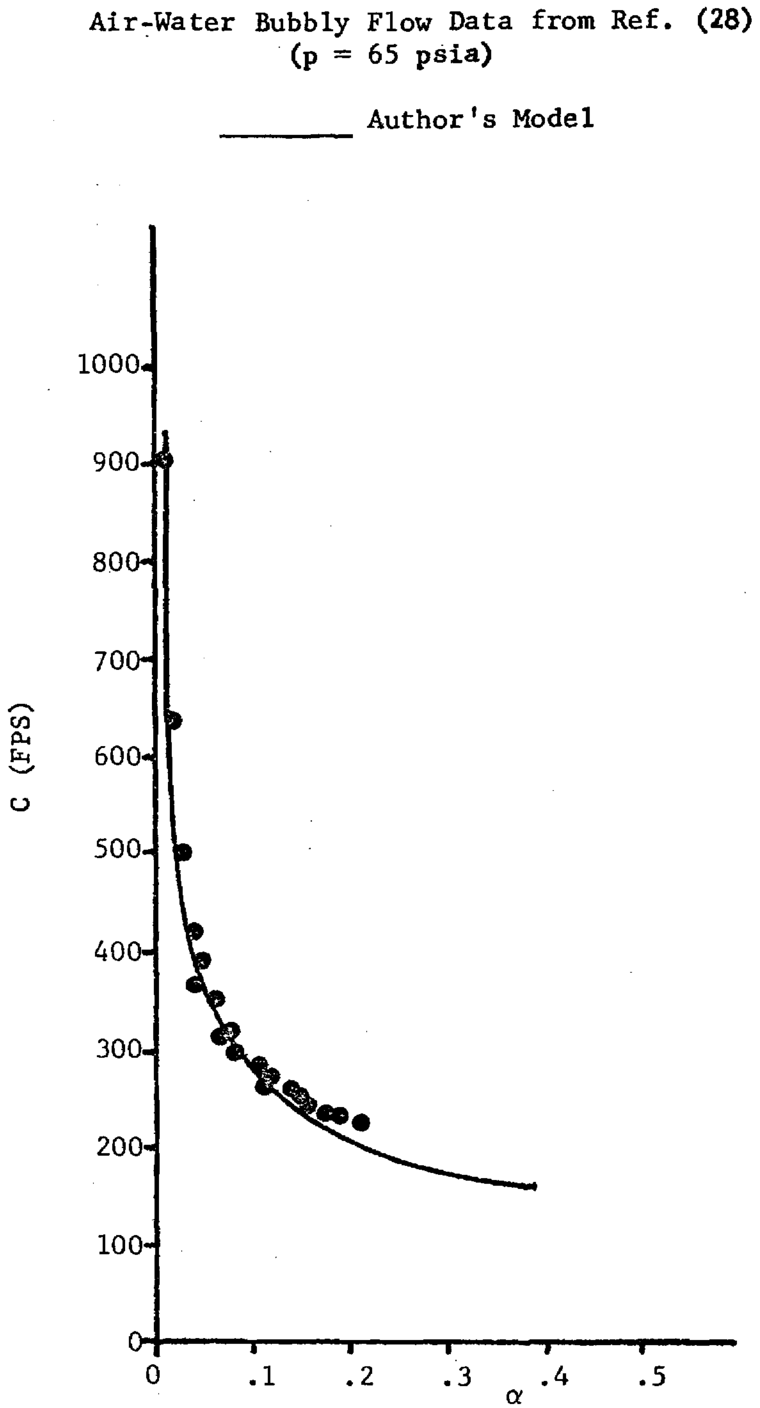

Figure 5. Two-Component Pressure Pulse Speed

limit appears to be more appropriate since the thermal response of the vapor should become more pronounced. Presumably a continuous transition exists between the polytropic exponent of 1. ($\alpha \to 0$) and the isentropic exponent ($\alpha \to .1$). Sufficient scatter existed in the data to obscure the exact functional form of $n(\alpha)$ so no attempt was made to provide one. This same effect was noted in reference [28] for example.

The thermal equilibrium model provides values essentially identical to those produced by the isothermal assumption. This occurs because the liquid acts as a large thermal reservoir and hence the gas temperature varies little when complete thermal equilibrium is used as the thermodynamic constraint.

For all of the results presented, the thermal approximation $T_f = T_g$ was employed for the purpose of calculating the property values of the components. The small degree of static temperature nonequilibrium (a few degrees F) which may exist in the actual system does not affect either the thermodynamic quantities or the results very much (on the order of 1 percent, see reference [24]), and since the actual amount of thermal nonequilibrium is not known this assumption is almost a requisite. The assumption of the particular thermodynamic evolution does however affect the results and the isentropic assumption may be thought of in the same sense that simple heating or cooling results are used in 1-D Fanno line flow [1]. This implies that whatever heat transfer does occur through the passage of the wave front velocity which is the measured quantity. This is analogous to the concept of frozen wave speeds in combustion processes with the bulk of the wave traveling at a speed more in line with the equilibrium (thermal) velocity.

The effect of static values of relative humidity on the predicted wave speeds was expected to be small. In fact the variation in predicted propagation velocities at low pressure with a variation of relative humidity from 0% to 95% was smaller than the tolerance of the root finding program.

Since the exact slip relationship (or relation for V_{gj}) does not affect the predicted velocity of sound propagation very much at low mass fluxes as long as the value of the slip ratio remains in a range reasonable for bubbly flow at low void fractions ($S \leq 1.2$), it would appear that the non-dimensional field equations could be reduced to provide a simple approximate relationship for the speed of sound.

If we limit our attention to relatively low mass velocities and use the isothermal speed of sound as our reference velocity V_o, we may simplify Equations (33)-(35). If we consider only the highest order terms the equations become:

<u>Void propagation</u>

$$\frac{\partial \alpha^*}{\partial t^*} + \alpha^*(1-\alpha^*)\left[\frac{1}{\rho_g^*} M_{Tg}^2 - \frac{1}{\rho_f^*} M_{Tf}^2\right] \frac{\partial p^*}{\partial t^*} \tag{47}$$

$$+ \frac{\alpha^*(1-\alpha^*)}{\rho_g^*} N_{pg} \frac{\partial T_g^*}{\partial t^*} = 0$$

<u>Continuity</u>

$$\rho_m^* \frac{\partial V_m^*}{\partial z^*} + \Delta\rho^* \frac{\partial \alpha^*}{\partial t^*} + \left[\alpha^* M_{Tg}^2 + (1-\alpha^*) M_{Tf}^2\right] \frac{\partial p^*}{\partial t^*} \tag{48}$$

$$+ \alpha^* N_{pg} \frac{\partial T_g^*}{\partial t^*} = 0$$

Momentum

$$\rho_m^* \frac{\partial V_m^*}{\partial t^*} + \frac{\partial P^*}{\partial z^*} = 0 \tag{49}$$

Actually the terms involving the temperature are of order (δ), but it should be recognized that under our isentropic assumption the temperature terms combine with the pressure terms in Equations (47) and (48) to yield the isentropic speed of sound of the gas rather than the isothermal speed of sound as a reference. Also, the highest order liquid compressibility terms were included so the result remains finite as $\alpha \to 0$.

The energy equation is not needed for this simplified analysis because we are specifying the thermodynamic constraint on the gaseous phase and the liquid temperature does not appear in the reduced equations. This is similar to the situation in single phase flow when

$$d\rho = \left(\frac{\partial \rho}{\partial P}\right)_s dP$$

is used rather than the more general form

$$d\rho = \left(\frac{\partial \rho}{\partial P}\right)_T dP + \left(\frac{\partial \rho}{\partial T}\right)_P dT$$

along with the energy equation.

Combining (47) and (48) and invoking the isentropic condition we may examine the characteristics of the system by writing the resulting equations in matrix form

$$\begin{bmatrix} a_{11} & 0 & 0 & \rho_m^* \\ 0 & 1 & \rho_m^* & 0 \\ dt^* & dz^* & 0 & 0 \\ 0 & 0 & dt^* & dz^* \end{bmatrix} \begin{bmatrix} \frac{\partial p^*}{\partial t^*} \\ \frac{\partial p^*}{\partial z^*} \\ \frac{\partial V_m^*}{\partial t^*} \\ \frac{\partial V_m^*}{\partial z^*} \end{bmatrix} = \begin{bmatrix} 0 \\ 0 \\ dp^* \\ dV_m^* \end{bmatrix}$$

where

$$a_{11} = \alpha^* M_{sg}^2 \left[1 - (1-\alpha^*) \frac{\Delta\rho^*}{\rho_g^*}\right] + (1-\alpha^*) M_{sf}^2 \left[1 + \alpha^* \frac{\Delta\rho^*}{\rho_f^*}\right] \tag{51}$$

the characteristic directions are (returning to a dimensional form)

$$C = \frac{dz}{dt} = \pm \left[\alpha\left(\frac{\partial \rho_g}{\partial P}\right)_s + \frac{\alpha(1-\alpha)(\rho_f - \rho_g)}{\rho_g}\left(\frac{\partial \rho_g}{\partial P}\right)_s + (1-\alpha)\left(\frac{\partial \rho_f}{\partial P}\right)_s + \frac{\alpha(1-\alpha)(\rho_g - \rho_f)}{\rho_f}\left(\frac{\partial \rho_f}{\partial P}\right)_s\right]^{-1/2} \tag{52}$$

This result is identical to the standard homogeneous form used in the literature. For example, Henry, et al. [28] provide a form under the same general assumptions

$$C = \pm \left[\alpha^2 \left(\frac{\partial \rho_g}{\partial P}\right)_s + \alpha(1-\alpha)\frac{\rho_f}{\rho_g}\left(\frac{\partial \rho_g}{\partial P}\right)_s + (1-\alpha)^2\left(\frac{\partial \rho_f}{\partial P}\right)_s + \alpha(1-\alpha)\frac{\rho_g}{\rho_f}\left(\frac{\partial \rho_f}{\partial P}\right)_s \right]^{-1/2} \qquad (53)$$

Equation (52) is exactly equivalent to (53) as a simple expansion of the terms in (52) will show.

Tables 1 and 2 show a comparison of the full drift flux model with the simplified analysis. It is evident that the results of Equation (52) (or 53) correspond almost exactly with the more detailed analysis. Under these circumstances it would appear that the simplified model can successfully calculate wave propagation speeds at low mass fluxes.

Experience with the full drift flux model suggests that the appropriate fluid reference velocity for either Equation (52) or (53) is V_m, the velocity of the center of mass of the system.

However, this is true only at relatively low mass velocities. If the modified Armand correlation is used, as the assumed mass flux increases V_p deviates more and more from V_m and the speed of sound C becomes a weak function of V_m. This suggests that simplified relations such as (52) and (53) will deviate (as in fact the assumptions used to produce their derivations imply) more and more from the data as the fluid velocities increase. To the author's knowledge no pressure pulse data have been taken in high speed bubbly flow so that this remains an area largely unexplored at present.

b. Separated and Mist Flow

While the correspondence of the drift-flux model with wave speeds

Table 1. Air-Water Bubbly Flow

α	V_{gj} defined by Equation (27) $C_{isentropic}$	$C_{isothermal}$	C Equation (52) or (53)
.005	716.4	605.6	717.9
.05	234.	197.7	233.9
.1	170.1	143.7	170.0
.2	127.6	107.7	127.5
.3	111.4	94.0	111.3
.4	104.1	87.9	104.1
.5	102.0	86.1	101.9

P = 25 psia
T = 70°F
The speed of sound C is in FPS

Table 2. Air-Water Bubbly Flow

α	V_{gj} defined by Equation (27) $C_{isentropic}$	$C_{isothermal}$	C Equation (52) or (53)
.005	1136.4	962.3	1144.2
.05	367.7	318.2	367.7
.1	274.0	231.4	273.9
.2	205.6	173.6	205.4
.3	179.4	151.5	179.3
.4	167.7	141.6	167.6
.5	164.2	138.7	164.1

P = 65 psia
T = 70°F
The speed of sound C is in FPS

in bubbly flow is good, success was not achieved in providing pulse propagation speeds for separated or mist flows. In these cases, experimenters [28] have recorded single speeds of sound either at exactly the isentropic sonic velocity of the gas phase (purely separated) or just under the gas sonic velocity (in mist flows). This has been noted even though in separated flow the existence of a continuous liquid layer suggests that two speeds of sound should be observed with one representing propagation at the speed of sound of the liquid.

In any event the drift-flux model seriously underpredicted the propagation speeds when Equation (28) was used for the slip function with various values of C_o.

Since neither a good dynamic relationship for V_{gj} or the slip exists in separated or annular mist flow, it remains to be seen whether the development of such a function would improve the results. It is possible that the mathematical coupling inherent in the drift flux model (both V_m and V_{gj} are functions of both V_g and V_f) is responsible for the poor agreement since the successful analytic predictions in this type of flow topology have all resulted from two fluid models which essentially uncoupled [28] or lightly coupled [30] the interphase momentum exchange during the wave passage. Fortunately, however, this problem is not significant with regard to critical flow results for reasons to be explained later.

2. Choking in Two-Component Flow

Henry [50] has taken data on air-water critical flow in a straight duct with a slightly flared end. The critical pressure was 17 psia and the void fraction was measured by gamma-ray attenuation. In order to accurately check any properly formulated critical flow model, accurate data on the void fraction at the choking point are necessary. This is true because the mass flux ($\rho_m V_m$), which is the predicted quantity, is a strong function of α over most of the void fraction range, especially at low pressures where the density difference between the phases is large. If only the quality X is measured, a reasonable uncertainty in the value of α exists since the slip ratio S is not accurately known. This occurs through kinematic considerations since

$$\alpha = \frac{1}{1 + \left(\frac{1-X}{X}\right) S \frac{\rho_g}{\rho_f}} \tag{54}$$

Gamma ray attenuation provides a reasonably accurate means of measuring the void fraction and the data by Henry are therefore probably quite good.

An isentropic evolution was used for the model along with the Armand correlation for the slip ratio (C_o = 1.15) which was depicted in Figure 1. The results of the analysis are shown in Figure 6. Table 3 lists the actual data along with the predictions and relative error. It may be seen that quite good agreement exists between the model and the data with the error increasing slightly at higher void fractions.

If the mass flux predictions for a given α are used as an input to determine the characteristic directions, one root approaches zero. This indicates that from the standpoint of the model the rarefaction waves no longer propagate upstream at the critical point. This is mathematically analogous to the single phase critical condition and indicates that the normal single phase relationship exists between the characteristic

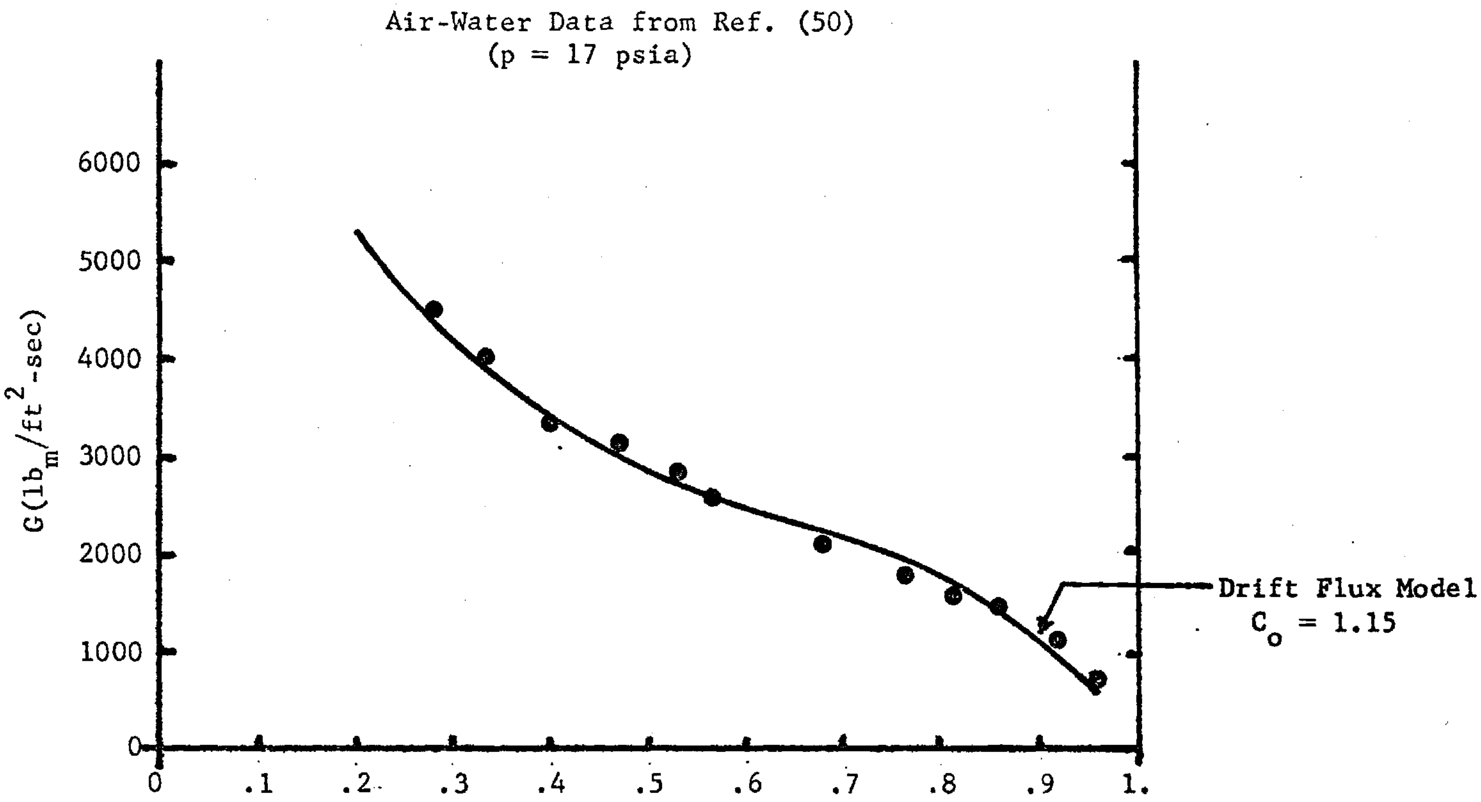

Figure 6. Two-Component Critical Flow

Table 3. Air-Water Critical Flow

α	G_m (measured)	G_p (predicted)	$\frac{G_p = G_m}{G_m} \times 100$ %	$G_{Eqn.\ (52)}$	$\frac{G_{Eqn.\ (52)} - G_m}{G_m} \times 100$ %
.277	4500	4382	- 2.6	4235	- 5.9
.336	4000	3860	- 3.5	3685	- 7.9
.405	3300	3353	+ 1.6	3178	- 3.7
.474	3100	2969	- 4.2	2763	- 10.9
.528	2800	2720	- 2.9	2480	- 11.4
.558	2600	2603	+ .1	2335	- 10.2
.689	2100	2151	+ 2.4	1764	- 16
.768	1800	2014	+ 11.9	1444	- 19.8
.817	1600	1733	+ 8.3	1244	- 22.3
.860	1450	1409	- 2.8	1061	- 26.8
.913	1100	989	- 10.1	815	- 25.9
.964	640	552	- 13.8	516	- 19.4

P = 17 psia
T = 70°F

directions and the latent roots of the steady state system (see Abbott [23] for example).

At low to moderate values of the void fraction the same drift-flux model predicts both wave propagation speeds and choking conditions accurately. This suggests physically that the mechanism for choking is identical for bubbly flow to the single phase analogue.

At high values of α where an annular mist condition probably exists the drift flux model predicts the critical condition with reasonable accuracy, but not the corresponding wave speeds. However, if the air-water choking data by Henry are analyzed in the high void fraction range, they indicate that the speed of the gas in what should be a mist or annular mist regime is less than the speed of sound information indicates for wave propagation results. For example, at a void fraction of .964, the recorded quality was .0827, and the mass flux G = 640 lbm/ft^2-sec. Since

$$\chi = \frac{G_{gas}}{G_{TOTAL}} = 0.827 = \frac{(.964)(.087)V_g}{640}$$

then

$$V_g = 631 \text{ FPS}$$

or significantly less than the sonic velocity of the gas. If these data are accurate, specifically, if the measured void fraction is accurate, then the choking mechanism which is <u>mathematically</u> related in the drift flux model to wave propagation may not however be physically related to measured wave propagation results under stratified or annular mist conditions.

Several researchers [19,22] have tried to connect speed of sound information with the critical conditions at high values of the void fraction, but Henry's experimental evidence suggests that this is in error. More good data in which both void fraction and quality are accurately measured may be needed to clarify this point.

It does, therefore, appear that the single phase analogy between wave propagation and choking holds for at least the bubbly flow regime in two-component flow. The one-component situation is somewhat more complicated, however, due to the relative importance of flashing. This point is discussed in more detail in Appendix A.

In order to formulate a simplified model to predict choking in two-component flow, the non-dimensional equations (33-35) were again examined, this time using V_m as the reference velocity V_o. After some rearrangement, a form identical to Equation (52) was derived for $V_{m_{crit}}$ and the results tabulated in Table 3. It may be noted that in this case, at high mass velocities, the effect of slip becomes more pronounced than in the low speed wave propagation case, and hence the more complete drift-flux model provides a much better fit of the data.

If the same model is applied to Vogrin's [49] air-water critical flow data, a large overprediction of the mass flux results. Vogrin took his data in a converging-diverging nozzle using gamma-ray attenuation to measure the void fraction. However, the scale drawing of the nozzle indicates a very small axial radius of curvature at the throat of the nozzle.

This suggests that two-dimensional effects may play a significant role in the flow field in the vicinity of the critical point. This same phenomenon has been noted in single phase flow in converging-diverging nozzles [47,48] where the two-dimensional aspects of the flow became important if the ratio of the axial radius of curvature at the throat to the throat diameter was less than 1. As this ratio decreased, so did the ratio of the actual single phase mass flux to the mass flux prediction, based on a one-dimensional analysis [47].

This suggests that the inclusion of a covariant term to account for the two-dimensionality of the velocity profile in the vicinity of the critical point might be useful in correlating not only Vogrin's data, but also critical flows in sharp edged orifices. It is assumed that the most significant covariant term is the one appearing in the momentum equation (Equation (3)) since this term accounts for the main effect of the two-dimensionality in the velocity profile. In fact, the assumption of a uniform pressure across the cross section would also break down, but this would require at least one additional constitutive equation for the pressure variation along with at least one more covariant term. This information is not presently available.

The additional term in the momentum equation is

$$\frac{\partial}{\partial z} \operatorname{cov}(\mathrm{mom}\ T)$$

but

$$\operatorname{cov}(\mathrm{mom}\ T) = (1-\alpha)\,\rho_f \operatorname{cov}(V_f \cdot V_f) + \alpha\,\rho_g \operatorname{cov}(V_g \cdot V_g)$$

The individual covariance terms represent the difference between the average of the velocity squared and the square of the mass averaged velocity (a positive quantity in cocurrent flow)

$$\mathrm{cov}\,(V_K \cdot V_K) = \langle V_K^2 \rangle - \langle V_K \rangle^2$$

These terms may be approximated as some constant b times the mass averaged velocity squared or

$$\mathrm{Cov}\,(V_K \cdot V_K) = b_K \langle V_K \rangle^2 = b_K V_K^2$$

(In laminar single phase fully developed flow, b would equal 1/3. Of course, in fully developed flow which is not our condition here, $\frac{\partial}{\partial z}$ cov (mom T) = 0 by definition.) If in addition, it is assumed that the primary regime of interest is a turbulent bubbly flow at intermediate values of the void fraction, we should be able to use a single constant to describe both covariant terms. Therefore

$$\mathrm{cov}\,(V_f \cdot V_f) = b V_f^2$$

and

$$\mathrm{cov}\,(V_g \cdot V_g) = b V_g^2$$

so

$$\frac{\partial}{\partial z}\left[\text{cov}\,(\text{mom}\,T)\right] = \frac{\partial}{\partial z}\left[(1-\alpha)\rho_f\, b\, V_f^2\right.$$

$$\left. + \alpha\, \rho_g\, b\, V_g^2\right]$$

If these additional terms are added to the momentum equation with b = .8, significantly improved correspondence exists with Vogrin's data. What this implies is that as the critical point is approached the velocity profiles become more irregular, which would appear to be a reasonable assumption. Table 4 lists the results of the original choking model (isentropic flow, Armand correlation), the improved model (inclusion of covariant term), and some predictions Vogrin included in his report.

While it must be noted that the correspondence of the modified prediction is still far from excellent, it is clearly better than either the original drift-flux model or the two predictions included in Vogrin's report. It would be expected that a better fit of the data would occur if b were assumed to be a function of void fraction and pressure, or possibly simply ρ_m. However, the purpose of this is to show that for a given orifice or nozzle a covariant correlation coefficient may prove (in the same sense that nozzle discharge coefficients are used) to be useful in accommodating the two-dimensional aspects of the flow.

It should also be pointed out that the insertion of the covariant term is related to the inclusion of partial derivatives in the interfacial shear stress relationship used by some investigators [45] with a two-fluid model. However, it is felt that the formulation suggested in the preceding section is more representative of the correct reason for the inclusion of the derivative term than that advanced by Boure, et al. [45].

Table 4. Vogrin's Air-Water Critical Flow Data

P_{throat} psia	α_{throat}	G_{data}	G_{p1}	G_{p2}	$\frac{G_{p2} - G_D}{G_D} \times 100$ %	$G_{homogeneous}$	G_{Fauske}
19.9	.473	2119	3232	2410	+ 13.7	990	4400
33.8	.640	2140	3255	2422	+ 13.2	1200	
52.8	.698	2119	3734	2784	+ 31.4	1380	6950
31.6	.568	2960	3494	2602	- 12.1	1546	
28.4	.839	1280	2000	1492	+ 16.6	710	2380
46.8	.878	1305	2025	1510	+ 15.7	876	
31.5	.540	2960	3632	2712	- 8.4	1500	4690

$T \approx 70^{o}F$

G in lbm/ft^2-sec

G_{p1} was calculated on the basis of an isentropic assumption with the Armand correlation

G_{p2} same as G_{p1} with covariant coefficient of .8

$\left.\begin{matrix} G_{homogeneous} \\ G_{Fauske} \end{matrix}\right\}$ two predictions included in Vogrin's report

3. Range of Hyperbolicity

For a given set of pressure, temperature, fluid constituents, and void fraction, an iterative procedure (starting at $G = 0$) was used to determine the range of mass flux over which the characteristic directions were real. This establishes the extent of the region over which the method of characteristics can be applied and also seems related to the stability of the solution obtained when other methods of finite difference integration are employed.

For two-component air water flows at low pressures the roots were always real when Equation (27) was used for V_{gj} even when the mass flux was increased to twice the value of the critical condition for the given situation. If the Armand correlation was used ($C_o = 1.15$), the absolute range of hyperbolicity was reduced to less than the critical value of the mass flux as low α's, but the value of the imaginary part of the roots was on the order of 10^{-7}. Under these conditions the complex roots were also not conjugate and due to the small magnitude of the imaginary part (much smaller than the accuracy of the root finding subroutine) it is suggested that this represents a numerical aberration in the root solution. If a value of 10^{-5} for example is established as the minimum magnitude of the imaginary part of the characteristics for the purpose of determining the range of hyperbolicity, then the required mass flux is much larger than the predicted critical flux for the given set of conditions.

This indicates that the drift-flux model may be successfully used in the numerical integration of two-component flow problems up to and including the critical condition. Some investigators have had difficulty with specific two-fluid models due to a limited range of hyperbolicity.

4. Conclusions

The following conclusions may be drawn from the present investigation.

1. The drift-flux model can successfully predict leading edge pressure pulse velocities in bubbly two-component flow. At low mass fluxes the simplified form (Equation (52)) is very accurate and may be substituted for the full model. At higher mass fluxes then it would be expected that more and more deviation from Equation (52) would result although no data exist to support this conclusion.

2. At low mass fluxes in bubbly blow V_m is the appropriate reference velocity for the pulse propagation. As the mass flux increases, the model suggests that the propagation reference velocity may deviate from V_m. Again, data taken at high mass fluxes are needed to verify this assumption.

3. The drift-flux model will not provide the measured propagation velocities in separated or annular mist flow. This may result from the lack of a good dynamic expression for V_{gj} or the slip under these conditions.

4. The model does provide good agreement with the critical flux in straignt pipes for two-component flow. The correspondence of the model with both critical flow and wave propagation in bubbly flow indicates that the Reynolds mechanism for choking occurs in bubbly flow. In annular flow the choking mechanism is suggested by the Reynolds mechanism with the sonic condition of the mist being the criteria, but more good two-component data are needed to clarify this point.

5. The two-dimensional aspects of a flow in sharp edged orifices and nozzles can be successfully handled by a covariant correlation.

6. The range of hyperbolicity appears sufficient to allow the successful numerical integration of the equations up to and including the critical condition.

APPENDICES

APPENDIX A

WAVE PROPAGATION AND CHOKING IN ONE-COMPONENT FLOW

If the model employed for two-component flow is applied to one-component (steam-water) wave propagation in a bubbly mixture, the picture becomes less clear. The frozen isentropic model corresponds reasonably well to data taken by Karplus [26] and Henry, et al. [28] (see Figures 7 and 8), but the large amount of scatter makes it difficult to conceive of any sort of model making accurate predictions. If the same formulation is used on data by DeJong, et al. [44], the model seriously underpredicts their results, except at very low α, even though the regime should clearly be bubbly flow. The effect of non-equilibrium may account for the discrepancies and large scatter, although this is still to be determined.

If the same frozen isentropic model is applied to the critical flow situation the results consistently overpredict by wide margins the available data (see Figures 9-11). This suggests that the effect of the flashing present in critical flow contributes significantly to the conditions at the critical point. In general, it appears that while the wave front in one-component wave propagation travels in a substantially frozen manner, the critical condition is representative of non-equilibrium flashing even though, as previously mentioned, the large degree of scatter and inability of a frozen model to predict some of the available wave propagation data leave some room for doubt. This difference between wave propagation and critical flow conditions is however physically appealing. The wave front

Steam-Water Data from Ref. (26)
(p = 10 psia)

________ Author's Frozen Model

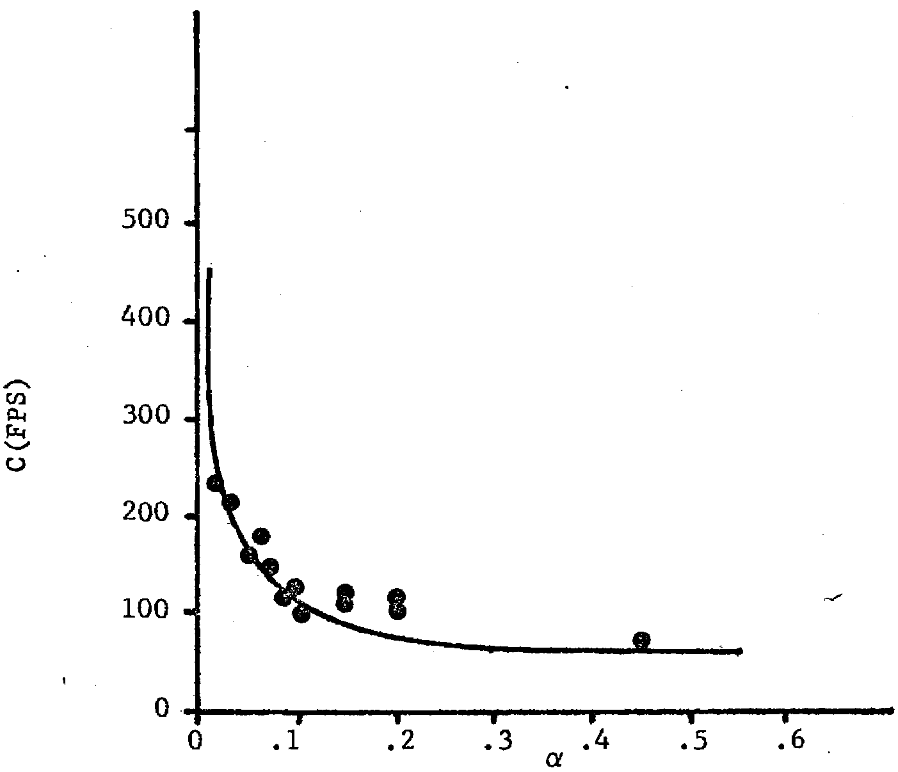

Figure 7. One-Component Pressure Pulse Speed

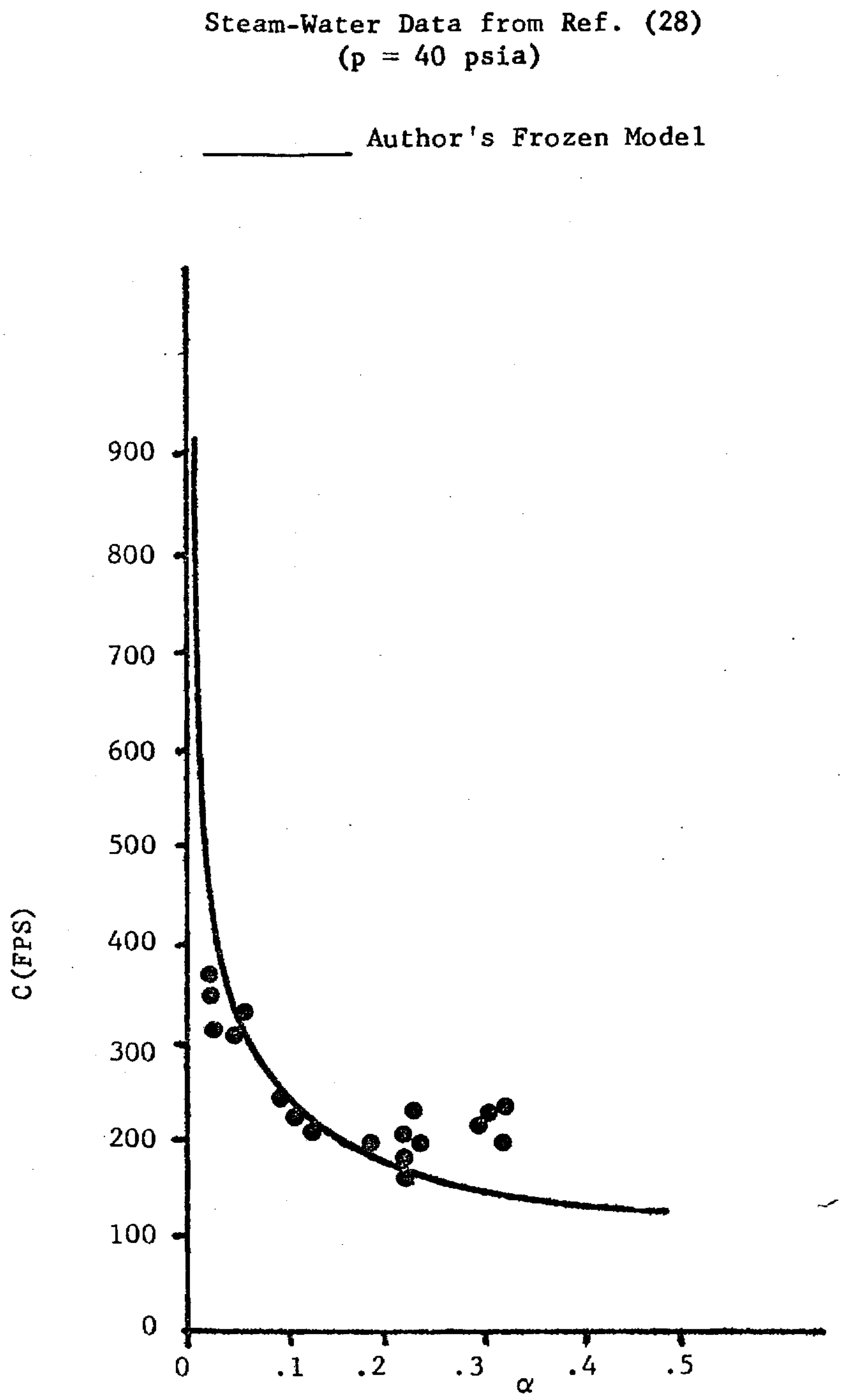

Figure 8. One-Component Pressure Pulse Speed

represents the leading edge of the pressure pulse in a mathematical sense although in actual fact some effect of the pulse may be felt ahead of what the 1-D model predicts as the wave front, due to the fact that the isentropic speed of sound of both vapor and liquid are higher than the observed and predicted average velocities of the pressure pulse (except at high α's and as $\alpha \to 0$). In the case of critical flow the observed choking point however is situated near the center of a region in which there is a large pressure drop. This suggests that in the case of one-component choking the concept of frozen equilibrium cannot be supported as indeed the data indicate. Numerous authors (for example [51]) have suggested that such non-equilibrium effects are important.

In order to account for the effect of flashing in one-component flow, J. Boure, et al. [45] have suggested a constitutive equation of the form

$$\Gamma_{gi} = \Gamma_{gio} + C_1 \frac{d\Delta i_g}{dz} + C_2 \frac{d\Delta i_f}{dz} \tag{A1}$$

where

$$\Delta i_g = - i_g(P, T_g) + i_{g\,sat}(P)$$

$$\Delta i_f = - i_f(P, T_f) + i_{f\,sat}(P)$$

However, no mention of the functional form of C_1 or C_2 was made nor were any results presented. If elementary kinetic theory is examined, a simplified more explicit form of A1 may be deduced. The net vaporization flux in evaporization from reference [52] is

$$j_v = \alpha_v (P_{SAT} - P) / (2\pi m K T)^{1/2} \qquad \text{(A2)}$$

where α_v is an evaporization coefficient ≈ 1. However A2 is derived on the assumption that the external pressure field has no steep pressure gradients in the region of interest. If we define

$$\Delta P = P - P_{SAT}$$

and consider a region where such steep pressure gradients exist, but where variation in $T^{-\frac{1}{2}}$ is small compared to this pressure variation, then from a first order Taylor approximation

$$\Gamma_{gi} = \frac{1}{A_{TC}} \frac{m \alpha_v}{(2\pi m K T)^{1/2}} \left[\int_{\xi_i} \Delta P \frac{dA}{dz} + \int_{\xi_i} \left(\frac{d\Delta P}{dz} dz \right) \frac{dA}{dz} \right] \qquad \text{(A3)}$$

If we assume in the vicinity of the critical point that $\frac{\partial \Delta P}{\partial z}$ ≈ constant, then A3 may be rewritten as

$$\Gamma_{gi} = \Gamma_{gio} + \frac{1}{A_{TC}} \left(\int_{\xi_i} dA \right) \frac{m \alpha_v}{(2\pi m K T)^{1/2}} \frac{d\Delta P}{dz} \qquad \text{(A4)}$$

where

$$\Gamma_{gio} = \frac{1}{A_{TC}} \frac{m \alpha_v}{(2\pi m K T)^{1/2}} \int_{\xi_i} \Delta P \frac{dA}{dz}$$

If we assume further that the pressure non-equilibrium ΔP is small and consider the isothermal process (almost isentropic) at T_g between P_{sat} and P then

$$T\,ds = di - \frac{1}{\rho_g}\,dP \approx \Delta i - \frac{1}{\rho_g}\,\Delta P \approx 0$$

or $\Delta P \approx \rho_g\ \Delta h$ where ρ_g is assumed to vary less than Δh.

Since $\frac{1}{A_{Tc}} \int \xi dA_s$ should be a strong function of the void fraction we have upon conversion to British engineering units

$$\Gamma_{gi} = \Gamma_{gio} + \frac{C_v\ F(\alpha)\ \rho_g}{(RT)^{1/2}}\ \frac{d\Delta i_g}{dz} \tag{A5}$$

where C_v is a constant for a given critical pressure.

This is of course a highly simplified analysis, but if

$$F(\alpha) = \alpha\,(1-\alpha)^{.1} \tag{A6}$$

and C_v is allowed to be a function of the pressure at the critical point, reasonable correspondence with the data is shown (Figures 9, 10, and 11). Of course, only the second part of Equation A5 enters into the determinant which provides a prediction of the conditions at the critical point.

For the model displayed in Figures 9-11, a value of $C_o = 1.1$ was used with a cutoff alpha of 80% of the value at which the slip ratio becomes infinite. The reason that the reduced cutoff was used (rather than the 90% used previously) was because a slight hook occurred in the predicted

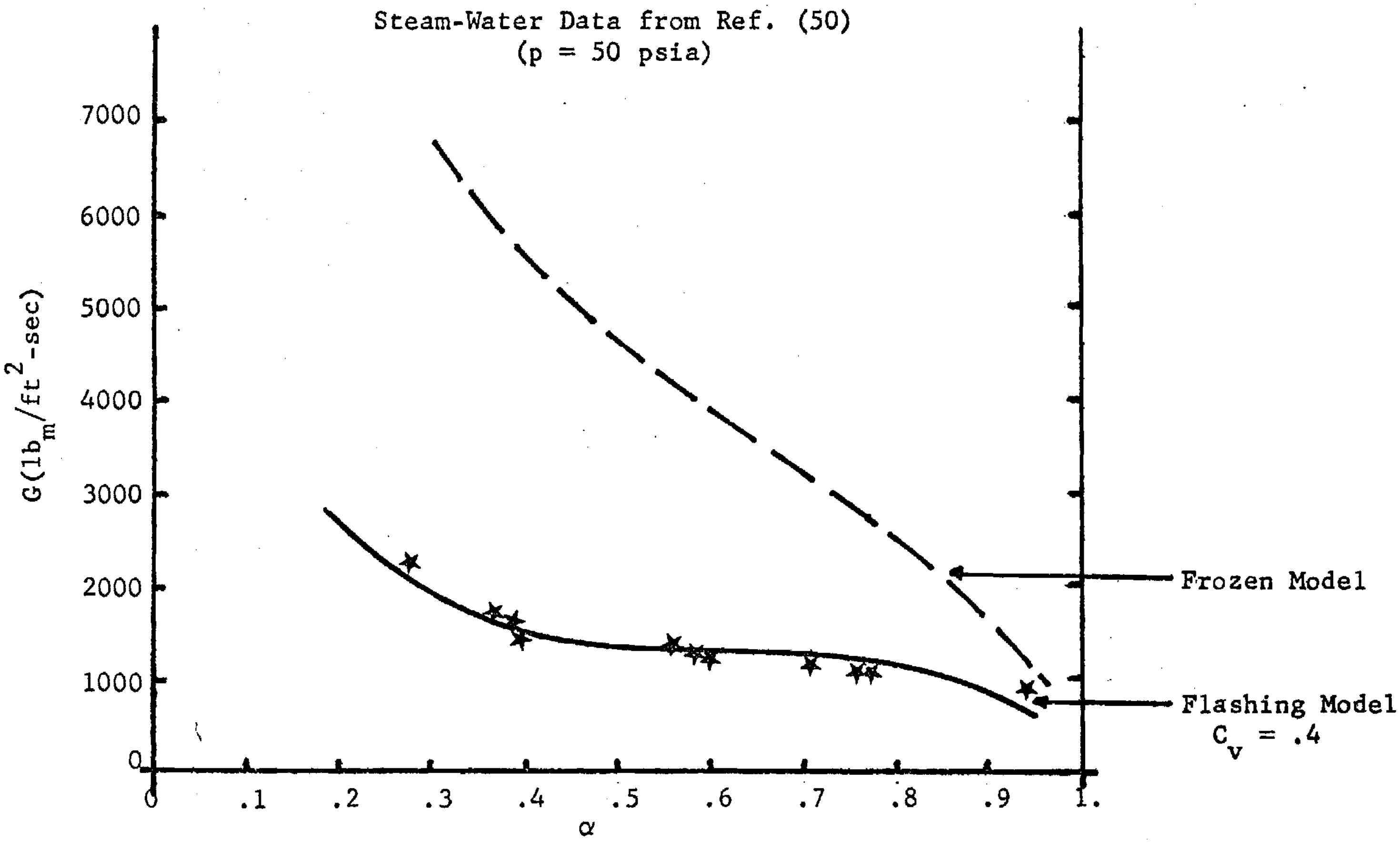

Figure 9. One-Component Critical Flow

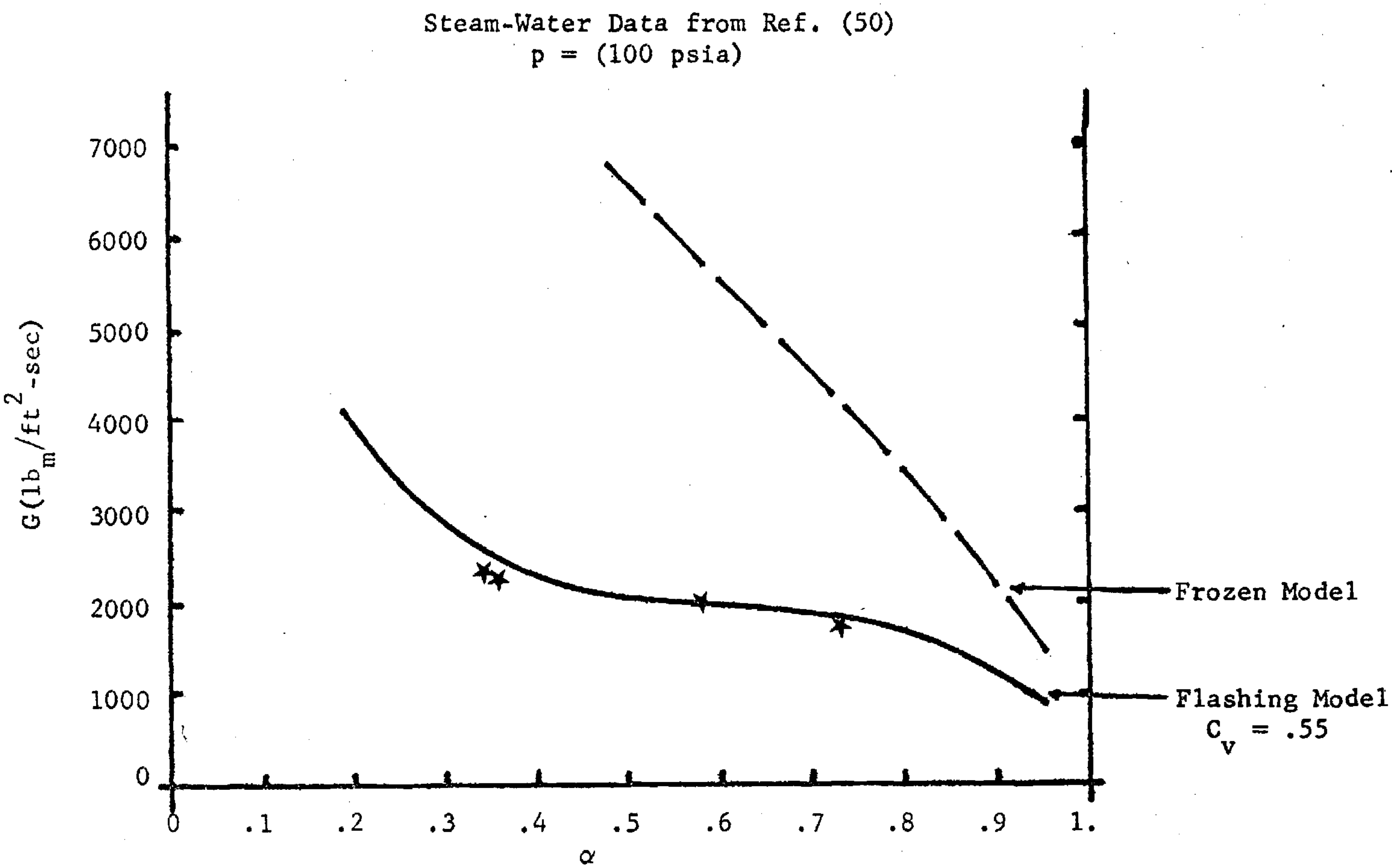

Figure 10. One-Component Critical Flow

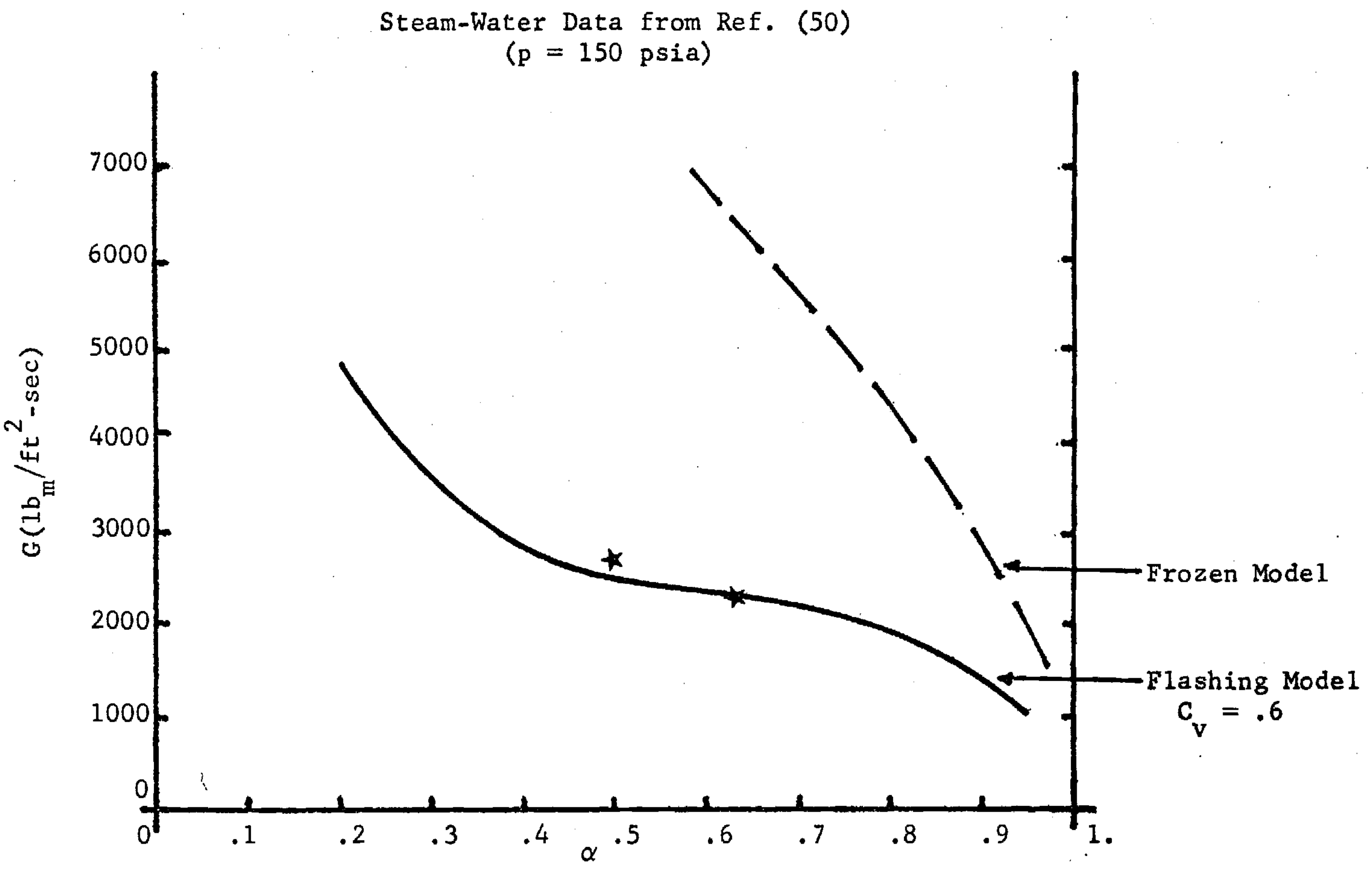

Figure 11. One-Component Critical Flow

curve in the vicinity of the cutoff alpha if the 90% figure was used. In addition, a C_o of 1.1 provided a slightly better fit of the data than the C_o of 1.15 used earlier and, of course, provides a slip ratio in the same range as that suggested by Henry, et al. [50]. While a more complex function of α might provide a somewhat better fit of the data, it was felt that the simplicity of A6 outweighed any gain in accuracy achieved through greater complexity. Also, if more good data were available (where α is measured directly) at varying pressures, then a functional relationship could be derived for C_v and of course provide a better test for what is admittedly a highly simplified model of a complex phenomenon.

The suggestion here is that in single component flow wave propagation information may not be directly related to the critical condition as it apparently can in two-component bubbly flow. In single component flow, the critical mass velocity is smaller (except as $\alpha \rightarrow 0, 1$) than that predicted by the sort of frozen model which may be used to predict wave speeds in most of the available data. This shows the importance of flashing in critical flow although from the standpoint of the model, the Reynold's analogy still holds up.

APPENDIX B

a_{ij}'s

(Note $K^* = \frac{c_{Pg}}{c_{vg}}$)

$$a_{11} = 0$$

$$a_{12} = \alpha^* N_{gjm}$$

$$a_{13} = 1$$

$$a_{14} = V_m^* + \frac{\rho_f^*}{\rho_m^*} V_{gj}^* + \alpha^* N_{gj\alpha}$$

$$a_{15} = \alpha^*(1-\alpha^*)\left[\frac{M_{Tg}^2}{\rho_g^*} - \frac{M_{Tf}^2}{\rho_f^*}\right] + \frac{\alpha^*(1-\alpha^*) N_{Pg}(K^*-1) T_g^*}{\rho_g^* K^* P^*}$$

$$a_{16} = \alpha^*\left[N_{gjf} M_{Tf}^2 + N_{gjg} M_{Tg}^2\right] + \frac{\alpha^*(1-\alpha^*)}{\rho_g^*}\left(V_m^* + \frac{\rho_f^*}{\rho_m^*} V_{gj}^*\right) M_{Tg}^2 + \frac{\alpha^*(1-\alpha^*)}{\rho_f^*}\left(V_m^* - \frac{\alpha^*}{(1-\alpha^*)} \frac{\rho_g^*}{\rho_m^*} V_{gj}^*\right) M_{Tf}^2 + \frac{(K^*-1) T_g^* \alpha^*}{K^* P^*}\left[N_{Pg} N_{gjg} + \frac{(1-\alpha^*)}{\rho_g^*}\left(V_m^* + \frac{\rho_f^*}{\rho_m^*} V_{gj}^*\right) N_{Pg}\right]$$

$$a_{17} = -\frac{\alpha^*(1-\alpha^*)}{\rho_s^*} N_{ps}$$

$$a_{18} = \alpha^* \left[N_{ps} N_{gjs} - \frac{(1-\alpha^*)}{\rho_s^*} \left(V_m^* - \frac{\alpha^*}{(1-\alpha^*)} \frac{\rho_g^*}{\rho_m^*} V_{gj}^* \right) N_{ps} \right]$$

$$a_{21} = 0$$

$$a_{22} = \rho_m^*$$

$$a_{23} = \Delta p^*$$

$$a_{24} = V_m^* \Delta p^*$$

$$a_{25} = (1-\alpha^*) M_{Ts}^2 + \alpha^* M_{Tg}^2 + \frac{(K^*-1)\, T_g^* N_{pg} \alpha^*}{K^* \; P^*}$$

$$a_{26} = V_m^* \left[(1-\alpha^*) M_{Ts}^2 + \alpha^* M_{Tg}^2 \right] + \frac{(K^*-1)\, T_g^* V_m^* \alpha^* N_{pg}}{K^* \; P^*}$$

$$a_{27} = (1-\alpha^*) N_{ps}$$

$$a_{28} = V_m^* (1-\alpha^*) N_{ps}$$

$$a_{31} = \rho_m^*$$

$$a_{32} = \rho_m^* V_m^* + \frac{\alpha^*}{1-\alpha^*} \frac{\rho_f^* \rho_g^*}{\rho_m^*} \, 2V_{gj}^* \, N_{gjm}$$

$$a_{33} = 0$$

$$a_{34} = \frac{\alpha^*}{(1-\alpha^*)} \frac{\rho_f^* \rho_g^*}{\rho_m^*} V_{gj}^2 \left[\frac{1}{\alpha^*(1-\alpha^*)} - \frac{\Delta\rho^*}{\rho_m^*} + \frac{2}{V_{gj}^*} N_{gj\alpha} \right]$$

$$a_{35} = 0$$

$$a_{36} = 1 + \frac{\alpha^*}{(1-\alpha^*)} \frac{\rho_f^* \rho_g^*}{\rho_m^*} V_{gj}^* \left[V_{gj}^* \left(\frac{1}{\rho_f^*} - \frac{(1-\alpha^*)}{\rho_m^*} \right) M_{Tf}^2 \right.$$

$$+ V_{gj}^* \left(\frac{1}{\rho_g^*} - \frac{\alpha^*}{\rho_m^*} \right) M_{Tg}^2 + 2 N_{gjf} M_{Tf}^2 + 2 N_{gjg} M_{Tg}^2$$

$$+ \frac{(K^*-1) T_g^* \alpha^*}{(1-\alpha^*) K^* P^*} \frac{\rho_f^* \rho_g^*}{\rho_m^*} V_{gj}^* \left[V_{gj}^* \left(\frac{1}{\rho_g^*} - \frac{\alpha^*}{\rho_m^*} \right) N_{Pg} \right.$$

$$\left. + 2 N_{gjg} N_{Pg} \right]$$

$$a_{37} = 0$$

$$a_{38} = \frac{\alpha^*}{(1-\alpha^*)} \frac{\rho_f^* \rho_g^*}{\rho_m^*} V_{gj}^* \left[V_{gj}^* \left(\frac{1}{\rho_f^*} - \frac{(1-\alpha^*)}{\rho_m^*} \right) N_{Pf} \right.$$

$$a_{41} = 0$$

$$a_{42} = \rho_m^* i_m^* + \frac{\alpha^* \rho_f^* \rho_g^*}{\rho_m^*} \Delta i^* N_{gjm}$$

$$a_{43} = \rho_g^* i_g^* - \rho_f^* i_f^*$$

$$a_{44} = V_m^* (\rho_g^* i_g^* - \rho_f^* i_f^*) + \frac{V_{gj}^* \rho_f^{*2} \rho_g^*}{\rho_m^{*2}} \Delta i^* \Big[1 + \frac{\alpha^* \rho_m^* N_{gj\alpha}}{V_{gj}^* \rho_f^*} \Big]$$

$$a_{45} = (1-\alpha^*) \Big[\frac{T_f^*}{\rho_f^*} N_{Pf} + i_f^* M_{Tf}^2 \Big] + \alpha^* \Big[\frac{T_g^*}{\rho_g^*} N_{Pg} + i_g^* M_{Tg}^2 \Big] + \frac{(K^*-1) T_g^* \alpha^*}{K^* P^*} \big[\rho_g^* C_{Pg}^* + i_g^* N_{Pg} \big]$$

$$a_{46} = V_m^* \Big[(1-\alpha^*) \Big(\frac{T_f^*}{\rho_f^*} N_{Pf} + i_f^* M_{Tf}^2 \Big) + \alpha^* \Big(\frac{T_g^*}{\rho_g^*} N_{Pg} + i_g^* M_{Tg}^2 \Big) \Big] + \frac{\alpha^* V_{gj}^*}{\rho_m^*} \Big[\frac{T_g^* \rho_f^*}{\rho_g^*} N_{Pg} - \frac{T_f^* \rho_g^*}{\rho_f^*} N_{Pf}$$

$$+ \frac{\Delta i^* \alpha^* \rho_g^{*2}}{\rho_m^*} M_{Tf}^2 + \frac{\Delta i^* (1-\alpha^*) \rho_f^{*2}}{\rho_m^*} M_{Tg}^2$$

$$+ \frac{\alpha^* \rho_f^* \rho_g^*}{\rho_m^*} \Delta i^* \big[N_{gjf} M_{Tf}^2 + N_{gjg} M_{Tg}^2 \big]$$

$$+ \frac{(K^*-1) T_g^*}{K^* P^*} \Big\{ V_m^* \alpha^* \big[\rho_g^* C_{Pg}^* + i_g^* N_{Pg} \big]$$

$$+ \frac{\alpha^* V_{gj}^*}{\rho_m^*} \left[\rho_f^* \rho_g^* c_{pg}^* + \frac{\Delta i^* (1-\alpha^*) \rho_f^{*2}}{\rho_m^*} N_{pg} \right]$$

$$+ \frac{\alpha^* \rho_f^* \rho_g^* \Delta i^*}{\rho_m^*} N_{gjg} N_{pg} \Big\}$$

$$a_{47} = (1-\alpha^*) \left[\rho_f^* c_{pf}^* + i_f^* N_{pf} \right]$$

$$a_{48} = V_m^* (1-\alpha^*) \left[\rho_f^* c_{pf}^* + i_f^* N_{pf} \right]$$

$$+ \frac{\alpha^* V_{gj}^*}{\rho_m^*} \left[- \rho_f^* \rho_g^* c_{pf}^* + \frac{\Delta i^* \alpha^* \rho_g^{*2}}{\rho_m^*} N_{pf} \right]$$

$$+ \frac{\alpha^* \rho_f^* \rho_g^* \Delta i^*}{\rho_m^*} N_{gjf} N_{pf}$$

APPENDIX C

PROGRAM WAVE

```
      DIMENSION S(10),Q(10),G(10),A(5),X(4)
       DIMENSION ALL(40)
      DIMENSION AB(15)
      DIMENSION XY(505),YMVM(505)
      DIMENSION C(4,8),E(6),B(4,4)
      DIMENSION XX(4)
      COMPLEX A,X
      REAL KI
      EPS=.00001
      KMAX=200
C     IA=1,AIR      NE1 STEAM
      WRITE(6,477)
 477  FORMAT(1H,23HIPP,KKK,IZ,IKK,IY,RHUM    )
      READ(5,998)IPP,KKK,IZ,IKK,IY,RHUM
       IF(RHUM.LT.0.0)GO TO 6780
       IA=1
       GO TO 6790
6780    IA=2
6790   IF(IZ-3)6777,6677,6777
6677   WRITE(6,9900)
9900   FORMAT(1H,25H HYPERBOLICITY TOLERANCE        )
        READ(5,998)EPZ
6777    CONTINUE
  998 FORMAT()
         WRITE(6,7800)
7800   FORMAT(1H,15H CON,CO,CUTOFF       )
       READ(5,998)CON,ALB,COFF
         IF(CON.LT.3.)GO TO 6700
      IJK=1
      IY=2
       GO TO 5500
6700   CONTINUE
       IJK=2
5500   CONTINUE
    2 FORMAT (8F10.3)
      WRITE(6,4700)
4700  FORMAT(1H,9H GAS EXP        )
      READ(5,998)KI
      IF(IJK.GT.1)GO TO 476
      WRITE(6,475)
 475  FORMAT(1H,5HSIGMA   )
      READ(5,998)SG
 476   DB=.1667
       WRITE(6,8900)
8900   FORMAT(1H,26H CN,CF,DHG/DP,AL**,AL1**                  )
       READ(5,998) SC2,AA12,TTT3,TTAL,TTAL1
      TTT2=0.0
      TTT4=0.0
      IF(IKK.EQ.1) GO TO 345
       WRITE(6,479)
```

```
 479  FORMAT(1H,4HRCVM  )
      READ(5,998)RCVM
 345   IF(IPP.GT.1)GO TO 4000
       WRITE(6,4001)
4001   FORMAT(1H,8H P,T1,T2 )
       READ(5,998)P,T1,T2
4000   DO 1000 KJ=1,KKK
       IF(IPP.GT.1)GO TO 4005
        IF(IPP.EQ.1)GO TO 1234
       IF(KJ.GT.1)GO TO 1556
         DO 1444 I=1,KKK
1444     READ(5,2)ALL(I)
1556   AL=ALL(KJ)
         GO TO 4006
1234    READ(5,2)AL
       GO TO 4006
4005   WRITE(6,4007)
4007   FORMAT(1H,8H P,T,AL  )
       READ(5,998)P,T1,AL
       T2=T1
4006   CONTINUE
      CALL DAT(RHUM,P,T1,T2,AB)
      CT1=AB(1)
      RCT1=AB(2)
      CT1=1./(4200.**2.)
      CT2=AB(3)
      RCT2=AB(4)
      U1=AB(5)
      U2=AB(6)
      H1=AB(7)
      H2=AB(8)
      CP1=AB(9)
      CP2=AB(10)
      RC1=AB(11)
      RC2=AB(12)
      AAA1=RC2*(CT2**.5)
      KJI=1
      IKJ=2
        IIK=1
      IF(IY.NE.1) GO TO 177
      XO1=AL
      AL=.0001
 177   IF(IKK.EQ.1.OR.IZ.EQ.3)GO TO 544
       GO TO 164
 544   RCVM=10.
 164 GO=32.174
      IF(IKJ.GT.2)GO TO 175
      IF(IJK.EQ.1)GO TO 171
      IF(CON.GT.1.)GO TO 803
      WRITE(6,801)CON
 801 FORMAT(1H,//20X16HSLIP=(RC1/RC2)**     ,F3.2)
      GO TO 175
 803 IF(CON.GT.2.) GO TO 804
      WRITE(6,802)
 802 FORMAT(1H,//20X19HHOMOGENOUS FLOW       )
      GO TO 175
 804    ALCUT=COFF/ALB
       WRITE(6,805)ALB,COFF,ALCUT
 805   FORMAT(1H,//10X4H CO= ,F4.2,5X11H CUTOFF % =,F4.2,5X3HAL=,F5.3)
      GO TO 175
```

```
171 WRITE (6,346)
346 FORMAT(1H0,35X15HBUBBLY FLOW        )
175 CONTINUE
    N=4
    DO 3 I=1,10
    S(I)=0.0
    Q(I)=0.0
    G(I)=0.0
  3 CONTINUE
    AL1=1.0-AL
     ABCB=(AL**TTAL)*(AL1**TTAL1)
     ROM=AL*RO2+(1.-AL)*RO1
    ALD=AL/AL1
    S(2)=SO2*ROVM
    VM=ROVM/ROM
    IF (IJK.EQ.1)GO TO 69
    AL3=AL**.5
    AL4=AL3/(1.+AL3)
    IF(CON.GT.1.)GO TO 156
    SL=((RO1/RO2)**CON)
    SLAL=0.0
    SLRO1=CON*SL/RO1
    SLRO2=CON*(-SL/RO2)
    GO TO 157
156 IF(CON.GT.2.)GO TO 159
    SL=1.0
    SLAL=0.0
    SLRO1=0.0
    SLRO2=0.0
    GO TO 157
159  ALC=COFF/ALB
     IF(AL.GT.ALC)GO TO 2000
     SL=AL1/(1./ALB-AL)
     SLAL=-SL/AL1+SL*ALB/(1.-ALB*AL)
     GO TO 3000
2000 SL=(1.-ALC)/(1./ALB-ALC)
     SLAL=-SL/(1.-ALC)+SL*ALB/(1.-ALB*ALC)
3000 SLRO1=0.0
     SLRO2=0.0
157 S1=SL-1.
    DN=1.+AL*RO2*S1/ROM
    IF(S1.LT.0.000001) GO TO 154
    V2VM=AL1*S1/DN
    V2R7=(AL1*VM*RO2*S1*S1/(DN*DN*ROM))
    V2R8=ROM*DN/(RO2*S1*S1)-AL/S1
    V2AL=(-1.*S1*VM/DN)+V2R7*((AL*(RO2-RO1)/ROM)-1.+V2R8*SLAL)
    V2RO1=V2R7*((AL*AL1/ROM)+V2R8*SLRO1)
    V2RO2=V2R7*((AL*AL/ROM)-(AL/RO2)+V2R8*SLRO2)
    GO TO 155
154 V2AL=0.0
    V2RO1=0.0
    V2RO2=0.0
    V2VM=0.0
155 V2J=AL1*S1*VM/DN
    GO TO 71
 69 V=(1.41   )*((GC*GC*SC)**.25)
    V2J=V*(((RO1-RO2)/(RO1*RO1))**.25)
    V2RO=(2.5E-1)*(((RO1*RO1)/(RO1-RO2))**.75)*V
    V2RO1=V2RO*((-1./(RO1*RO1))+2.*RO2/(RO1**3.))
    V2RO2=-V2RO/(RO1*RO1)
```

```
      V2VM=0.0
      V2AL=0.0
   71 IF(IKJ.GT.2) GO TO 176
      IF(IY.NE.1) GO TO 176
      DS=((1.-XO1)/XO1)*(RO2/RO1)*SL
      FF=AL-1./(DS+1.)
      FF1=1.+(1./((DS+1.)**2.))*DS*SLAL/SL
      AY=AL-(FF/FF1)
      AC=ABS(AY-AL)
      AL=AY
      IIK=IIK+1
      IF(IIK.GT.200) GO TO 19
      IF(AC.GT..001) GO TO 175
  176 CONTINUE
C     MAIN BODY
C     S(I)= DIFFERENTIAL TERMS FOR SHEAR STRESS
C     O(I)= DIFFERENTIAL TERMS FOR HEAT TRANSFER
C     G(I)= DIFFERENTIAL TERMS FOR MASS TRANSFER
      P=P*144.*GC
       V2XX=1./(CT2**.5)
       RO=(ROM/(RO1*RO2))
      TTT1=(-AA12*ABCD*RO2)/(V2XX)
      C(1,1)=RO*G(1)
      C(1,2)=RO*G(2)+AL*V2VM
      C(1,3)=RO*G(3)+1.0
      C(1,4)=VM+(RO1/ROM)*V2J+RO*G(4)+AL*V2AL
      VT2T=(AL*AL(/RO2)*ROT2
      VT2X=AL*(V2RO2*ROT2+(AL1/RO2)*(VM+(RO1/ROM)*V2J)*ROT2)
      IF(IA.NE.1) GO TO 654
      EVL=((KI-1.0)/KI)*(T2/P)
      GO TO 656
  654 EVL=(T2/(RO2*RO2))*(-ROT2)/(CP2*778.*GC)
  656 CONTINUE
      VPT=AL*AL1*(CT2/RO2-CT1/RO1)
      VPX=AL*(V2RO1*CT1+V2RO2*CT2)+(AL*AL1/RO2)*(VM+(RO1/ROM)*V2J)*CT2-(
     1AL*AL(/RO1)*(VM-(ALD*RO2/ROM)*V2J)*CT1
      VT1T=       -(AL*AL1/RO1)*ROT1
      VT1X=AL*(V2RO1*ROT1-(AL1/RO1)*(VM-(ALD*RO2/ROM)*V2J)*ROT1 )
       TTT3=TTT3*778./144.
       TTT4=TTT4*778./144.
       VT2X=VT2X-(TTT1*CP2)*RO*778.*GC
       VT1X=VT1X-(TTT2*CP1)*RO*778.*GC
       CVP1=RO*TTT1*(1./RO2+(T2*ROT2)/(RO2*RO2)-TTT3)
       CVP1=CVP1+RO*TTT2*(1./RO1+(T1*ROT1)/(RO1*RO1)-TTT4)
       TTT3=TTT3*144./778.
       TTT4=TTT4*144./778.
       VPX=VPX-CVP1
      IF (KI.GT.0.0) GO TO 30
      C(1,5)=VPT+RO*G(5)
      C(1,6)=VPX+RO*G(6)
      C(1,7)=VT1T+VT2T+RO*G(7)
      C(1,8)=VT1X+VT2X+RO*G(8)
      GO TO 31
   30 C(1,5)=VPT+EVL*VT2T+RO*G(5)
      C(1,6)=VPX+EVL*VT2X+RO*G(6)
      C(1,7)=VT1T+RO*G(7)
      C(1,8)=VT1X+RO*G(8)
   31 CONTINUE
      C(2,1)=0.0
      C(2,2)=ROM
```

```
      C(2,3)=RC2-RC1
      C(2,4)=VM*(RC2-RC1)
      CPX=VM*(AL1*CT1+AL*CT2)
      CPT=AL1*CT1+AL*CT2
      CT1T=AL1*RCT1
      CT1X=VM*AL1*RCT1
      CT2T=AL*RCT2
      CT2X=VM*AL*RCT2
      IF(KI.GT.0.0) GO TO 32
      C(2,5)=CPT
      C(2,6)=CPX
      C(2,7)=CT1T+CT2T
      C(2,8)=CT1X+CT2X
      GO TO 33
   32 C(2,5)=CPT+EVL*CT2T
      C(2,6)=CPX+EVL*CT2X
      C(2,7)=CT1T
      C(2,8)=CT1X
   33 CØNTINUE
       VJJ=V2J*(1.+SC2/2.)
      C32=(AL/AL1)*2.*VJJ/RØ
       VMSC=VM*VM*SC2/2.
       S(4)=VMSC*(RØ2-RØ1)
       S(4)=S(4)*DE/4.
       S(2)=S(2)*DE/4.
      C(3,1)=RØM+(4.0/DE)*S(1)
      C(3,2)=RØM*VM+(4.0/DE)*S(2)+C32*V2VM
      C(3,3)=(4.0/DE)*S(3)
      CA34=(ALD/RØ)*VJJ*V2J*(1./(AL*AL1)-((RØ2-RØ1)/RØM))+C32*V2AL
       C(3,4)=CA34+(4./DE)*S(4)
      CMPX=1. +(ALD/RØ)*VJJ*(V2J*(1./RØ1-AL1/RØM)*CT1+V2J*(1./RØ2-AL/RØM

     1)*CT2+2.*V2RØ1*CT1+2.*V2RØ2*CT2)
       CMPX=CMPX+VMSC*(AL*CT2+AL1*CT1)
      CMT1X= (ALD/RØ)*VJJ*(V2J*(1./RØ1-AL1/RØM)*CT1+2.*V2RØ1*CT1)
      CMT2X= (ALD/RØ)*VJJ*(V2J*(1./RØ2-AL /RØM)*CT2+2.*V2RØ2*CT2)
       CMT1X=CMT1X+VMSC*AL1*RØT1
       CMT2X=CMT2X+VMSC*AL*RØT2
      IF(KI.GT.0.0) GØ TØ 34
      C(3,6)=CMPX+(4./DE)*S(6)
       C(3,8)=CMT1X+CMT2X+(4./DE)*S(8)
      GØ TØ 35
   34 C(3,6)=CMPX+CMT2X*EVL+(4./DE)*S(6)
      C(3,8)=CMT1X+(4./DE)*S(8)
   35 C(3,5)=(4.0/DE)*S(5)
      C(3,7)=(4./DE)*S(7)
      CØNTINUE
      H1=H1*778.*GC
      H2=H2*778.*GC
      CP1=CP1*778.*GC
      CP2=CP2*778.*GC
      DH=H2-H1
      C42=AL*RØ1*RØ2*DH/RØM
       PP9=P*(RØ1-RØ2)/(RØ2*RØ1)
      C(4,1)=(4./DE)*Q(1)
      C(4,2)=AL1*RØ1*H1+AL*RØ2*H2+(4./DE)*Q(2)+C42*V2VM
      C(4,3)=RØ2*H2-RØ1*H1+(4./DE)*Q(3)
      C(4,4)=(V2J*RØ1/(RØ*RØM))*DH+VM*(RØ2*H2-RØ1*H1)+4.*S(4)/DE+C42*V2A

     1L
      ENPT=AL1*(1.+(T1/RØ1)*RØT1+H1*CT1)+AL*(1.+(T2/RØ2)*RØT2+H2*CT2)-1.

      ENPX=VM*(AL1*((T1/RØ1)*RØT1+H1*CT1)+AL*((T2/RØ2)*RØT2+H2*CT2))+(AL
```

```
     1*V2J/RØM)*((T2*RØ2/RØ1)*RØT2-(T1*RØ2/RØ1)*RØT1+DH*AL*RØ2*RØ2*CT1/R
     2ØM+DH*AL1*RØ1*RØ1*CT2/RØM)+(AL*DH/RØ)*(V2RØ1*CT1+V2RØ2*CT2)
      ENT1T=AL1*(RØ1*CP1+H1*RØT1)
      ENT1X=VM*ENT1T+(AL*V2J/RØM)*(-RØ1*RØ2*CP1+DH*AL*RØ2*RØ2*RØT1/RØM)+
     1AL*DH*V2RØ1*RØT1/RØ
      ENT2T=AL*(RØ2*CP2+H2*RØT2)
      ENT2X=VM*ENT2T+(AL*V2J/RØM)*(RØ1*RØ2*CP2+DH*AL1*RØ1*RØ1*RØT2/RØM)+
     1AL*DH*V2RØ2*RØT2/RØ
      ENT2X=ENT2X+TTT1*CP2*PP9
      ENT1X=ENT1X+TTT2*CP1*PP9
      ENPX=ENPX+CVR1*PP9/RØ
      IF(K1.GT.0.0) GØ TØ 36
      C(4,5)=ENPT+(4./DE)*Q(5)
      C(4,6)=ENPX+(4./DE)*Q(6)
      C(4,7)=ENT1T+ENT2T+(4./DE)*Q(7)
      C(4,8)=ENT1X+ENT2X+(4./DE)*Q(8)
      GØ TØ 37
   36 C(4,5)=ENPT+EVL*ENT2T+(4./DE)*Q(5)
      C(4,6)=ENPX+EVL*ENT2X+(4./DE)*Q(6)
      C(4,7)=ENT1T+(4./DE)*Q(7)
      C(4,8)=ENT1X+(4./DE)*Q(8)
   37 CØNTINUE
C     THIS CØMPLETES THE CALCULATION OF C(I,J)
      P=P/(144.*GC)
      H1=H1/(778.*GC)
      H2=H2/(778.*GC)
      CP1=CP1/(778.*GC)
      CP2=CP2/(778.*GC)
      IF(IKK.EQ.1) GØ TØ 160
      IF(IZ.GT.1) GØ TØ 558
      WRITE(6,38)
   38 FØRMAT (1H0,40X10H   C(I,J)                )
      DØ 39 I=1,4
   39 WRITE(6,41) (C(I,KK),KK=1,8)
   41 FØRMAT (1H0,2X1P8E10.2)
C     THE NEXT PART CALCULATES THE VALUES ØF THE 16 DETERMINANTS
  558 CØNTINUE
      DØ 100 I=1,4
      B(I,1)=C(I,1)
      B(I,2)=C(I,3)
      B(I,3)=C(I,5)
  100 B(I,4)=C(I,7)
      CALL DETER(B,D)
      A(5)=CMPLX(D,0,0)
      DØ 201 I=1,4
  201 B(I,3)=C(I,6)
      CALL DETER(B,D)
      E(1)=-D
      DØ 202 I=1,4
      B(I,2)=C(I,4)
  202 B(I,3)=C(I,5)
      CALL DETER(B,D)
      E(2)=-D
      DØ 2 3 I=1,4
      B(I,2)=C(I,3)
  203 B(I,4)=C(I,8)
      CALL DETER(B,D)
      E(3)=-D
      DØ 204 I=1,4
      B(I,1)=C(I,2)
  204 B(I,4)=C(I,7)
```

```
      CALL DETER(B,D)
      E(4)=-D
      Y=0.0
      DO 50 I=1,4
   50 Y=Y+E(I)
      A(4)=CMPLX(Y,0.0)
      DO 301 I=1,4
      B(I,1)=C(I,1)
      B(I,2)=C(I,4)
  301 B(I,3)=C(I,6)
      CALL DETER(B,D)
      E(1)=D
      DO 302 I=1,4
      B(I,3)=C(I,5)
  302 B(I,4)=C(I,8)
      CALL DETER(B,D)
      E(2)=D
      DO 303 I=1,4
      B(I,2)=C(I,3)
  303 B(I,3)=C(I,6)
      CALL DETER(B,D)
      E(3)=D
      DO 304 I=1,4
      B(I,1)=C(I,2)
      B(I,2)=C(I,3)
  304 B(I,4)=C(I,7)
      CALL DETER(B,D)
      E(4)=D
      DO 305 I=1,4
      B(I,3)=C(I,5)
  305 B(I,4)=C(I,8)
      CALL DETER(B,D)
      E(5)=D
      DO 306 I=1,4
      B(I,2)=C(I,4)
  306 B(I,4)=C(I,7)
      CALL DETER(B,D)
      E(6)=D
      Y=0.0
      DO 51 I=1,6
   51 Y=Y+E(I)
      A(3)=CMPLX(Y,0.0)
      DO 401 I=1,4
  401 B(I,3)=C(I,6)
      CALL DETER(B,D)
      E(1)=-D
      DO 402 I=1,4
      B(I,3)=C(I,5)
  402 B(I,4)=C(I,8)
      CALL DETER(B,D)
      E(2)=-D
      DO 403 I=1,4
      B(I,2)=C(I,3)
  403 B(I,3)=C(I,6)
      CALL DETER(B,D)
      E(3)=-D
      DO 404 I=1,4
      B(I,1)=C(I,1)
  404 B(I,2)=C(I,4)
      CALL DETER(B,D)
      E(4)=-D
      Y=0.0
      DO 52 I=1,4
   52 Y=Y+E(I)
      A(2)=CMPLX(Y,0.0)
```

```
      DØ 500 I=1,4
  500 B(I,1)=C(I,2)
      CALL DETER(B,D)
      A(1)=CMPLX(D,0.0)
      IF(IZ.EQ.3)GØ TØ 599
      GØ TØ 161
  160 CØNTINUE
      DØ 162 I=1,4
      B(I,1)=C(I,2)
      B(I,2)=C(I,4)
      B(I,3)=C(I,6)
  162 B(I,4)=C(I,8)
      CALL DETER(B,D)
      IF(ABS(D).LT.0.001) GØ TØ 163
      IF(IKJ.GT.505) GØ TØ 19
      VMVM(IKJ)=VM
      XY(IKJ)=D
      XY(1)=XY(2)
      IF(KJI.EQ.2) GØ TØ 11
      Z=XY(IKJ)/XY(IKJ-1)
      GØ TØ 12
   11 Z=XY(IKJ)/XY(IKJ-2)
   12 IF(Z.LT.0.0)GØ TØ 17
  571  IF(KJI.GT.1)GØ TØ 5
       IF(IKJ.GT.505)GØ TØ 19
      VM=VM+10.
      RØVM=RØM*VM
      IKJ=IKJ+1
      VMVM(IKJ)=VM
      GØ TØ 175
   17 IF(KJI.GT.1)GØ TØ 18
    5 VM=(VMVM(IKJ-1))+1.
      VMVM(IKJ)=VM
      RØVM=RØM*VM
      KJI=KJI+1
      IKJ=IKJ+1
      IF(KJI.GT.11) GØ TØ 19
      GØ TØ 175
   18 VMVM(IKJ)=VM
       IF(IZ.NE.3)GØ TØ 572
       IF(KJI.EQ.2)GØ TØ 573
       VM=VMVM(IKJ-1)
       GØ TØ 15
  573  VM=VMVM(IKJ-2)
       GØ TØ 15
  572  CØNTINUE
      IF(KJI.EQ.2) GØ TØ 14
      VM=(VM-VMVM(IKJ-1))*(-XY(IKJ-1))/(D-XY(IKJ-1))+VMVM(IKJ-1)
      WRITE(6,41)D,XY(IKJ-1)
      GØ TØ 15
   14 VM=(VM-VMVM(IKJ-2))*(-XY(IKJ-2))/(D-XY(IKJ-2))+VMVM(IKJ-2)
      WRITE(6,41)D,XY(IKJ-2)
   15 RØVM=RØM*VM
      IF(IZ.EQ.3)GØ TØ 161
      GØ TØ 163
   19 WRITE(6,20)
       IF(IZ.EQ.3)GØ TØ 1000
   20 FØRMAT(1H,5HABØRT)
  163 CØNTINUE
        WRITE(6,166) IKJ
  166 FØRMAT(/1H,20X23HNUMBER ØF ITERATIØNS =     ,I4)
      WRITE(6,144)VM,RØVM
  144 FØRMAT(1H,20X24HCHØKING MASS VELØCITY =      ,F10.4,/20X20HCHØKING
     1MASS FLUX =      ,F12.4)
```

```
161 CONTINUE
    WRITE (6,555)
555 FORMAT (1H ,52H  ALPHA      TEMP1     TEMP2    PRESSURE    MASS FLUX
   1     )
    WRITE (6,2) AL,T1,T2,P,ROVM
    IF(IZ.GT.1) GO TO 559
    IF(IKK.GT.1) GO TO 556
    DO 307 I=1,4
307 WRITE(6,41) (B(I,KL),KL=1,4)
556  WRITE(6,666)
666 FORMAT (1H,51H   ROT1      RO1       DIA     ENTHALPY2 ENTHALPY1 )
    WRITE (6,2) ROT1,RO1,DE,H2,H1
    W
     RITE(6,255)
2
 55 FORMAT(1H,42H   CP1      CP2       GAS EXP     SIGMA      )
    WRITE(6,2)CP1,CP2,KI,SG
    WRITE(6,112)
112 FORMAT(/1H,50H    V2J      V2RO1      V2RO2      V2AL      V2VM    )
    WRITE (6,111) V2J,V2RO1,V2RO2,V2AL, V2VM
     WRITE(6,111) ROT2
    WRITE(6,257)
257 FORMAT(/1H,37H  ROM       VM       RO1       RO2       )
    WRITE(6,2)ROM,VM,RO1,RO2
111 FORMAT (1H,1P12E10.3//)
    AF=(1./CT1)**.5
     AG=(ABS(KI)/CT2)**.5
    WRITE(6,969)AG,AF
969 FORMAT(/1H,10X3HAG= F7.2,5X3HAF= F7.2)
559  CONTINUE
    V1=VM-ALD*RO2*V2J/ROM
    V2=VM+RO1*V2J/ROM
    VJ=AL1*V1+AL*V2
    SLIP=V2/V1
    VJ1=AL1*V1
    VJ2=AL*V2
    VVW=(V1*RO1/AL1+V2*RO2/AL)/(RO1/AL1+RO2/AL)
    VVVV=(V1*AL1/RO1+V2*AL/RO2)/(AL1/RO1+AL/RO2)
    VR=V2-V1
    V1J=-AL*VR
    V2J=AL1*VR
    VJ11=V1+VJ1/AL
    WRITE (6,333)
333 FORMAT (/1H,72H      V1           VM              V2
   1LIP              J          )
    WRITE (6,334) V1,VM,V2,SLIP,VJ
334   FORMAT(1H,6F14.3)
    IF(IZ.GT.1) GO TO 557
    WRITE(6,135)
135 FORMAT(/1H,55H    V1J            V2J            J1             .1
   1       )
    WRITE(6,334)V1J,V2J,VJ1,VJ2
557   XQ=AL*RO2*V2/ROVM
    WRTTE(6,339)XQ
339 FORMAT(/1H,25X10HQUALITY =     ,F7.4)
    IF(IKJ.GT.2) GO TO 1000
599   CONTINUE
    A(4)=A(4)/(REAL(A(5)))
    A(3)=A(3)/(REAL(A(5)))
    A(2)=A(2)/(REAL(A(5)))
```

```
      A(1)=A(1)/(REAL(A(5)))
      A(5)=CMPLX(1.,0.0)
C     THIS SECTION CALCULATES THE VELOCITIES OF PROPAGATION
      CALL ROOTCP (A,N,EPS,KMAX,X,J,599)
C     A=N+1 ELEMENTS REPRESENTING COEF. OF POLYNOMIAL
C     N= DEGREE OF POLYNOMIAL
C     EPS= MAX DIFFERENCE BETWEEN SUCESSIVE APPROXIMATIONS OF A ROOT
C     KMAX= MAX NO OF ITERATIONS
C     X=ROOTS OF POLYNOMIAL
C     J= ROOT CONVERGENCE INDICATOR
C     J=N IF ALL ROOTS CONVERGE
C     IF J IS LESS T
C     IF J IS LESS T HAN N THEN JTH ROOT FAILED TO CONVERGE
C     IF J IS LESS THAN  N THEN JTH ROOT FAILED TO CONVERGE
C     F(X)= A0 + A1X +''''''''+ ANX**N
      IF(IZ.NE.3)GO TO 99
      DO 568 I=1,J
      DDZ=ABS(AIMAG(X(I)))
568   IF(DDZ.GT.EPZ)GO TO 17
      VMVM(IKJ)=VM
      GO TO 571
   99 WRITE (6,88) J
   88 FORMAT (1H0,20XI4,6HROOTS       )
      DO 98 I=1,J
      XX(I)=CABS(X(I))
   98 WRITE (6,97) I,X(I),XX(I)
   97 FORMAT (1H,I4,2XF12.5,2X1PE15.4,2XF12.5)
      XX1=XX(1)-V1
      XX3=(-XX(3)+XX(4))/2.
      XX4=( XX(3)+XX(4))/2.
      IF(IJK.EQ.1)GO TO 589
      XX2=XX(2)-V1-VJ1/AL
      WRITE(6,389)
  389 FORMAT(//1H,10X80H      ROOT1-V1                ROOT2-V1-J1/AL        VP
     1                   SPEED OF SOUND                        )
      GO TO 222
  589 XX2=XX(2)-V2
      WRITE(6,399)
  399 FORMAT(//1H,10X80H      ROOT1-V1                ROOT2-V2
     1                   SPEED OF SOUND                        )
  222 WRITE (6,223) XX1,XX2,XX3,XX4
  223 FORMAT(1H,3X4F20.7)
 1000 CONTINUE
      END
```

```
      SUBROUTINE DETER(B,D)
      DIMENSION B(4,4)
      D1=B(1,1)*(B(2,2)*(B(3,3)*B(4,4)-B(3,4)*B(4,3))-B(3,2)*(B(2,3)*B(4
     1,4)-B(2,4)*B(4,3))+B(4,2)*(B(2,3)*B(3,4)-B(2,4)*B(3,3)))
      D2=B(2,1)*(-B(1,2)*(B(3,3)*B(4,4)-B(3,4)*B(4,3))+B(3,2)*(B(1,3)*B(
     14,4)-B(1,4)*B(4,3))-B(4,2)*(B(1,3)*B(3,4)-B(1,4)*B(3,3)))
      D3=B(3,1)*(B(1,2)*(B(2,3)*B(4,4)-B(2,4)*B(4,3))-B(2,2)*(B(1,3)*B(4
     1,4)-B(1,4)*B(4,3))+B(4,2)*(B(1,3)*B(2,4)-B(1,4)*B(2,3)))
      D4=B(4,1)*(-B(1,2)*(B(2,3)*B(3,4)-B(2,4)*B(3,3))+B(2,2)*(B(1,3)*B(
     13,4)-B(1,4)*B(3,3))-B(3,2)*(B(1,3)*B(2,4)-B(1,4)*B(2,3)))
      D=D1+D2+D3+D4
      RETURN
      END
```

```
      SUBROUTINE DAT(RHUM,P,T1,T2,AB)
        IF(RHUM.LT.0.0) GO TO 7500
        IA=1
        GO TO 7600
7500    IA=2
7600    CONTINUE
      DIMENSION AB(15)
      IF(T1.GT.660.) GO TO 580
      H1=.99994*(T1-492.)
      CP1=1.6
      H2=.417*(T1-492.)+1075.8
      GO TO 600
  580 IF(T1.GT.760.) GO TO 581
      H1=1.016*(T1-660.)+167.99
      CP1=1.02
      H2=.338*(T1-660.)+1145.9
      GO TO 600
  581 IF(T1.GT.860.) GO TO 582
      H1=1.0578*(T1-760.)+289.57
      CP1=1.05
      H2=.213*(T1-760.)+1179.7
      GO TO 600
  582 IF(T1.GT.910.) GO TO 583
      H1=1.103*(T1-860.)+374.37
      CP1=1.1
      H2=.06*(T1-860.)+1201.
      GO TO 600
  583 IF(T1.GT.960.) GO TO 584
      H1=1.15*(T1-910.)+430.1
      CP1=1.15
      H2=-.06*(T1-910.)+1204.6
      GO TO 600
  584 H1=1.292*(T1-1060.)+487.8
      CP1=1.25
      H2=-.362*(T1-1060.)+1201.7
  600 CONTINUE
      H1=5.4*EXP(-(T1-492.)/100.)
      U2=.0000537*(T2-1460.)+.07
      TK=(T1-492.)*5./9.
      PR=P/14.6959
      TC=374.11-TK
      VX1=-.3151548*(TC**-.333)-.001203374*TC+(7489O8E-18)*(TC**4.)
      VX2=1.+.1342489*(TC**-.333)-.003946263*TC
      VLX=(3.1975+VX1)/VX2
      VL=VLX
      RO1=62.43/VLX
      IF(T1.GT.559.) GO TO 8000
      RO1=62.3
8000  CONTINUE
      VLT=(+.89902*.147166*((374.1-TK)**-.8528)-1.6*.4*((385.-TK)**-2.6)
     1*(PR-218.5))*5./9.
      VLP=-.4*((385.-TK)**-1.6)
      ROT1=-(RO1/VL)*VLT
      CT1=(RO1/VL)*(-VLP/32.174)
      CT1=CT1/(14.6959*144.)
      TK=(T2-492.)*5./9.
      TK3=TK+273.16
      T1=1./(TK+273.16)
      G21=82.546*T1-(162460.    )*T1*T1
      G22=.21828-(126970.    )*T1*T1
```

```
      G23=(((T1*1000.)**4.)**5.)*((T1*10.)**4.)
      G33=.0003635-6.768*G23
      G3=G33
      BO=1.89-2641.62*T1*(10.**(80870.*(T1*T1)))
      B11=BO+BO*BO*G21*T1*PR
      B22=(BO**4.)*G22*(T1**3.)*(PR**3.)
      B33=((BO*T1*PR)**12.)*BO*(-G33)
      VG2=(4.55504*TK3/PR)+B11+B22+B33
      RO2=62.43/VG2
      DTT=-(T1**2.)
      G1T=(82.546-2.*(162460.    )*T1)*DTT
      G2T=-2.*(126970.    )*T1*DTT
      G3T=-24.*(G23/T1)*DTT*6.768
      BOT=((BO-1.89 )/T1)*DTT+(BO-1.89)*DTT*ALOG(10.)*161740.*T1
      BT1=BOT+2.*BO*BOT*G21*T1*PR+BO*BO*G1T*T1*PR+BO*BO*G21*DTT*PR
      BT2=(BO**4.)*G22*(T1**3.)*(PR**3.)*(4.*BOT/BO+G2T/G22+3.*DTT/T1)
      BT3=B33*(13.*BOT/BO+G3T/G3+12.*DTT/T1)
      BT=BT1+BT2+BT3
      ROT2=-(RO2/VG2)*(4.5504/PR+BT)*5./9.
      BP=BO*BO*G21*T1+(BO**4.)*G22*(T1**3.)*(PR**2.)*3.+B33*12./PR
      CT2=-(RO2/VG2)*(-4.55504*TK3/(PR*PR)+BP)/32.174
      CT2=CT2/(14.6959*144.)
      CP2=      (1.4720+( 75566E-8) *TK3+97.8365*T1)*(5./9.)*.42998
      IF(IA.NE.1) GO TO 64
      U2=( 7E-5) *(T2-460.)-( 37E-9) *((T2-460.)**2.)+.042
      XY=(647.27-TK3)
      Z1=3.2437814+.0058683*XY+(1170238E-14)*(XY**3)
      Z2=1.+(2187B5E-8)*XY
      Z=(XY/TK3)*(Z1/Z2)
      PG=(218.167*14.7)/(10.**Z)
      PV=RHUM*PG
      WR=(.95*.662*PG)/(P-PV)
      WFA=1./(1.+WR)
      R=WFA*53.34+(1.-WFA)*85.76
      CP2=WFA*.241+(1.-WFA)*CP2
      H2=WFA*(T2-492.)*.241+(1.-WFA)*H2
      RO2=(P*144.)/(R*T2)
      CT2=1.0/(R*T2)
      ROT2=-(P*144.)/(R*T2*T2)
      CT2=CT2/32.174
   64 CONTINUE
      AB(1)=CT1
      AB(2)=ROT1
      AB(3)=CT2
      AB(4)=ROT2
      AB(5)=U1
      AB(6)=U2
      AB(7)=H1
      AB(8)=H2
      AB(9)=CP1
      AB(10)=CP2
      AB(11)=RO1
      AB(12)=RO2
      RETURN
      END
```

BIBLIOGRAPHY

1. Shapiro, Ascher H., The Dynamics and Thermodynamics of Compressible Fluid Flow, Vol. 1, New York, the Ronald Press Company, 1953.

2. Kocamustafaogullari, Gunol, "Thermo-Fluid Dynamics of Separated Two-Phase Flow," Ph.D. Thesis, School of Mechanical Engineering, Georgia Institute of Technology, Atlanta, Georgia, December, 1971.

3. Ogasawara, Hideo, "A Theoretical Approach to Two-Phase Critical Flow," Bulletin JSME, 12, 1969, p. 827.

4. Boure, J., Fritte, A., and Giot, M., "Choking Flows and Propagation of Small Disturbances," Paper Fl European Two-Phase Flow Conference Flow Group Meeting, Brussels, June 4-7, 1973.

5. Van Wylen, Gordon J., Thermodynamics, New York, John Wiley and Sons, Inc., 1967.

6. Burnell, J. G., "Flow of Boiling Water Through Nozzles, Orifices, and Pipes," Engineering, 164, 1947, p. 572.

7. Zaloudek, F. R., "The Critical Flow of Hot Water Through Short Tubes," USAEC Report HW-77594, 1963.

8. Bailey, J. F., "Metastable Flow of Saturated Water," Transactions ASME, 73, 1959, p. 1109.

9. Isbin, H. S., May, J. E., and DaCruz, A. J. R., "Two-Phase Steam-Water Critical Flow," AIChE Journal, 3, 1957, p. 361.

10. Fauske, H. K., "Contribution to the Theory of Two-Phase, One-Component Critical Flow, ANL-6633, 1962.

11. Massena, W. A., "Steam-Water Critical Flow Using the Separated Flow Model," Report No. HW-65736, General Electric Co., 1960.

12. Faletti, D. W. and Moulton, R. W., "Two Phase Critical Flow of Steam-Water Mixtures," AIChE Journal, 9, 1963, p. 247.

13. Moody, F. J., "Maximum Flow Rate of a Single Component, Two-Phase Mixture," Journal of Heat Transfer, Transactions of ASME, 87, 1965, p. 134.

14. Zivi, S. M., "Estimation of Steady-State Steam Void Fraction by Means of the Principle of Minimum Entropy Production," Journal of Heat Transfer, Transactions ASME, 86, 1964, p. 247.

BIBLIOGRAPHY (Continued)

15. Moody, F. J., "Maximum Two-Phase Vessel Blowdown From Pipes," Journal of Heat Transfer, Transactions ASME, 88, 1966, p. 285.

16. Cruver, J. E. and Moulton, R. W., "Critical Flow of Liquid-Vapor Mixtures," AIChE Journal, 13, 1967, p. 52.

17. Henry, R. E. and Fauske, H. K., "The Two Phase Critical Flow of One Component Mixtures in Nozzles, Orifices, and Short Tubes," Journal of Heat Transfer, Transactions ASME, 93, 1971, p. 179.

18. Levy, S., "Prediction of Two-Phase Critical Flow Rate," Journal of Heat Transfer, Transactions ASME, 87, 1965, p. 53.

19. Smith, R. V., "Two-Phase Two-Component Critical Flow in a Venturi," Journal of Basic Engineering, Transactions ASME, 94, 1972, p. 147.

20. Henry, R. E. and Grolmes, M. A., Discussion of "Two-Phase, Two-Component Critical Flow in a Venturi," Journal of Basic Engineering, Transactions ASME, 94, 1972, p. 151.

21. Moody, F. J., "A Pressure Pulse Model for Two-Phase Critical Flow and Sonic Velocity," Journal of Heat Transfer, Transactions ASME, 91, 1969, p. 371.

22. D'Arcy, D. F., "On Acoustic Propagation and Critical Mass Flux in Two-Phase Flow," Journal of Heat Transfer, Transactions ASME, 93, 1971, p. 143.

23. Abbott, M. B., An Introduction to the Method of Characteristics, New York, American Elsevier, 1966.

24. Giot, M. and Fritte, A., "Two-Phase Two- and One-Component Critical Flows with the Variable Slip Model," Progress in Heat and Mass Transfer, Vol. 6, New York, Pergamon Press, 1972, p. 651.

25. Katto, Y., "Dynamics of Compressible Saturated Two-Phase Flow," Bulletin, JSME, 11, 1968, p. 1135.

26. Karplus, H. B., "Propagation of Pressure Waves in a Mixture of Steam and Water," AEC Report ARF 4132-12, 1961.

27. Grolmes, M. A. and Fauske, H. K., "Propagation Characteristics of Compression and Rarefaction Pressure Pulses in One-Component Vapor-Liquid Mixtures," Nuclear Engineering and Design, 11, 1969, p. 137.

28. Henry, R. E., Grolmes, M. A., and Fauske, H. K., "Pressure Pulse Propagation in Two-Phase and One- and Two-Component Mixtures," ANL-7792, 1971.

BIBLIOGRAPHY (Continued)

29. Radovskiy, I. S., "Speed of Sound in Two-Phase Vapor-Liquid Systems," Heat Transfer-Soviet Research, 3, 1971, p. 104.

30. Mecredy, R. C. and Hamilton, L. J., "The Effects of Nonequilibrium Heat, Mass and Momentum Transfer of Two Phase Sound Speed," International Journal of Heat and Mass Transfer, 15, 1972, p. 61

31. Hsieh, D. Y. and Plesset, M. S., "On the Propagation of Sound in a Liquid Containing Gas Bubbles," The Physics of Fluids, 4, 1961, p. 970.

32. Boure, J. and Reocreux, M., "General Equations of Two-Phase Flows, Applications to Critical Flows and to Non-Steady Flows," Fourth All-Union Heat and Mass Transfer Conference, Minsk, May 15-20, 1972.

33. Zuber, N. and Dougherty, D. E., "Liquid Metals Challenge to the Traditional Methods of Two-Phase Flow Investigations," Symposium on Two-Phase Flow Dynamics, Eindhoven, 1, September, 1967, p. 1091.

34. Ishii, M., "Thermally Induced Flow Instabilities in Two-Phase Mixtures in Thermal Equilibrium," Ph.D. Thesis, School of Mechanical Engineering, Georgia Institute of Technology, Atlanta, Georgia, June, 1971.

35. Saha, P., "Thermally Induced Two-Phase Flow Instabilities, Including the Effect of Thermal Non-Equilibrium Between the Phases," Ph.D. Thesis, School of Mechanical Engineering, Georgia Institute of Technology, Atlanta, Georgia, June, 1974.

36. Semenov, N. I. and Kosterin, S. I., "Results of Studying the Speed of Sound in Moving Gas-Liquid Systems," Teploenergetika, 11, 1964, p. 59.

37. Card, D. C., Sims, G. E., and Chant, R. E., "Ultrasonic Velocity of Sound and Void Fraction in a Bubbly Mixture," Journal of Basic Engineering, Transactions ASME, 93, 1971, p. 619.

38. Deich, M. E., Filippov, G. A., and Stekolshchikov, E. V., "The Speed of Sound in Two-Phase Media," Teploenergetika, 11, 1964, p. 44.

39. Ivandayey, A. I. and Nigmatulin, R. I., "Propagation of Weak Disturbances and Heat Transfer in Two-Phase Media with Phase Transitions," Heat Transfer-Soviet Research, 3, 1971, p. 98.

40. Deich, M. E., Filippov, G. A., Stekol'shchikov, E. V., and Anisimova, M. P., "Experimental Study of the Velocity of Sound in Wet Steam," Teploenergetika, 14, 1967, p. 59.

BIBLIOGRAPHY (Continued)

41. Deich, M. E. and Stekol'shchikov, E. V., "Velocity of Sound and the Damping Constant in Two-Phase Media," Tempenatur, 8, 1970, p. 989.

42. Collingham, R. E. and Firey, J. C., "Velocity of Sound Measurements in Wet Steam," I & EC Process Design and Development, 2, 1963, p. 197.

43. Dvornichenko, V. V., "Critical Conditions with Adiabatic Flow of Two-Phase Fluid from a DeLaval Nozzle," Teploenergetika, 14, 1967, p. 107.

44. DeJong, V. J. and Firey, J. C., "Effect of Slip and Phase Change on Sound Velocity in Steam-Water Mixtures and the Relation to Critical Flow," I & EC Process Design and Development, 7, 1968, p. 454.

45. Boure, J., Fritte, A., Giot, M., and Reocreux, M., "Choking Flows and Propagation of Small Disturbances," unpublished paper.

46. Zuber, N. and Findlay, J. A., "Average Volumetric Concentration in Two-Phase Flow Systems," Journal of Heat Transfer, Transactions ASME, 87, 1965, p. 453.

47. Hopkins, D. F. and Hill, D. E., "Effect of Small Radius of Curvature on Transonic Flow in Axisymmetric Nozzles," Journal of AIAA, 4, 1966, p. 1337.

48. Cuffel, R. F., Back, L. H., and Massier, P. F., "Transonic Flowfield in a Supersonic Nozzle with Small Throat Radius of Curvature," Journal of AIAA, 7, 1965, p. 1364.

49. Vogrin, J. A., "An Experimental Investigation of Two-Phase, Two Component Flow in a Horizontal Converging-Diverging Nozzle," ANL-6754, Argonne National Laboratory, 1963.

50. Henry, R. E., Fauske, H. K., and McComas, S. T., "Two-Phase Critical Flow at Low Qualities, Part I: Experimental," Nuclear Science and Engineering, 41, 1970, p. 79.

51. Henry, R. E., Fauske, H. K., and McComas, S. T., "Two-Phase Critical Flow at Low Qualities, Part II: Analysis," Nuclear Science and Engineering, 41, 1970, p. 92.

52. Hirth, J. P. and Pound, G. M., editors, Chalmes, B., Progress in Materials Science, 11, 1963, Pergamon Press, New York.

BIBLIOGRAPHY (Concluded)

53. Keenan, J. H. and Keyes, F. G., Thermodynamic Properties of Steam, John Wiley and Sons, Inc., New York.

VITA

Born on April 1, 1946, Dennis Richardson Liles is the only son of Mr. William J. Liles and Mrs. Vergie Richardson Liles of New Orleans, Louisiana. He graduated from Newman High School, New Orleans, in 1964 and entered the Georgia Institute of Technology, Atlanta, Georgia for his undergraduate education. In June 1968, he received his Bachelor of Mechanical Engineering and a commission in the United States Army.

Mr. Liles spent two years in the United States Army at Fort Bliss, Texas during which time he began graduate work at the University of Texas at El Paso. He received the degree of Master of Science in Mechanical Engineering from the University of Texas at El Paso in January 1972, one year after separation from the Army.

In September 1971 Mr. Liles returned to the Georgia Institute of Technology to continue his graduate studies in mechanical engineering. His educational emphasis has been in the area of the thermal and fluid sciences.

Mr. Liles is married to the former Laura Ann Reid. They have one child, a son, Daniel Trenton.